Fig. B.13.1.1. The average ^{137}Cs activities (pCi/g) in soil samples collected to a depth of 15 cm.

Fig. B.13.1.m. ^{60}Co isoexposure and isoconcentration contours. (Refer to alphabetic symbol key in this appendix.)

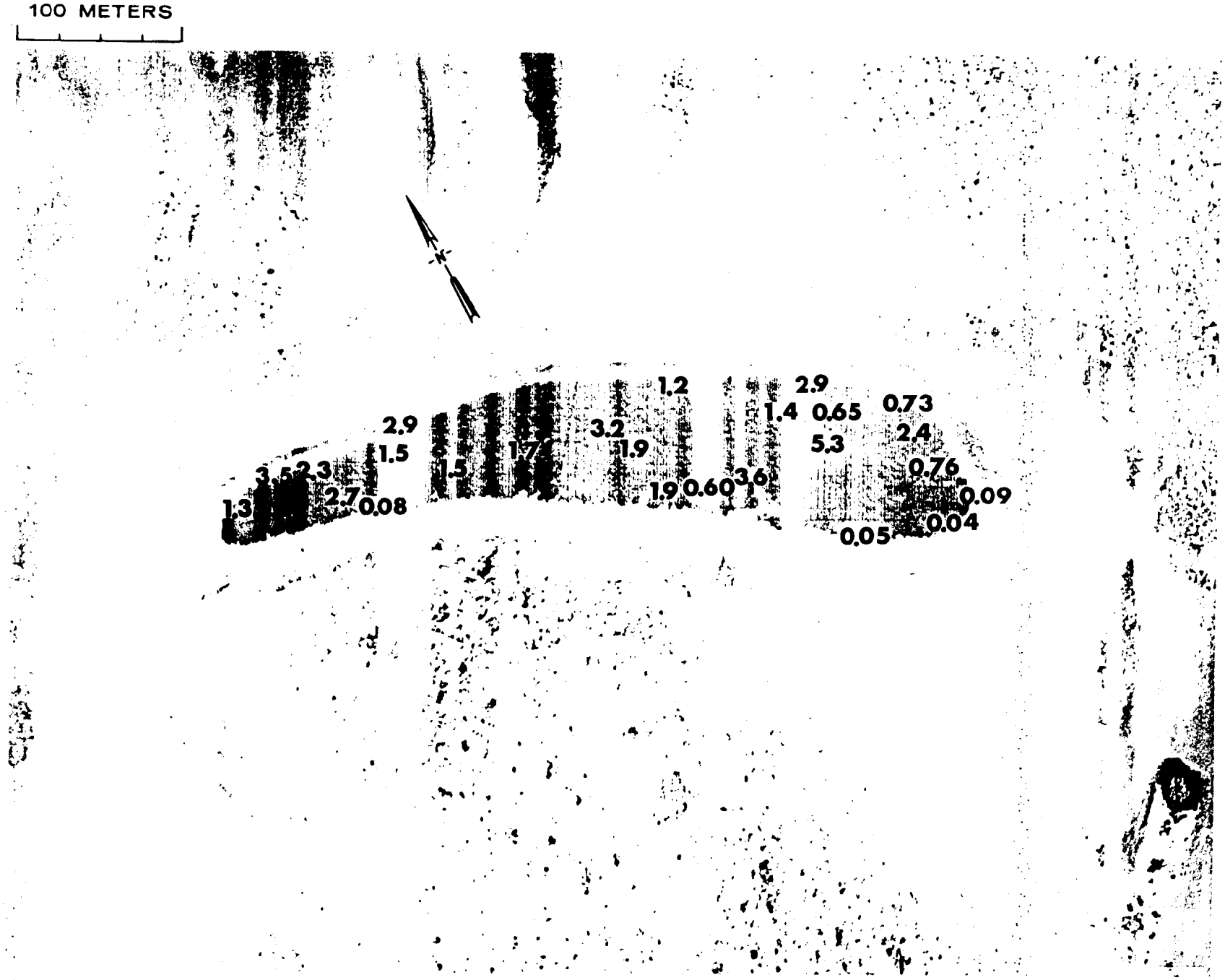

Fig. B.13.1.n. The average ^{60}Co activities (pCi/g) in soil samples collected to a depth of 15 cm.

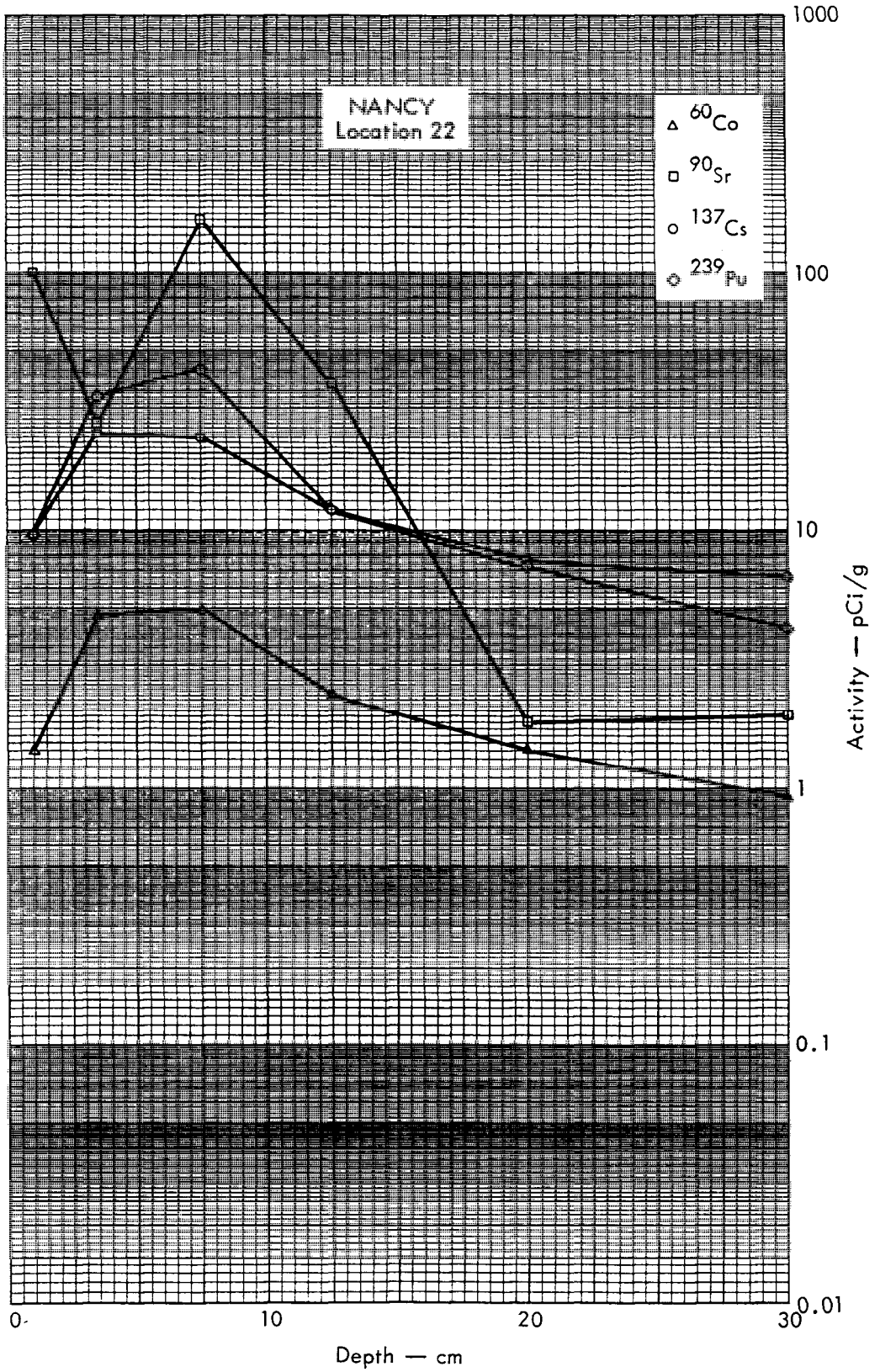

Fig. B. 13.2a. Activities of selected radionuclides as a function of soil depth.

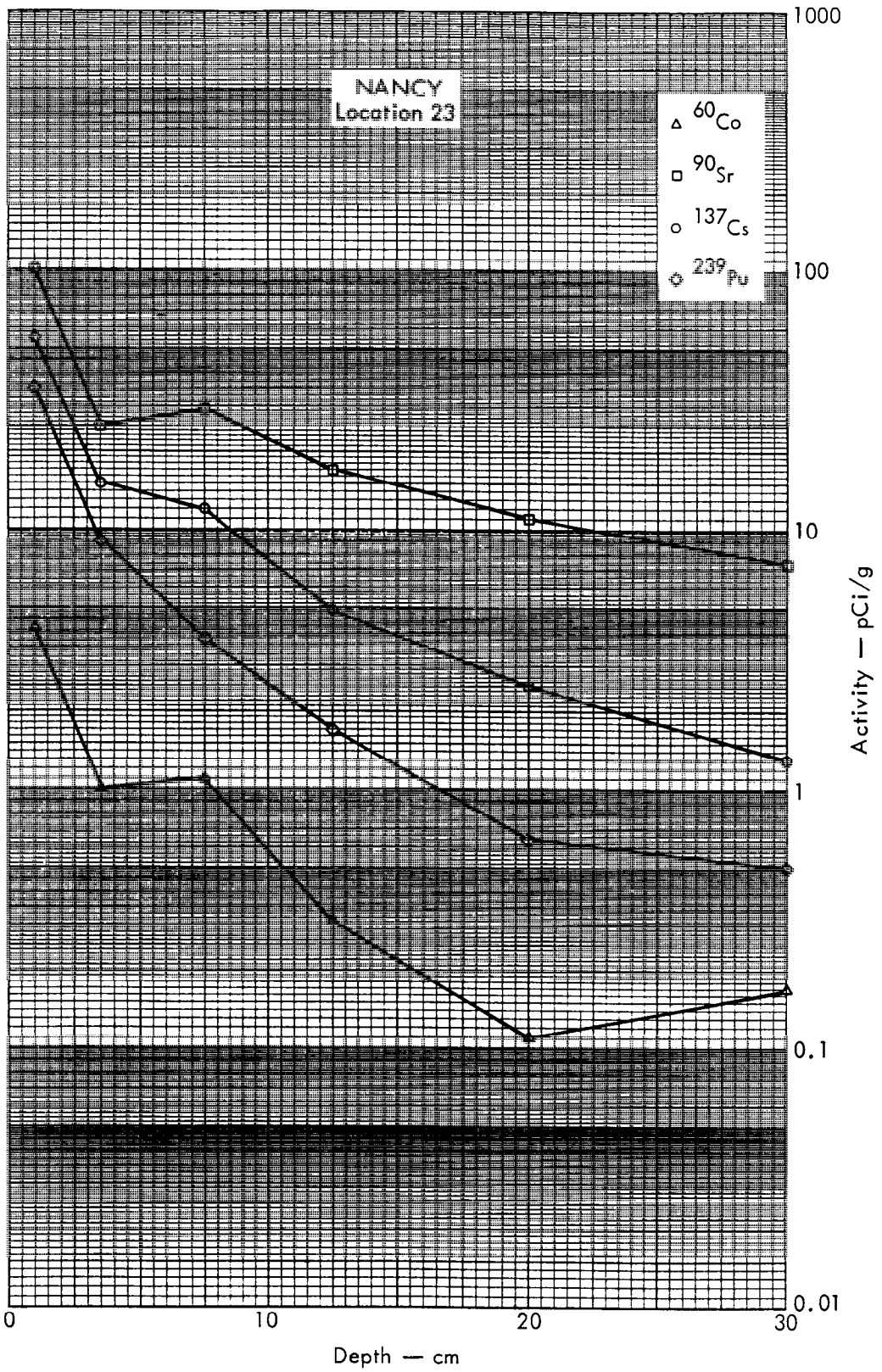

Fig. B.13.2b. Activities of selected radionuclides as a function of soil depth.

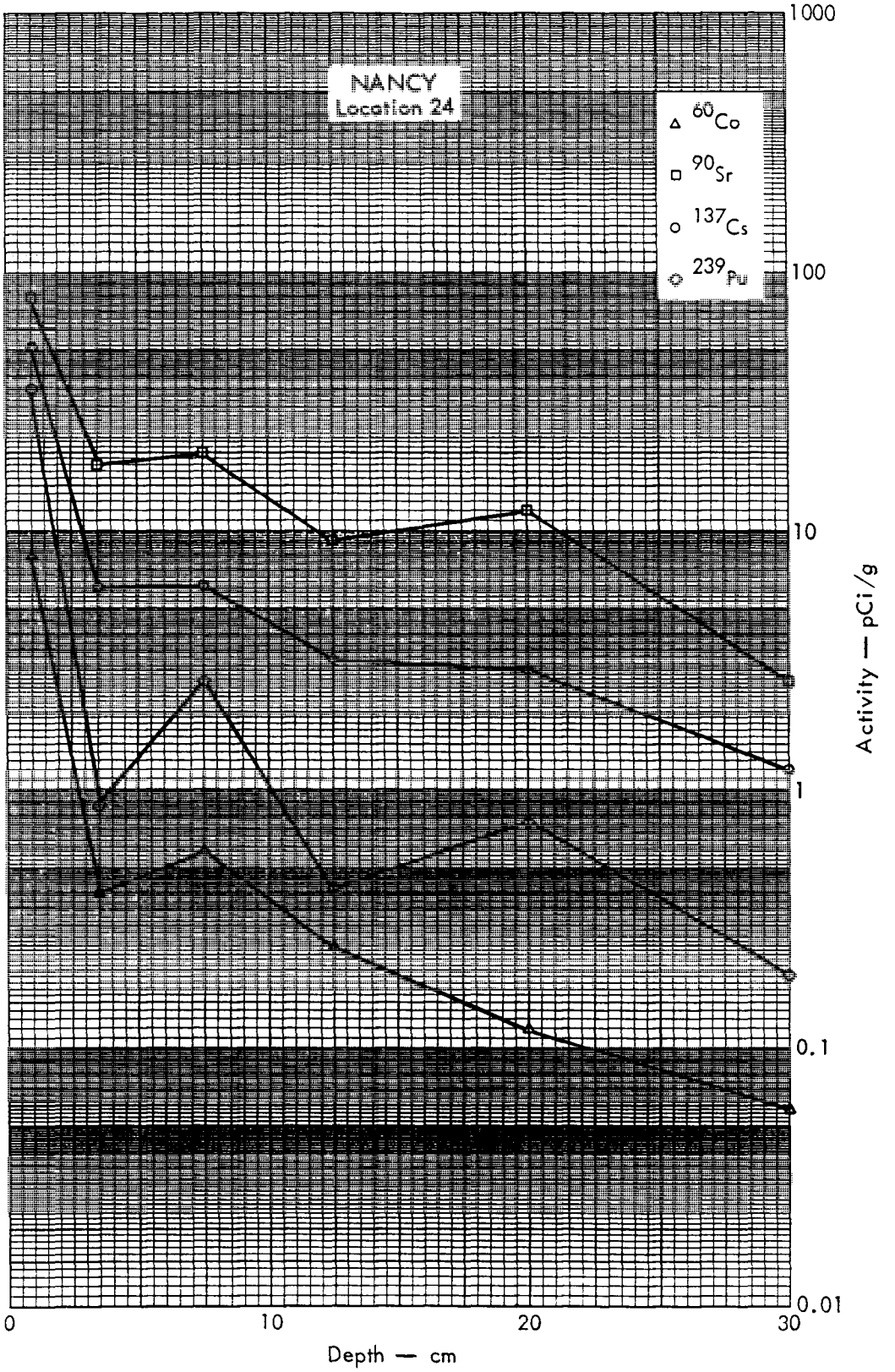

Fig. B. 13. 2c. Activities of selected radionuclides as a function of soil depth.

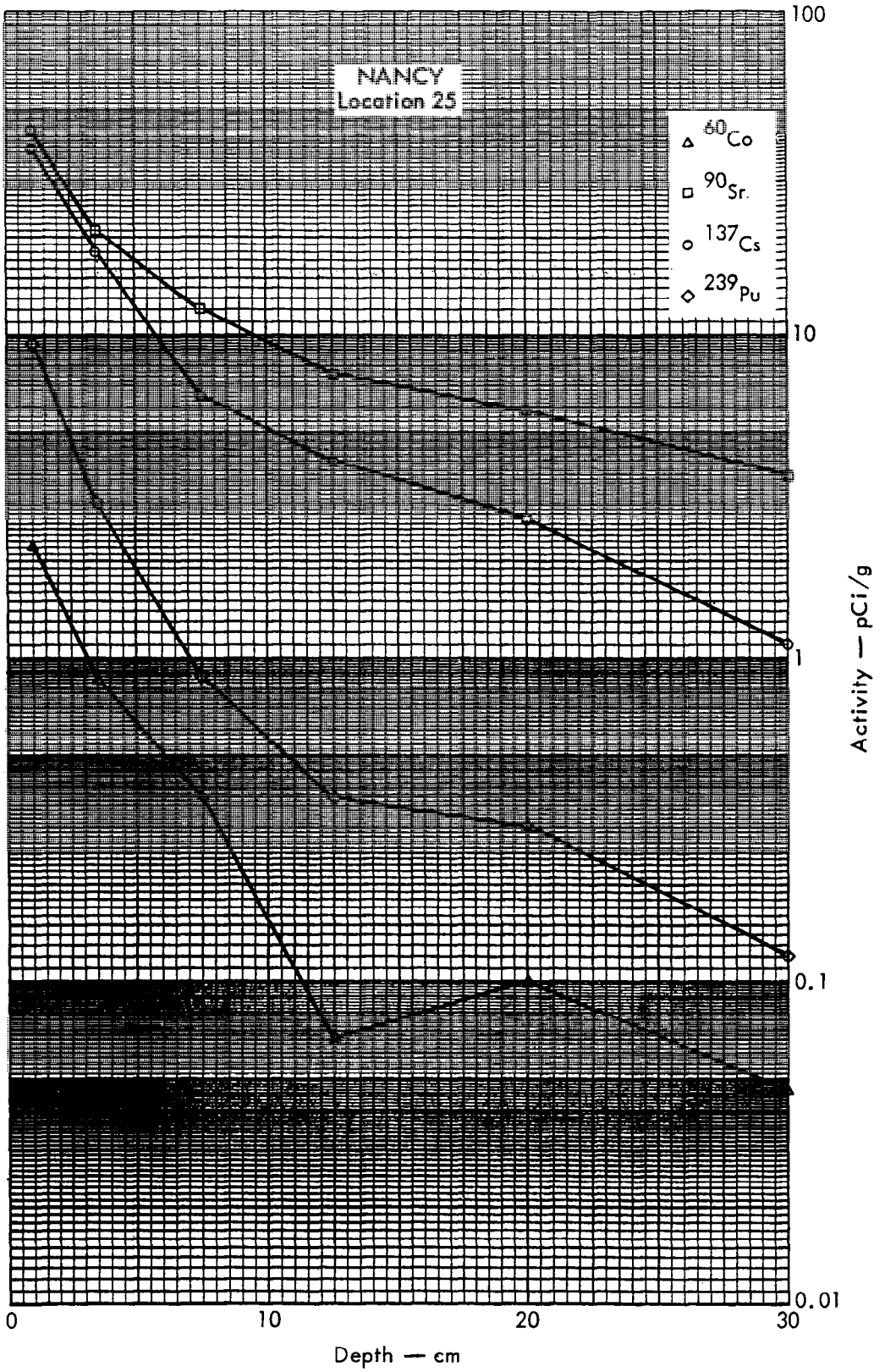

Fig. B.13.2d. Activities of selected radionuclides as a function of soil depth.

Fig. B.14.1.a.

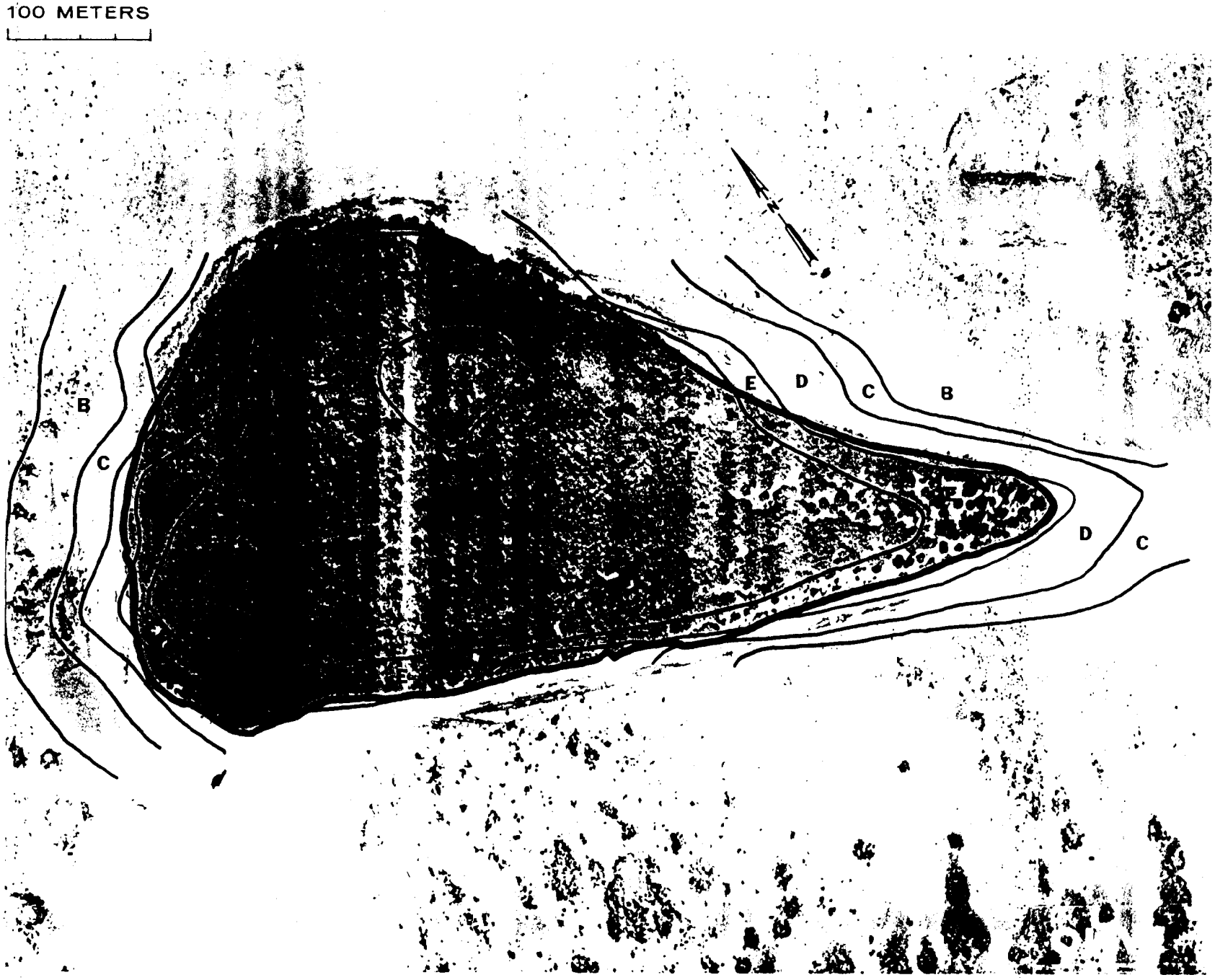

Fig. B.14.1.b. **Gross count** isoexposure contours. (Refer to alphabetic symbol key in this appendix.)

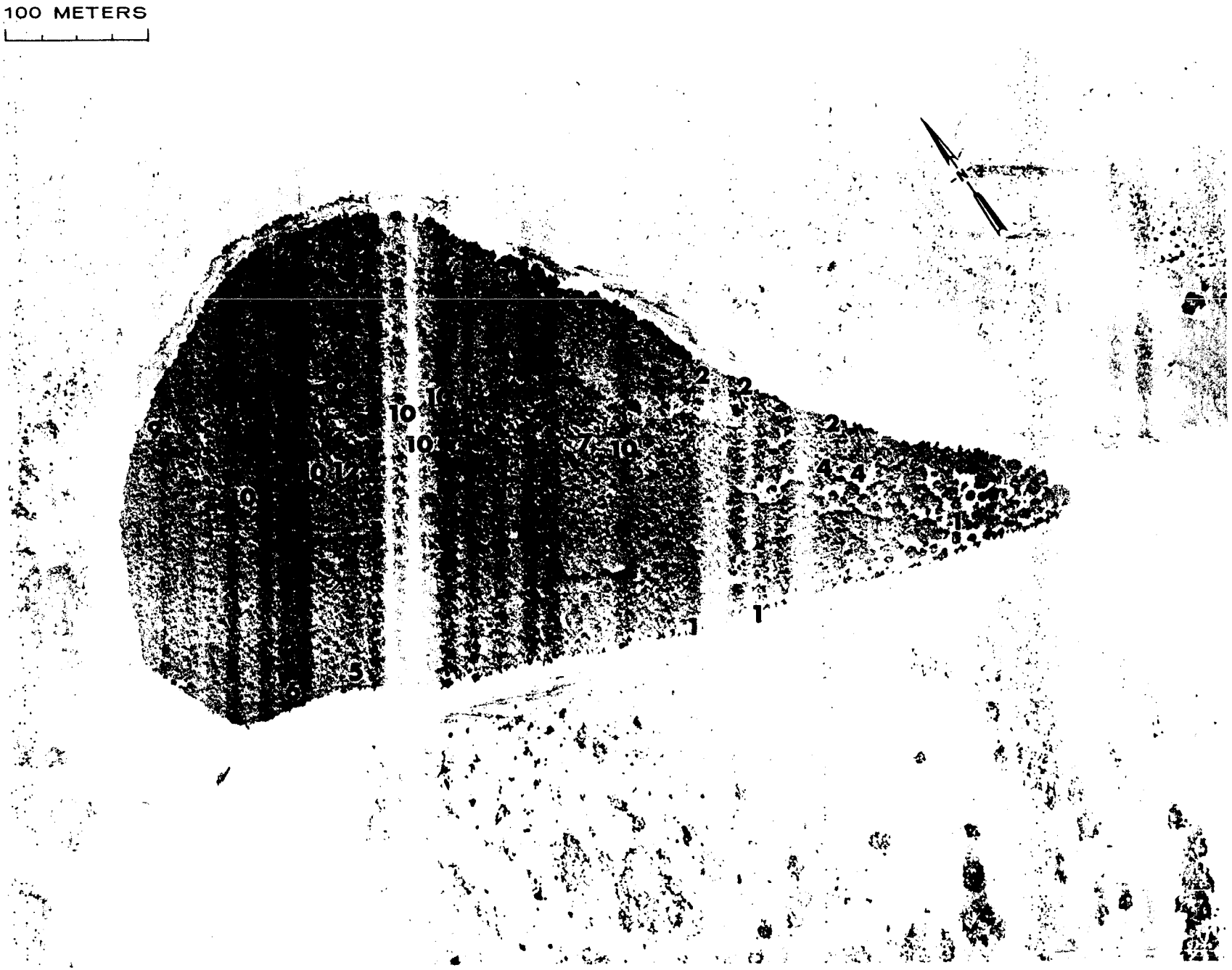

Fig. B.14.1.d. The gamma background exposure rate (μR/hr) at 1 m above the ground, measured with a portable NaI scintillation counter.

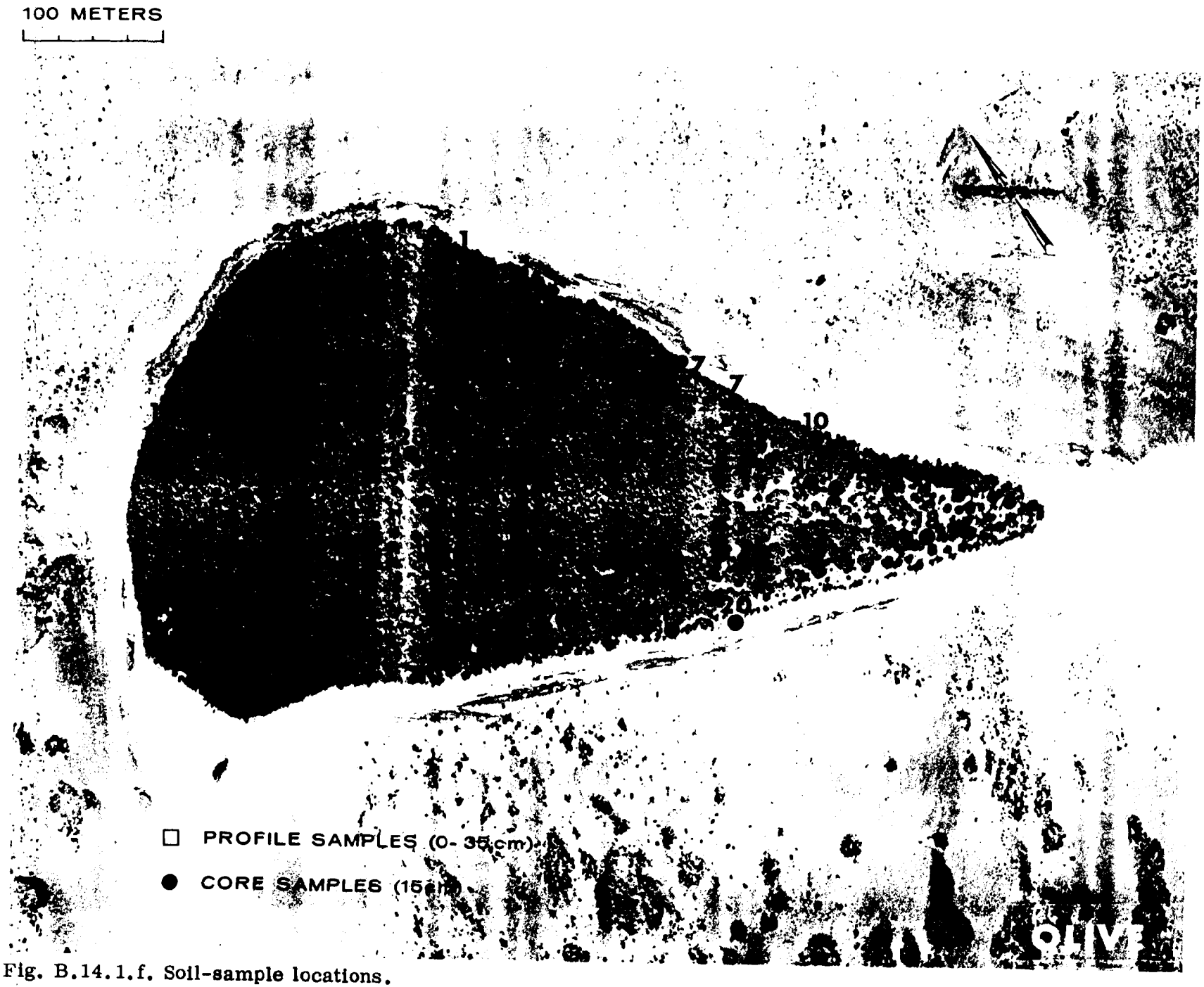

Fig. B.14.1.f. Soil-sample locations.

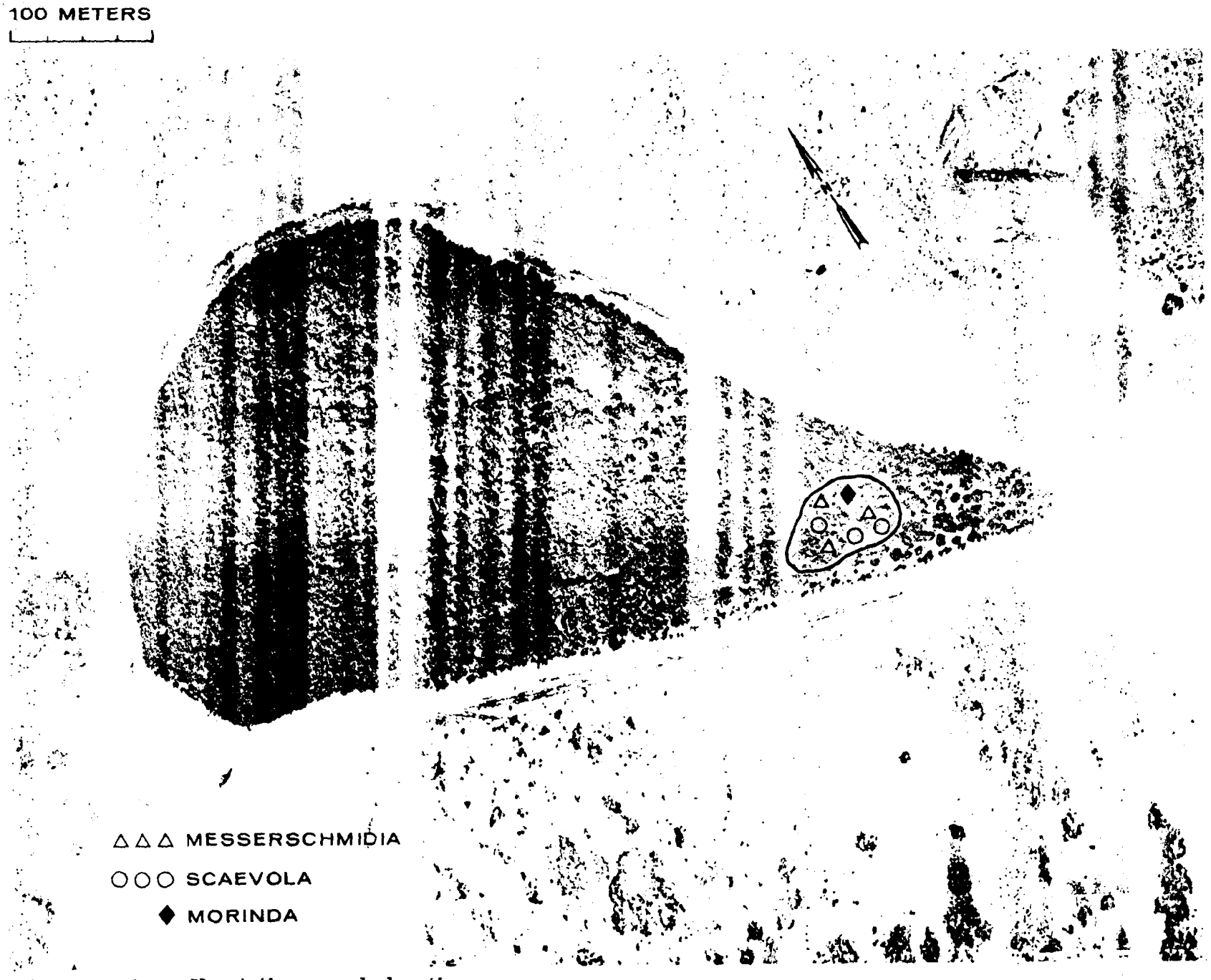

Fig. B.14.1.g. Vegetation sample locations.

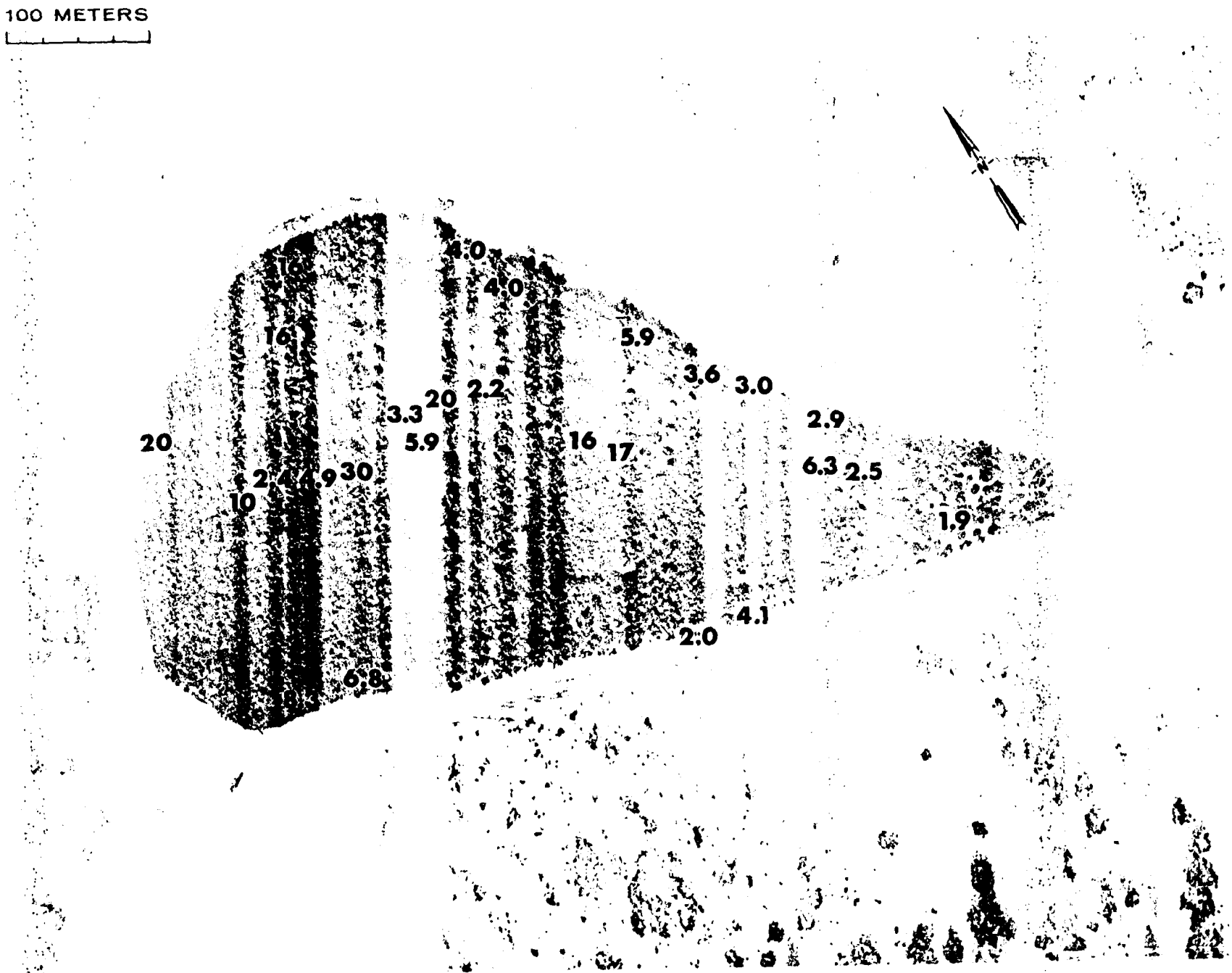

Fig. B.14.1.1. The average ^{239}Pu activities (pCi/g) in soil samples collected to a depth of 15 cm.

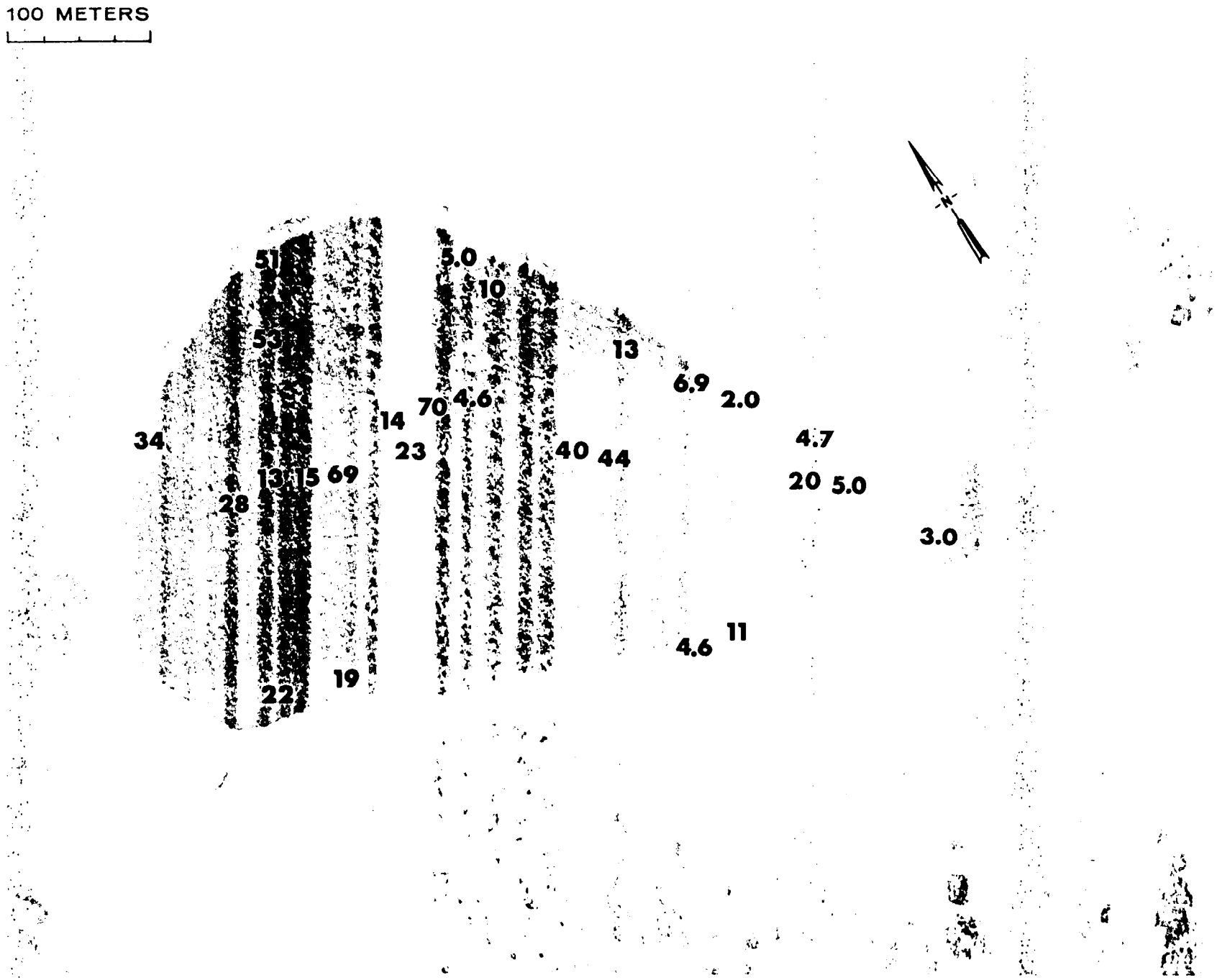

Fig. B.14.1.j. The average ^{90}Sr activities (pCi/g) in soil samples collected to a depth of 15 cm.

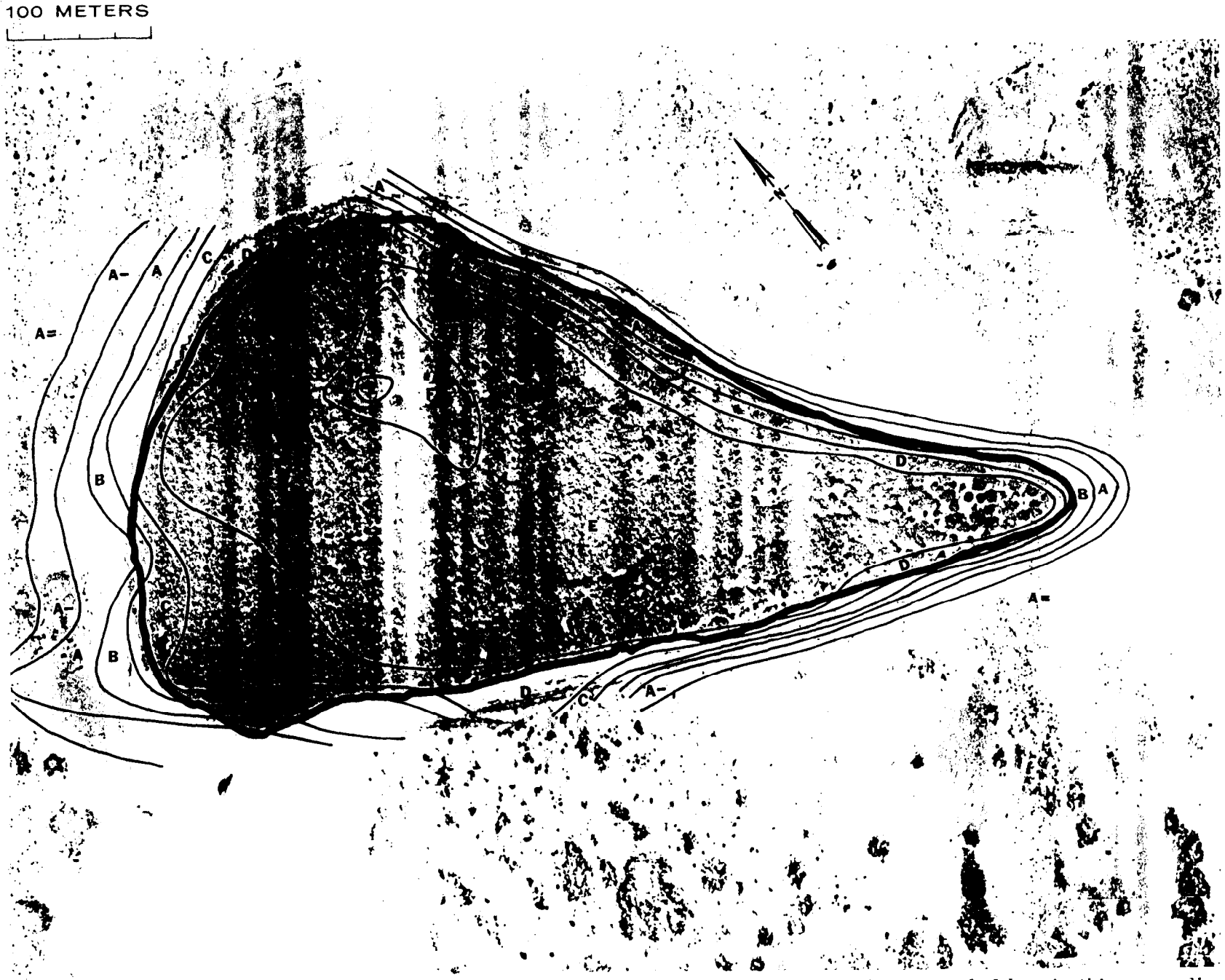

Fig. B.14.1.k. ^{137}Cs isoexposure and isoconcentration contours. (Refer to alphabetic symbol key in this appendix.)

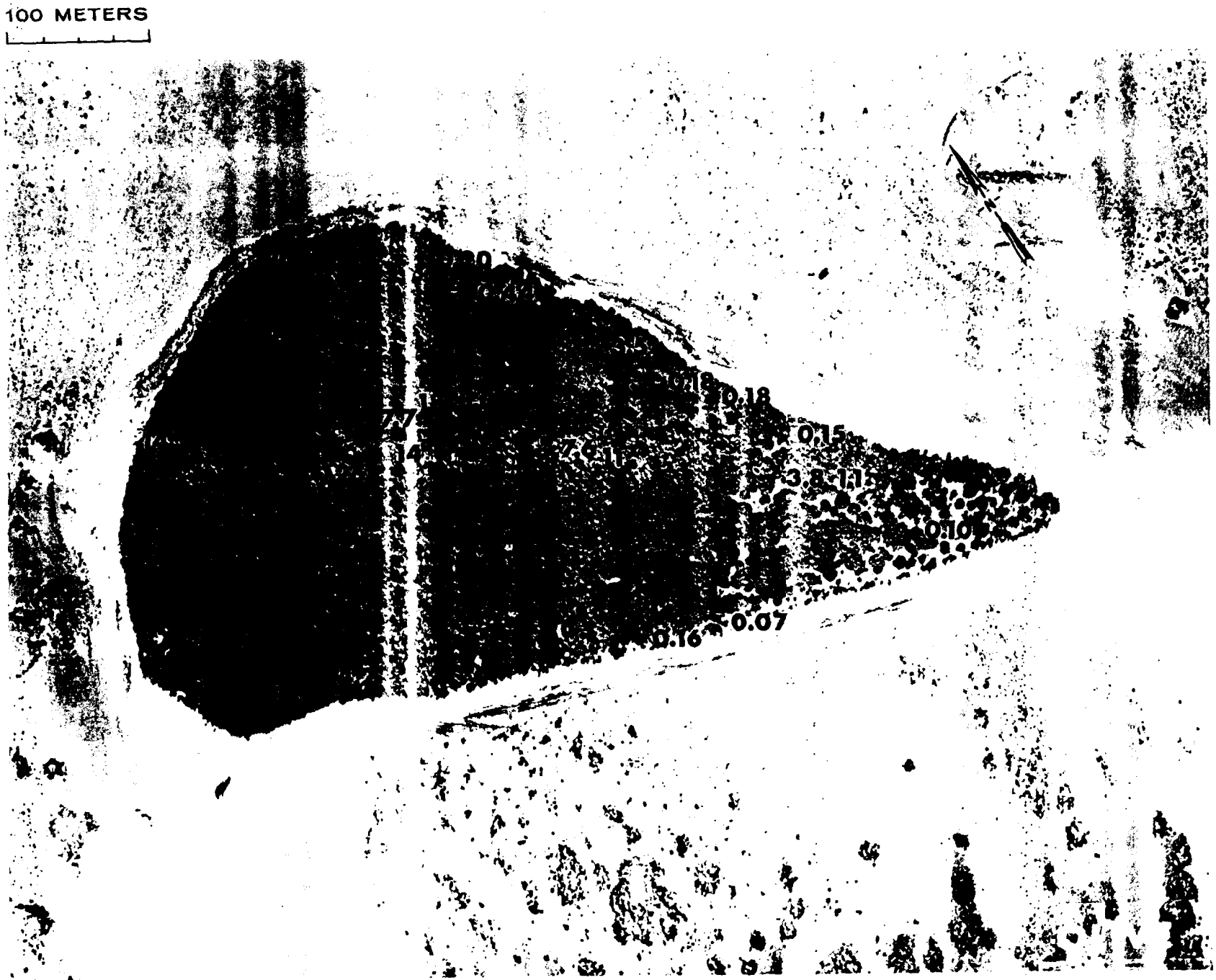

Fig. B.14.1.1. The average ^{137}Cs activities (pCi/g) in soil samples collected to a depth of 15 cm.

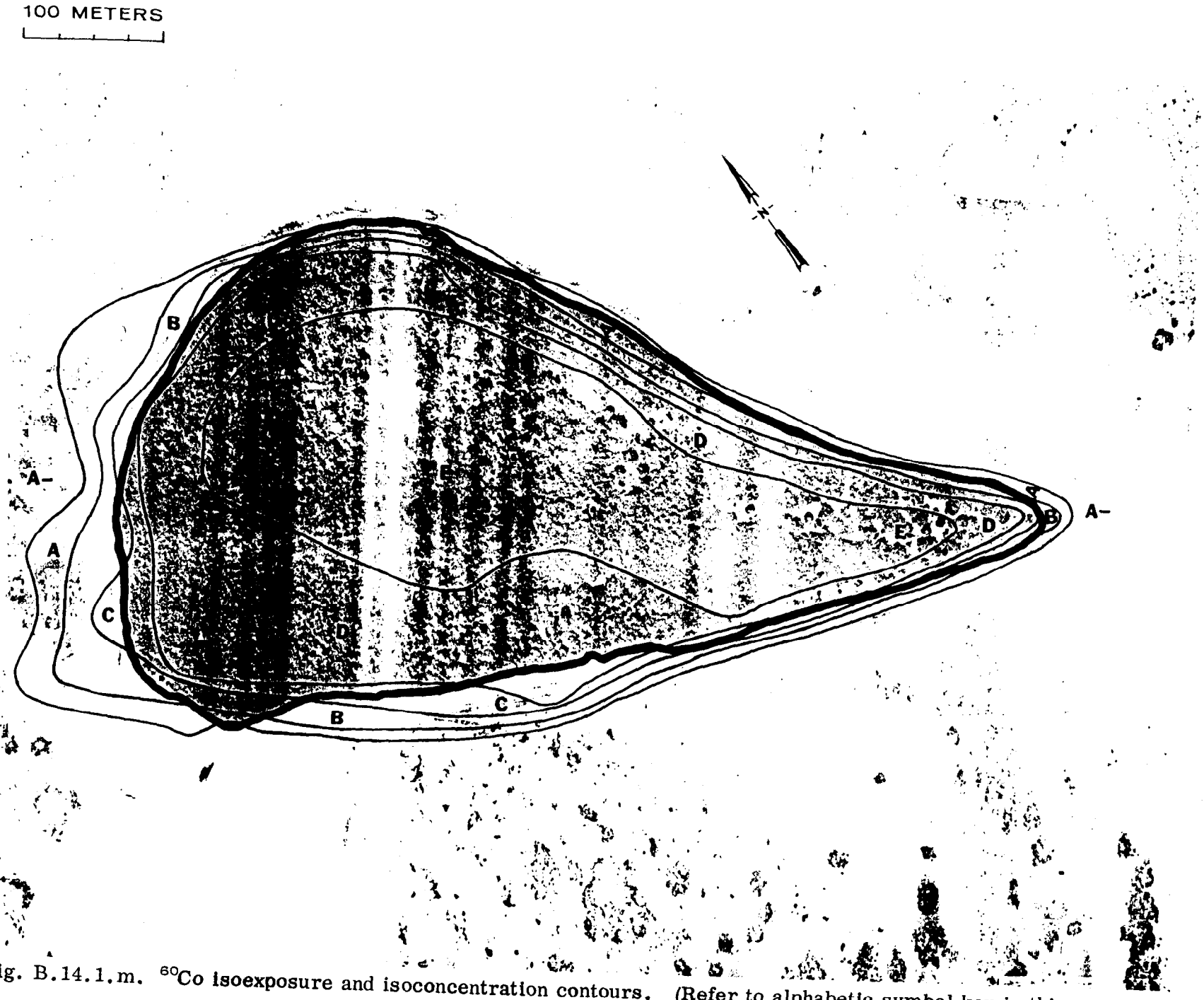

Fig. B.14.1.m. ^{60}Co isoexposure and isoconcentration contours. (Refer to alphabetic symbol key in this appendix.)

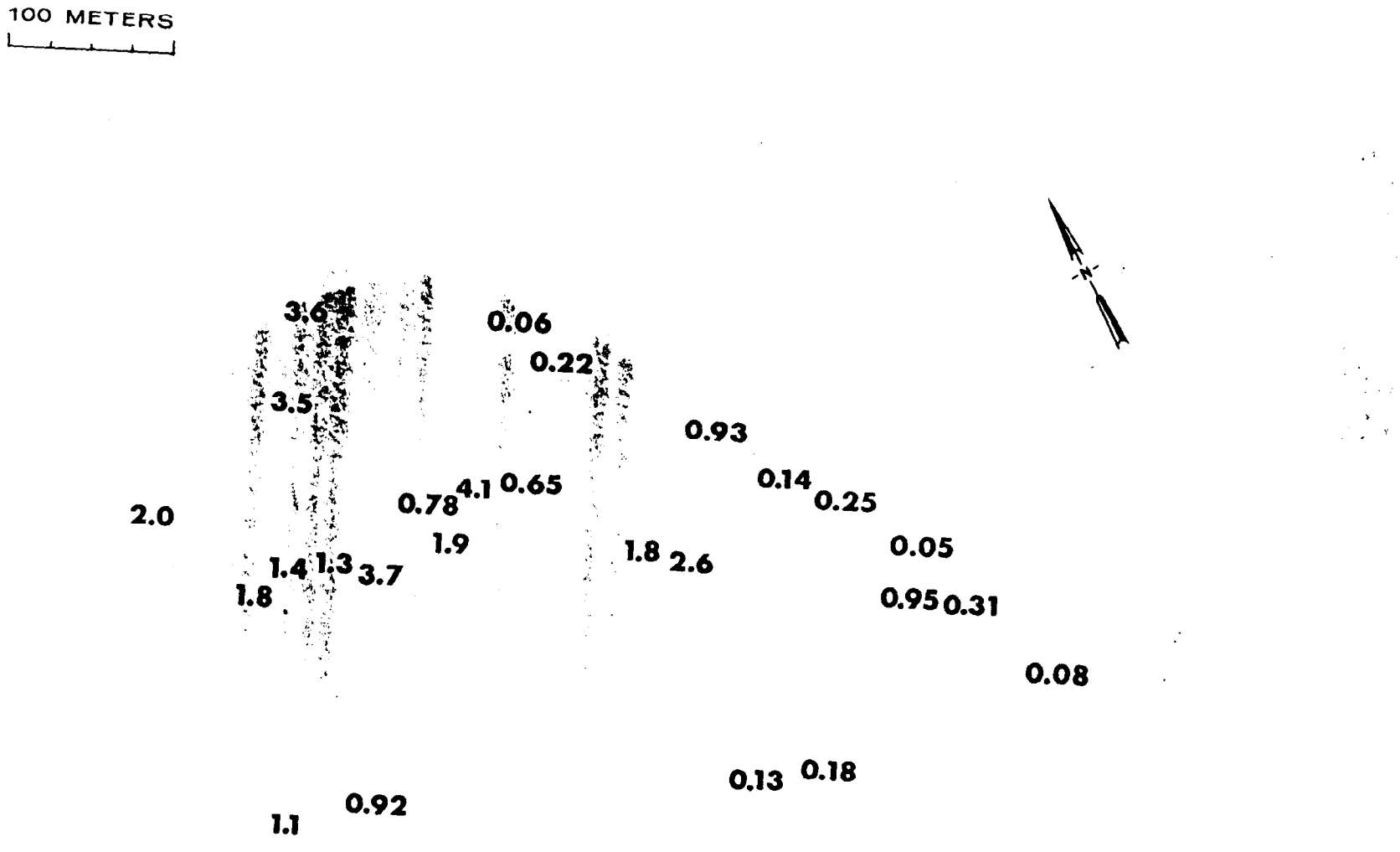

Fig. B.14.1.n. The average ^{60}Co activities (pCi/g) in soil samples collected to a depth of 15 cm.

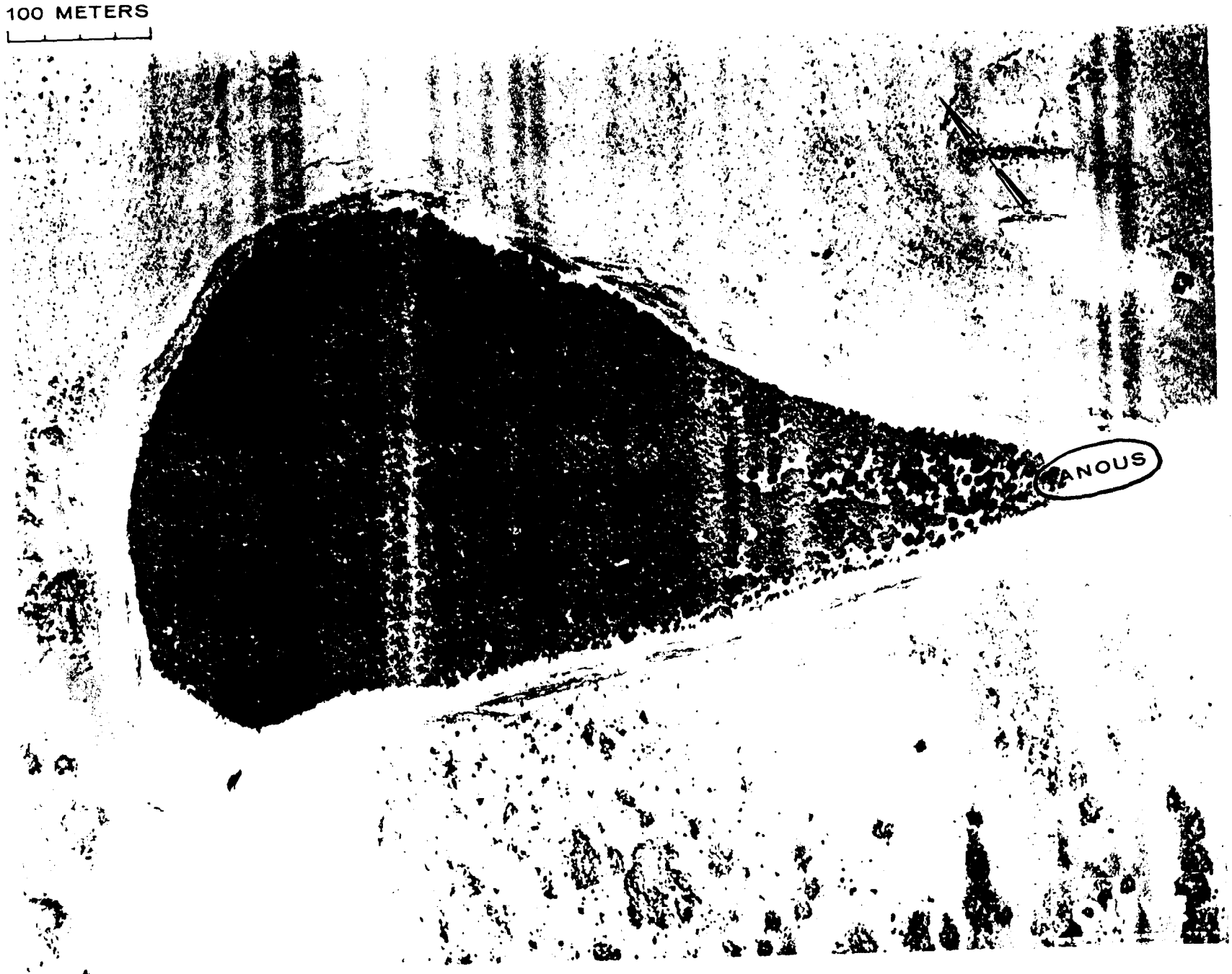

Fig. B.14.1.o. **Terrestrial animal sample locations.**

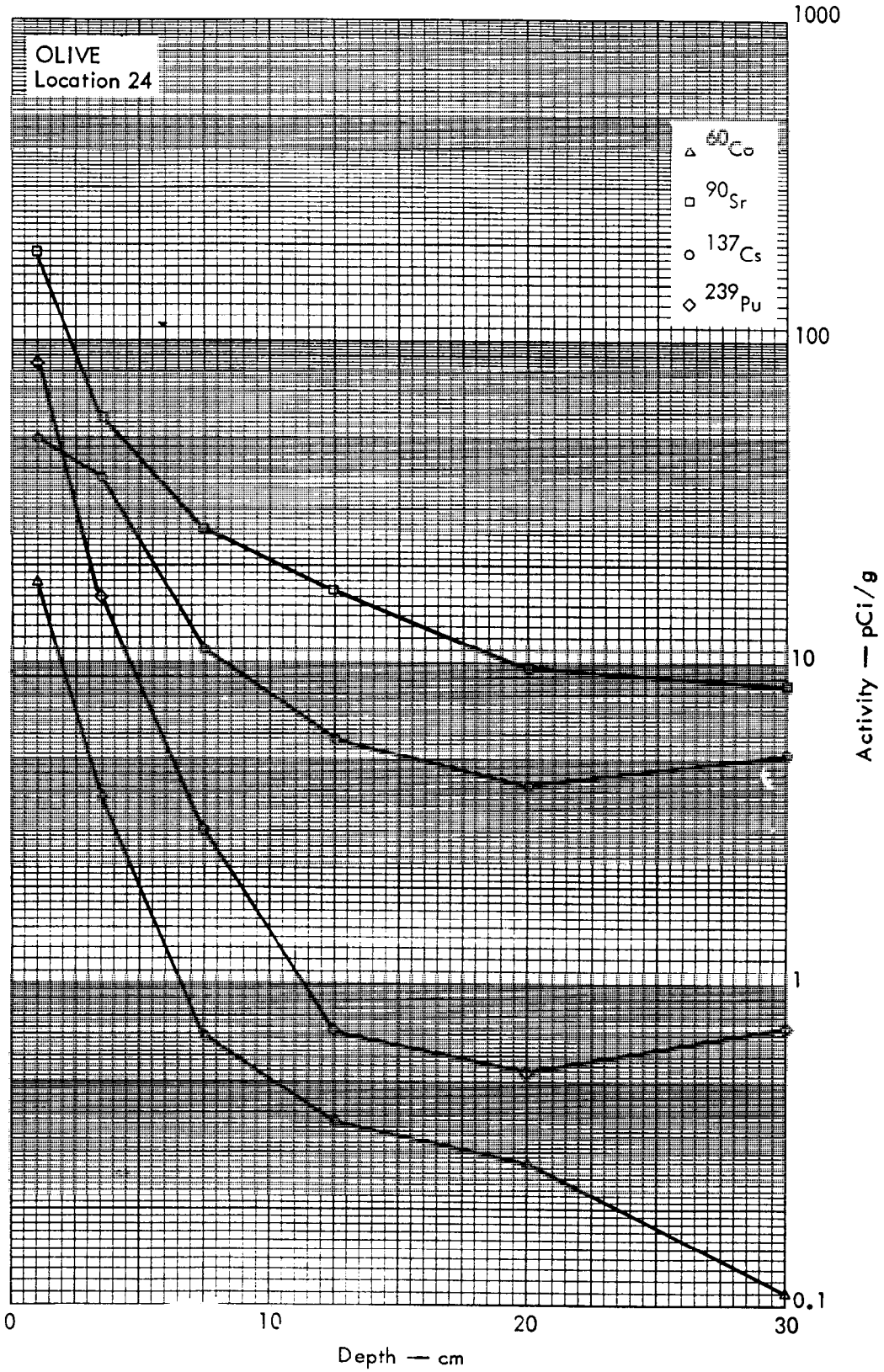

Fig. B. 14. 2a. Activities of selected radionuclides as a function of soil depth.

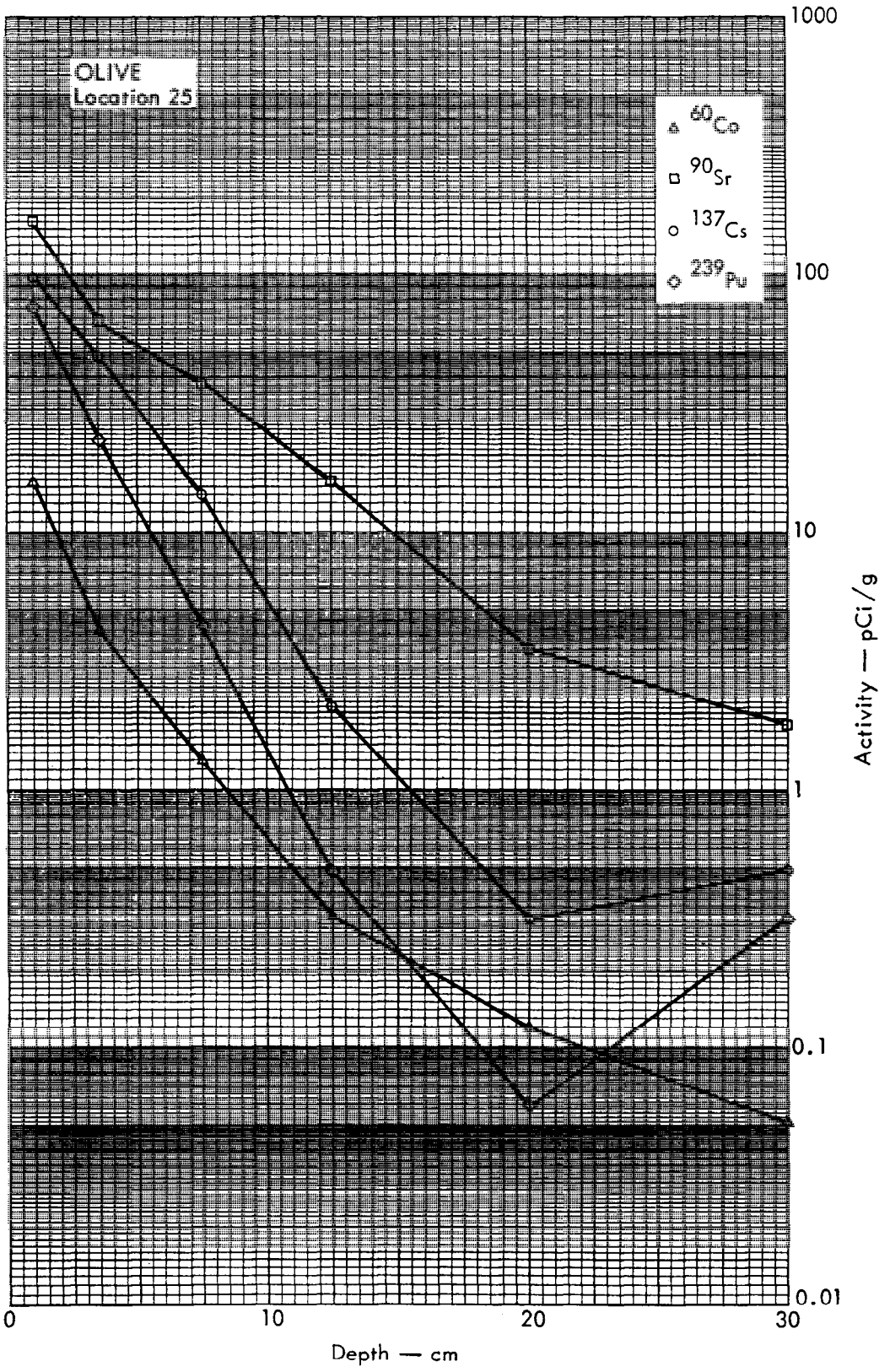

Fig. B. 14. 2b. Activities of selected radionuclides as a function of soil depth.

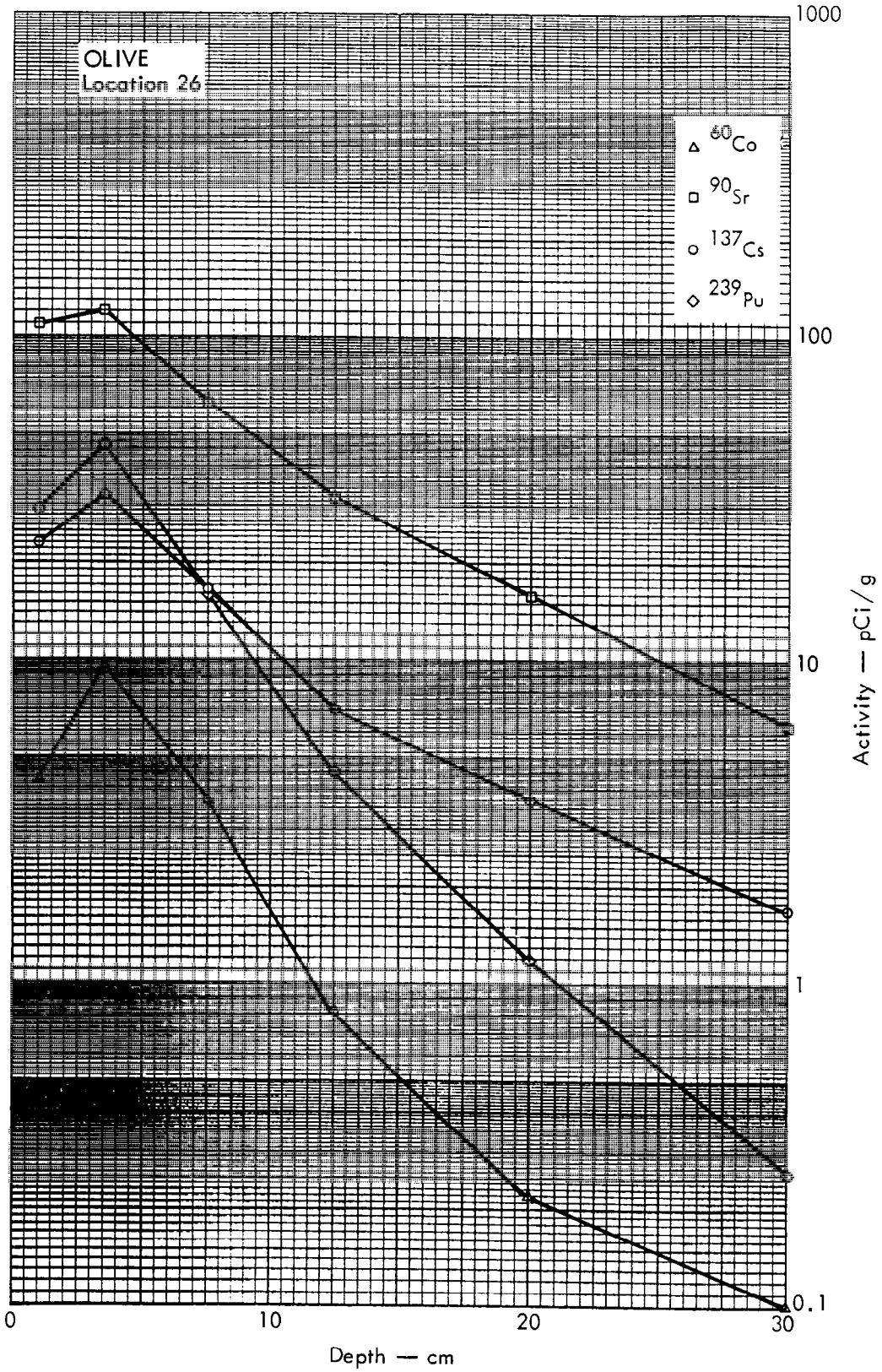

Fig. B.14.2c. Activities of selected radionuclides as a function of soil depth.

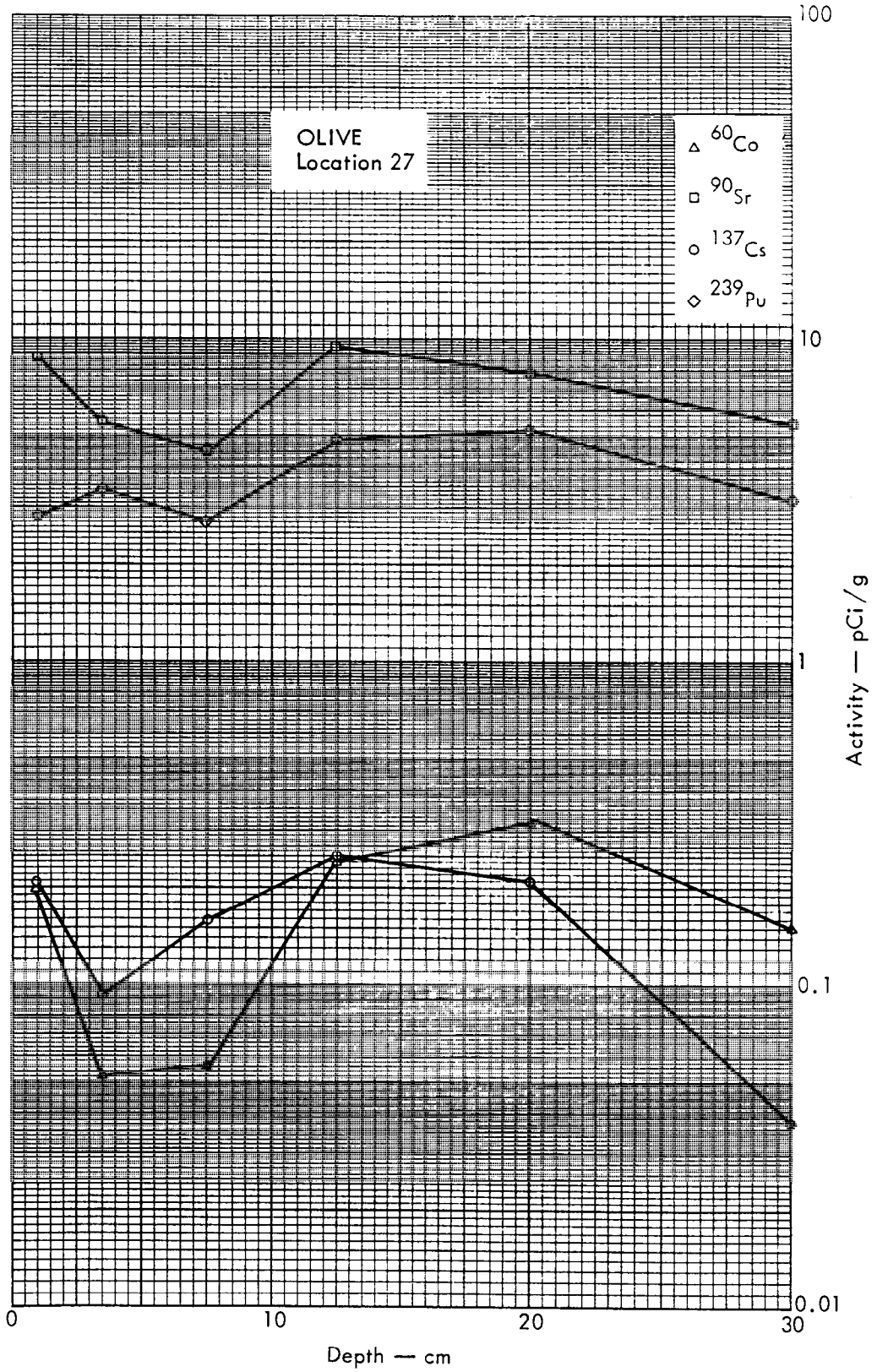

Fig. B. 14.2d. Activities of selected radionuclides as a function of soil depth.

Fig. B.15.1.a.

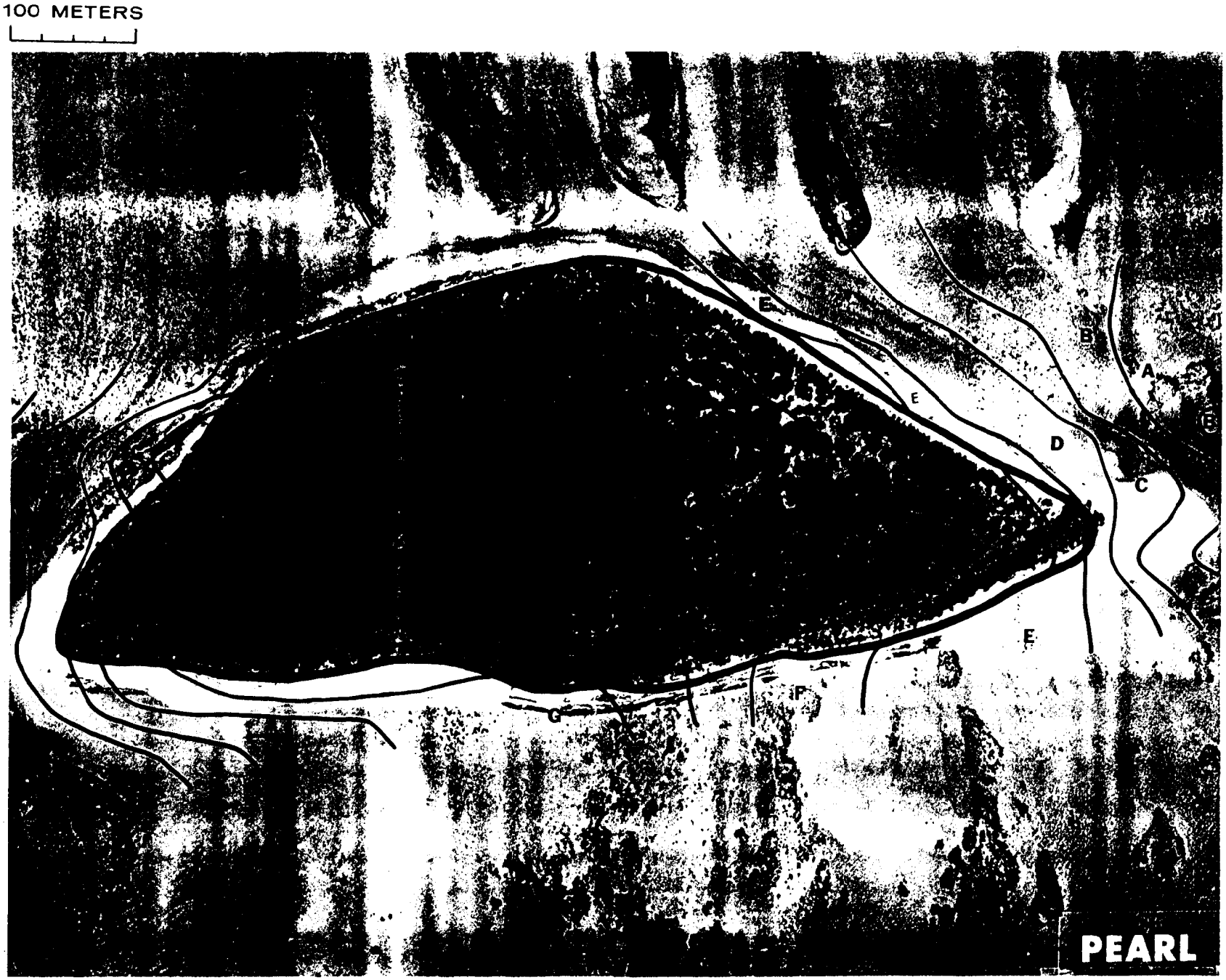

Fig. B.15.1.b. **Gross count isoexposure contours.** (Refer to alphabetic symbol key in this appendix.)

Fig. B.15.1.d. The gamma background exposure rate (μR/hr) at 1 m above the ground, measured with a portable NaI scintillation counter.

Fig. B.15.1.f. Soil-sample locations.

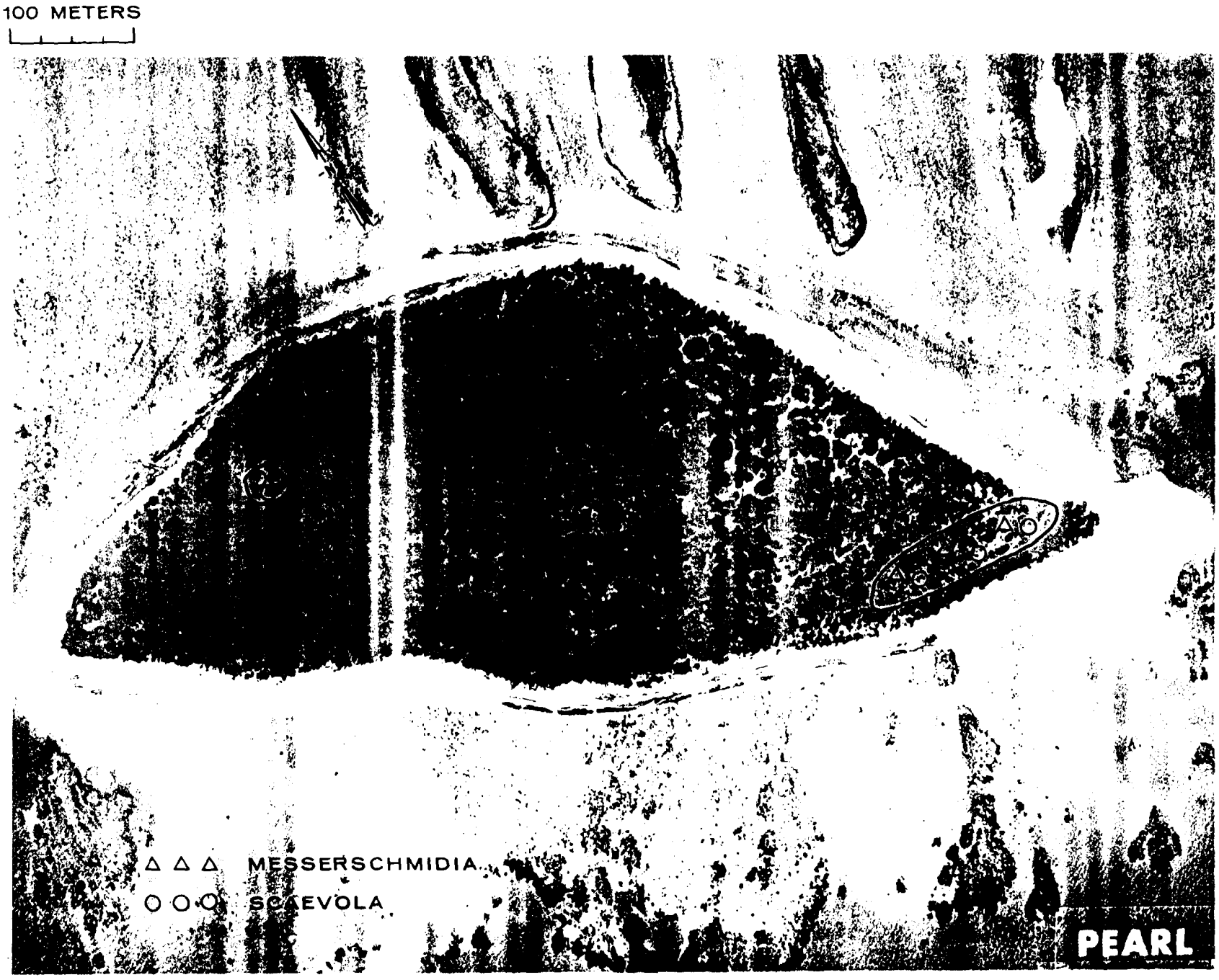

Fig. B.15.1.g. Vegetation sample locations.

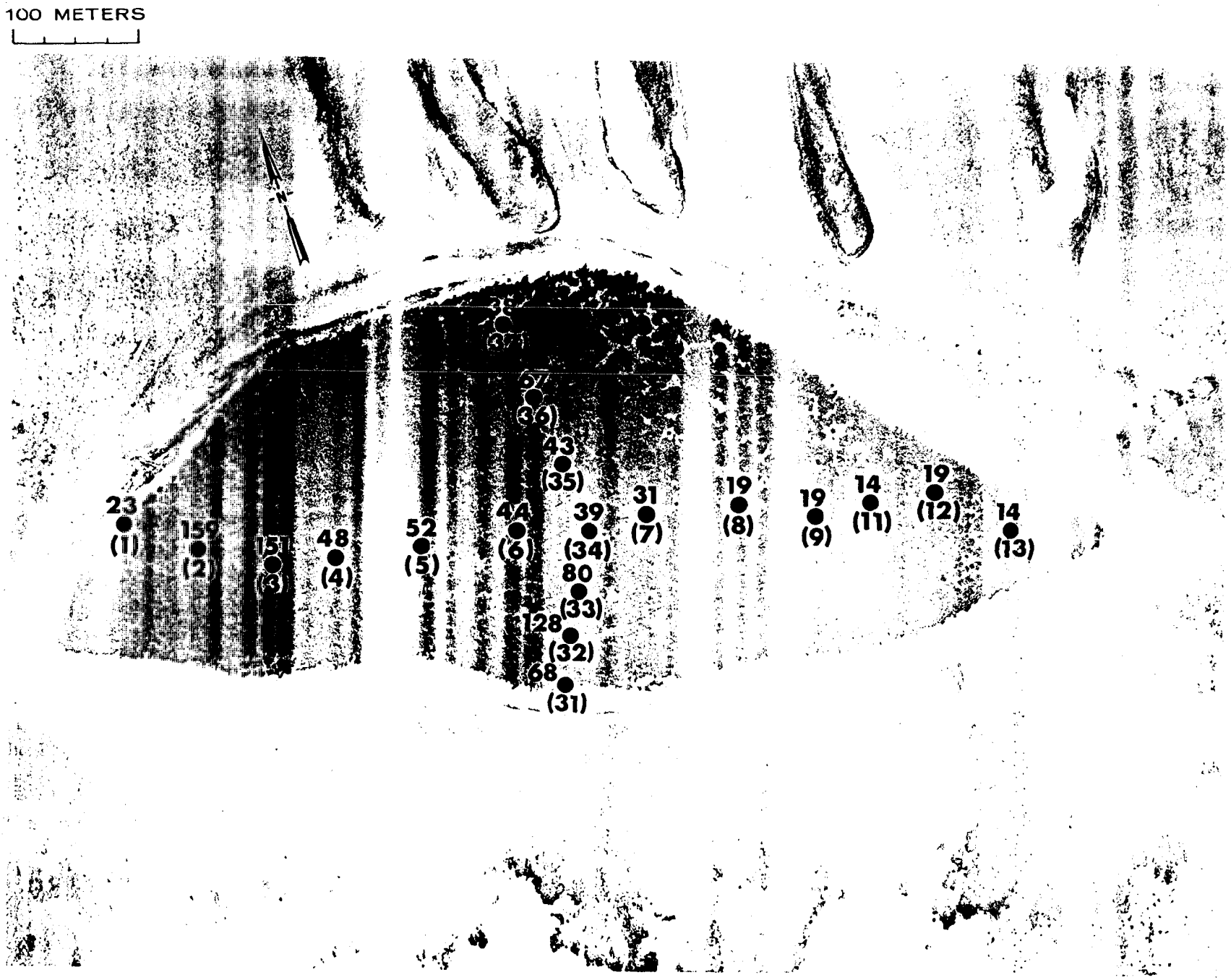

Fig. B.15.1.h. The gamma-ray exposure rates (uR/hr) measured 1 m above the ground by the LiF thermoluminescent dosimeters (TLD). The numbers shown in parentheses denote the location identification numbers.

Fig. B.15.1.1. The average ^{239}Pu activities (pCi/gm) in soil samples collected to a depth of 15 cm.

Fig. B.15.1.j. The average ^{90}Sr activities (pCi/gm) in soil samples collected to a depth of 15 cm.

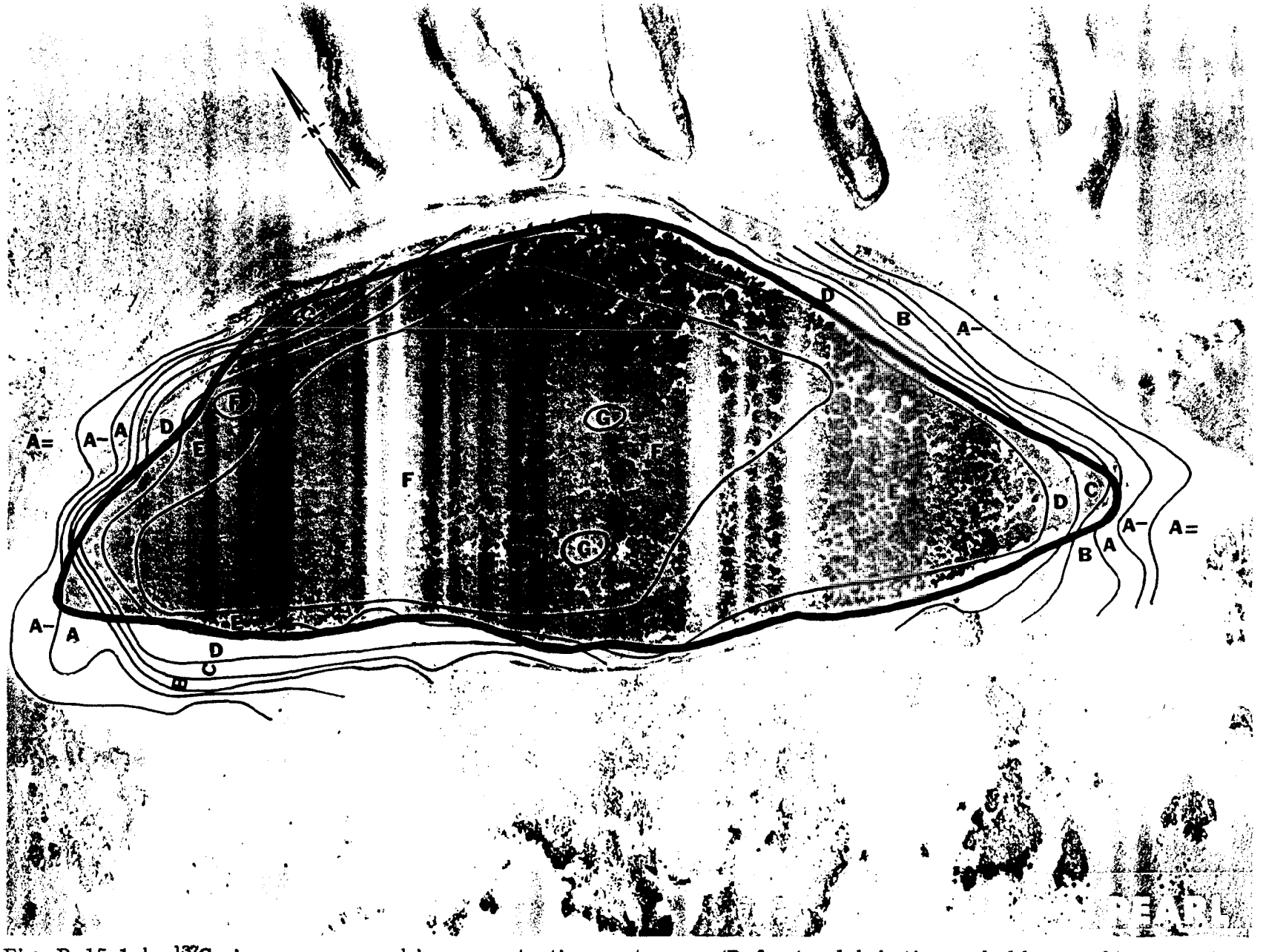

Fig. B.15.1.k. ^{137}Cs isoexposure and isoconcentration contours. (Refer to alphabetic symbol key in this appendix.)

Fig. B.15.1.1. The average ^{137}Cs activities (pCi/gm) in soil samples collected to a depth of 15 cm.

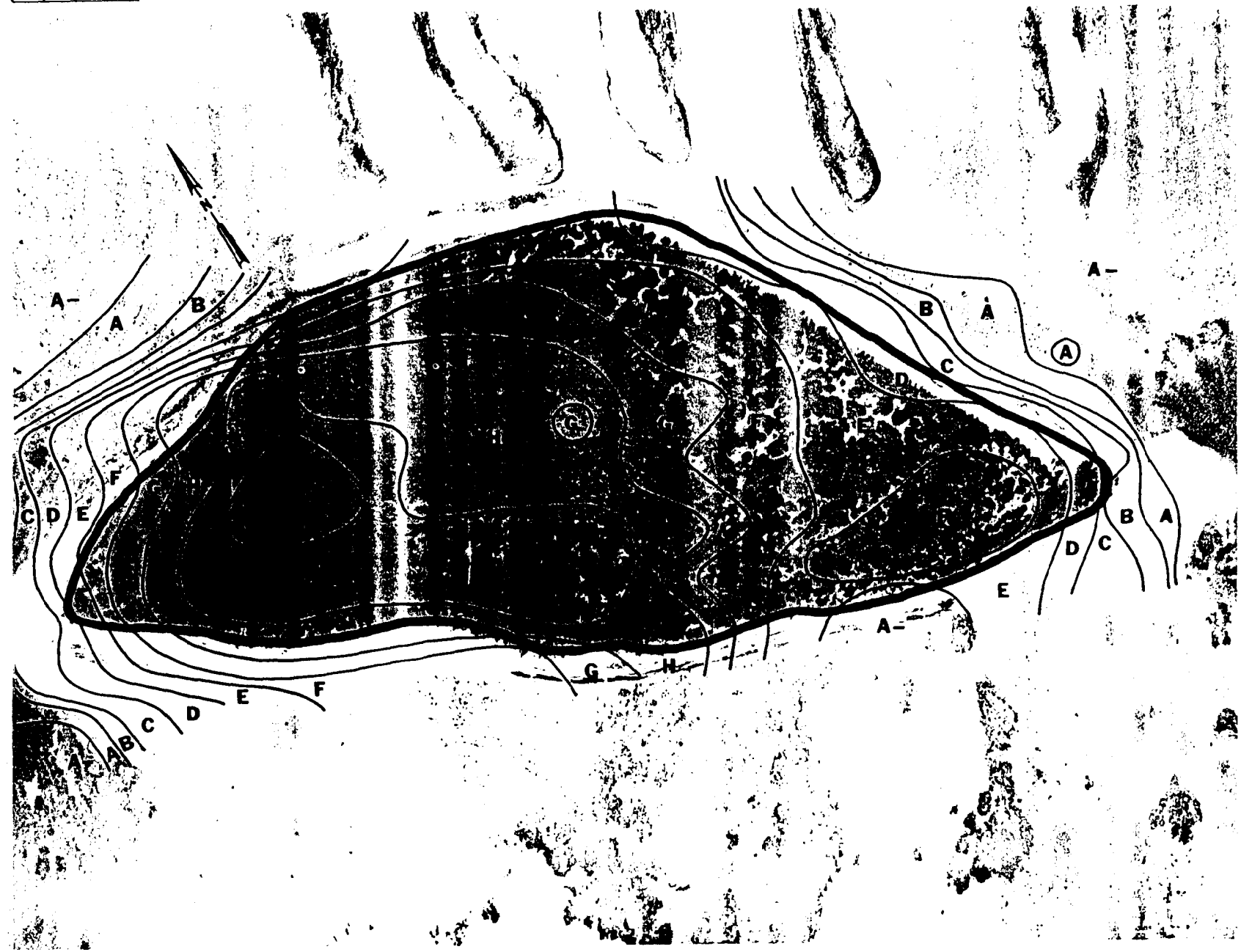

Fig. B.15.1.m. ^{60}Co isoexposure and isoconcentration contours. (Refer to alphabetic symbol key in this appendix.)

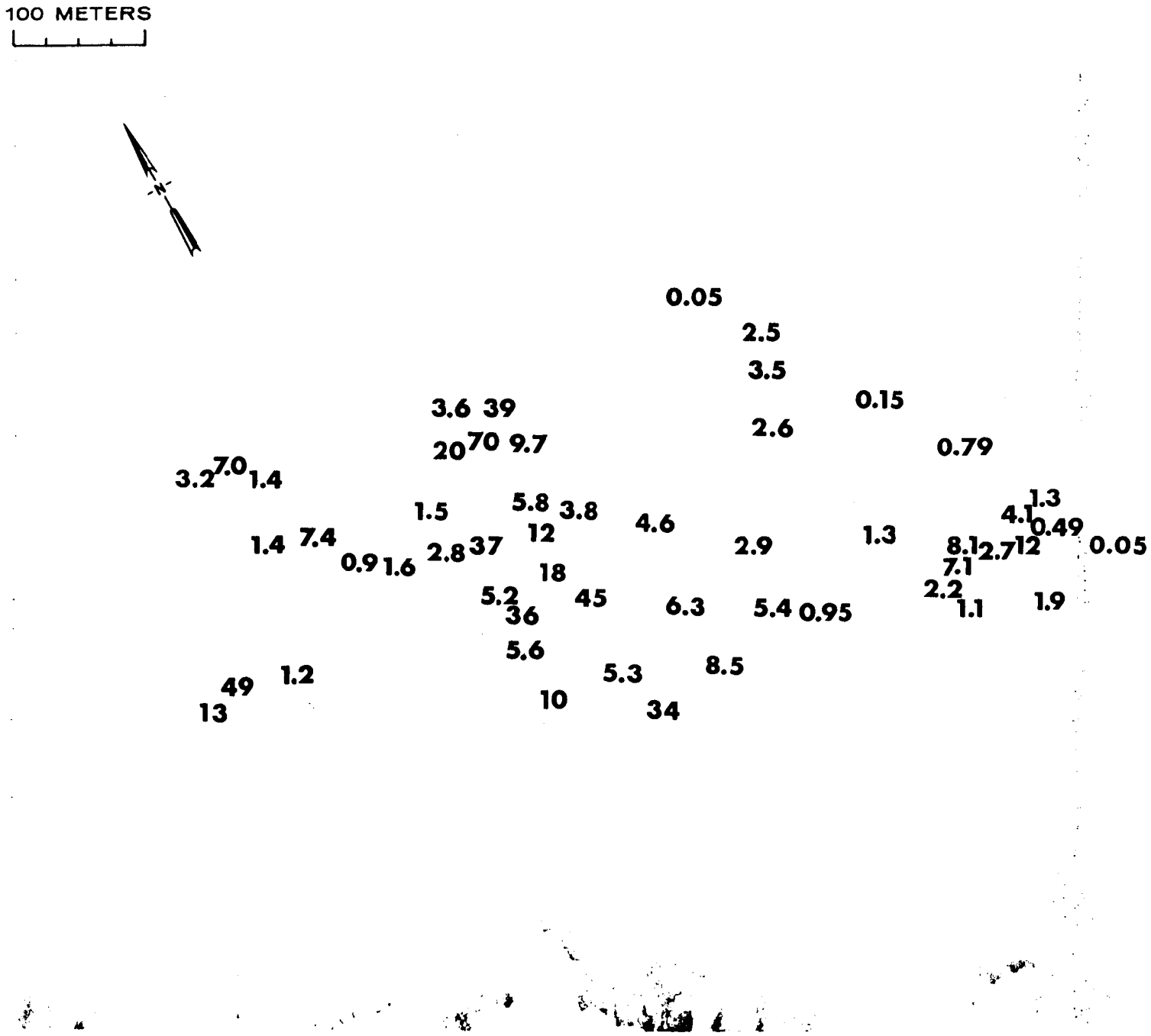

Fig. B.15.1.n. The average ^{60}Co activities (pCi/gm) in soil samples collected to a depth of 15 cm.

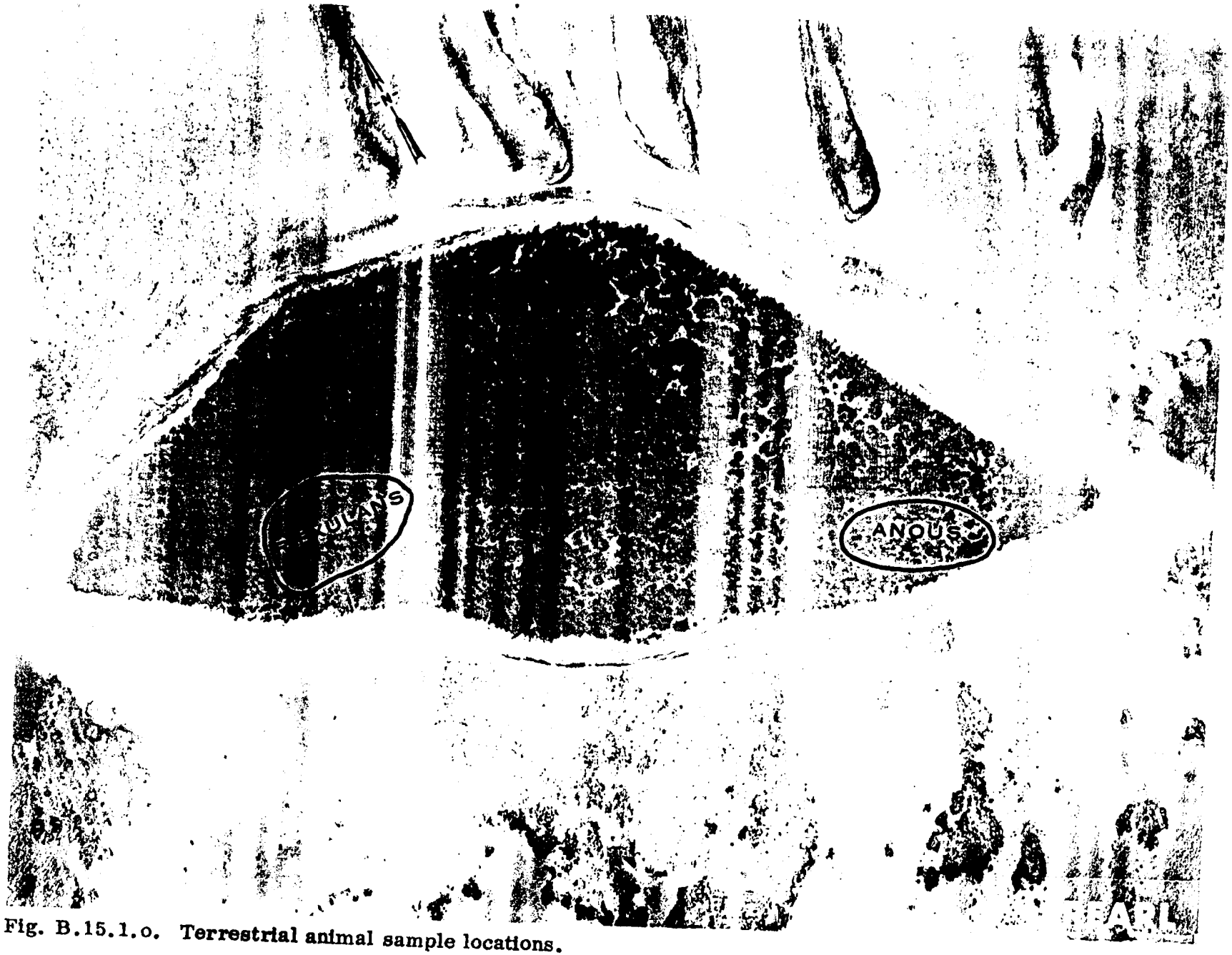

Fig. B.15.1.o. Terrestrial animal sample locations.

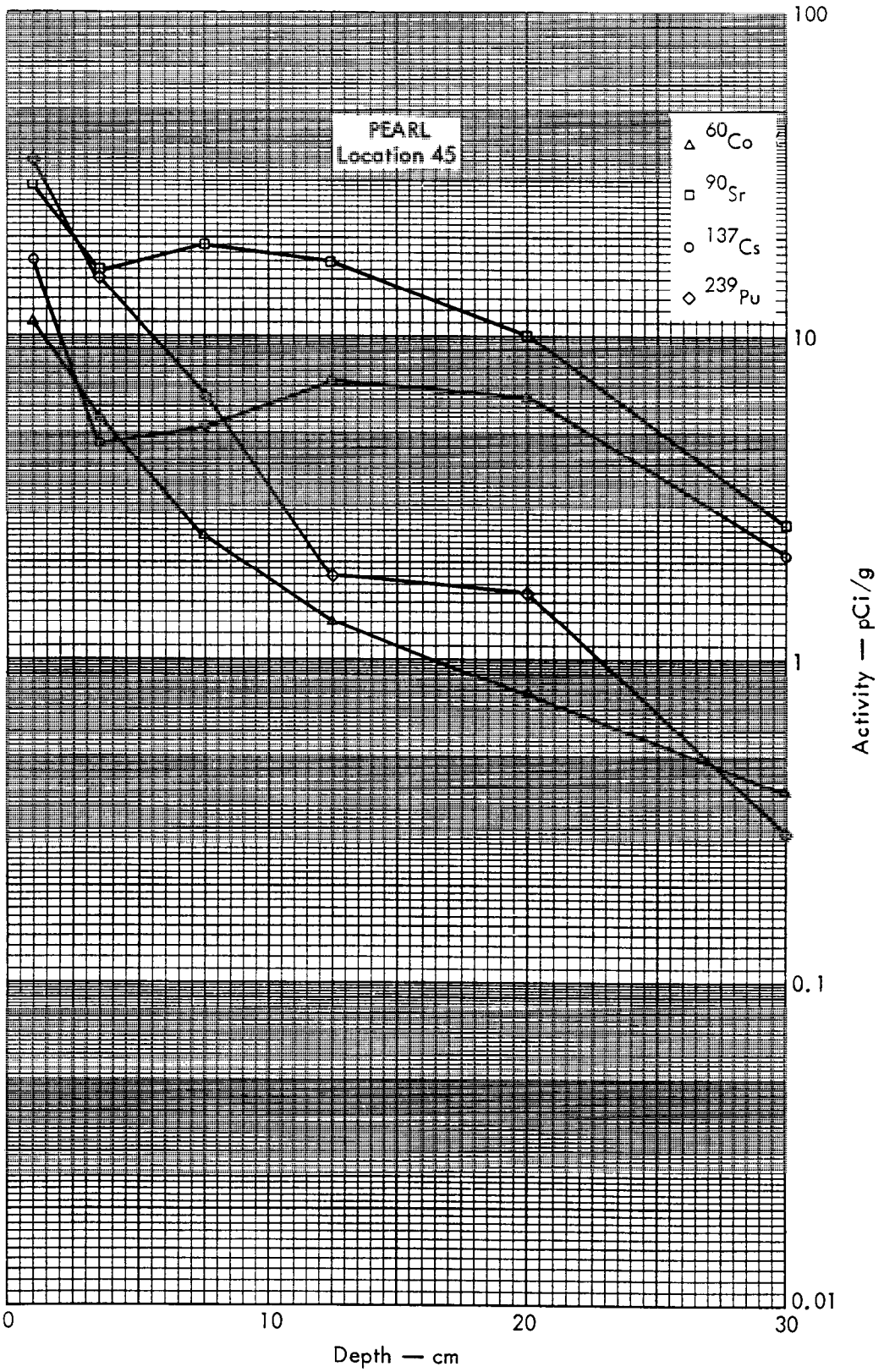

Fig. B. 15.2a. Activities of selected radionuclides as a function of soil depth.

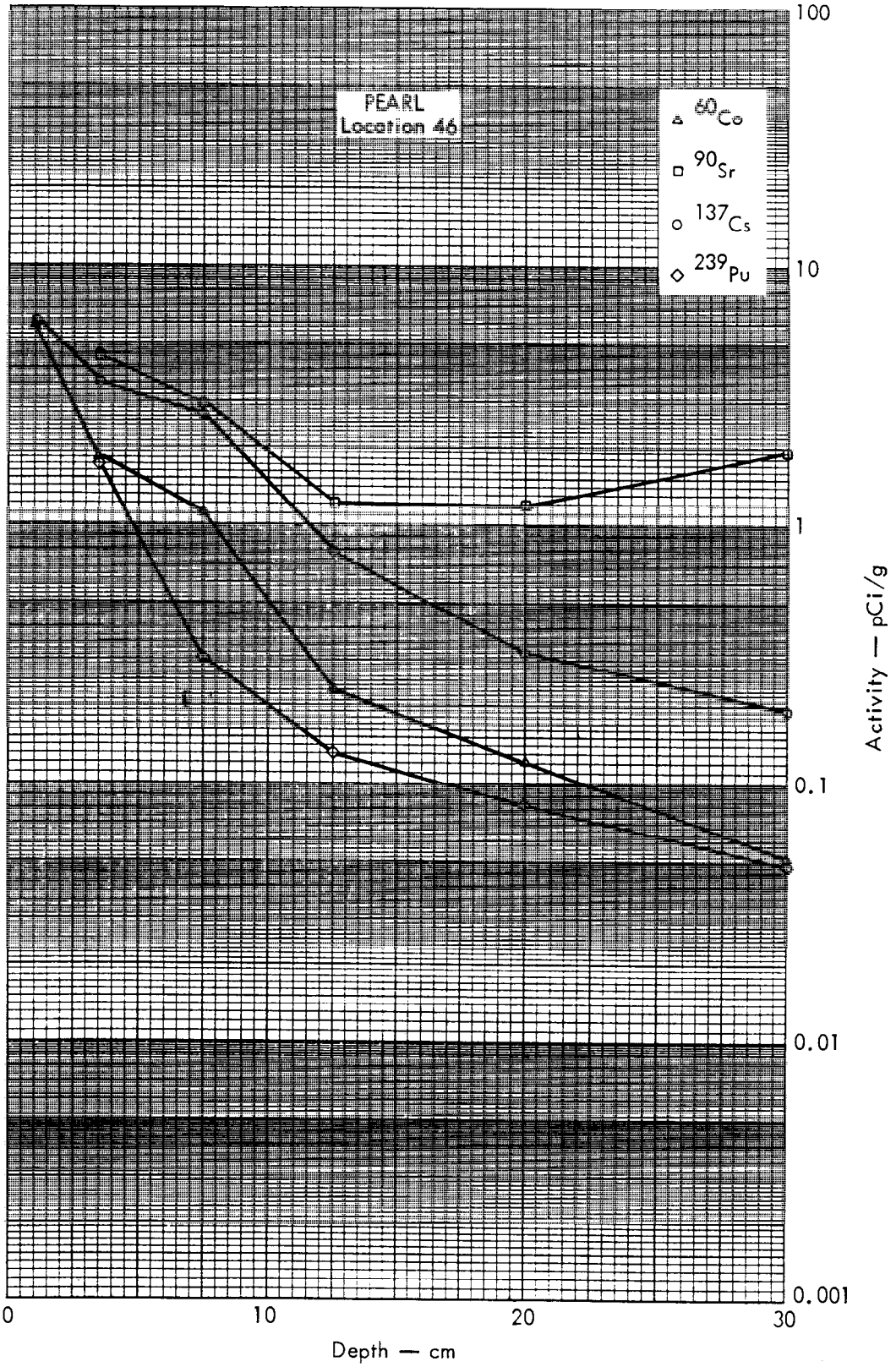

Fig. B. 15. 2b. Activities of selected radionuclides as a function of soil depth.

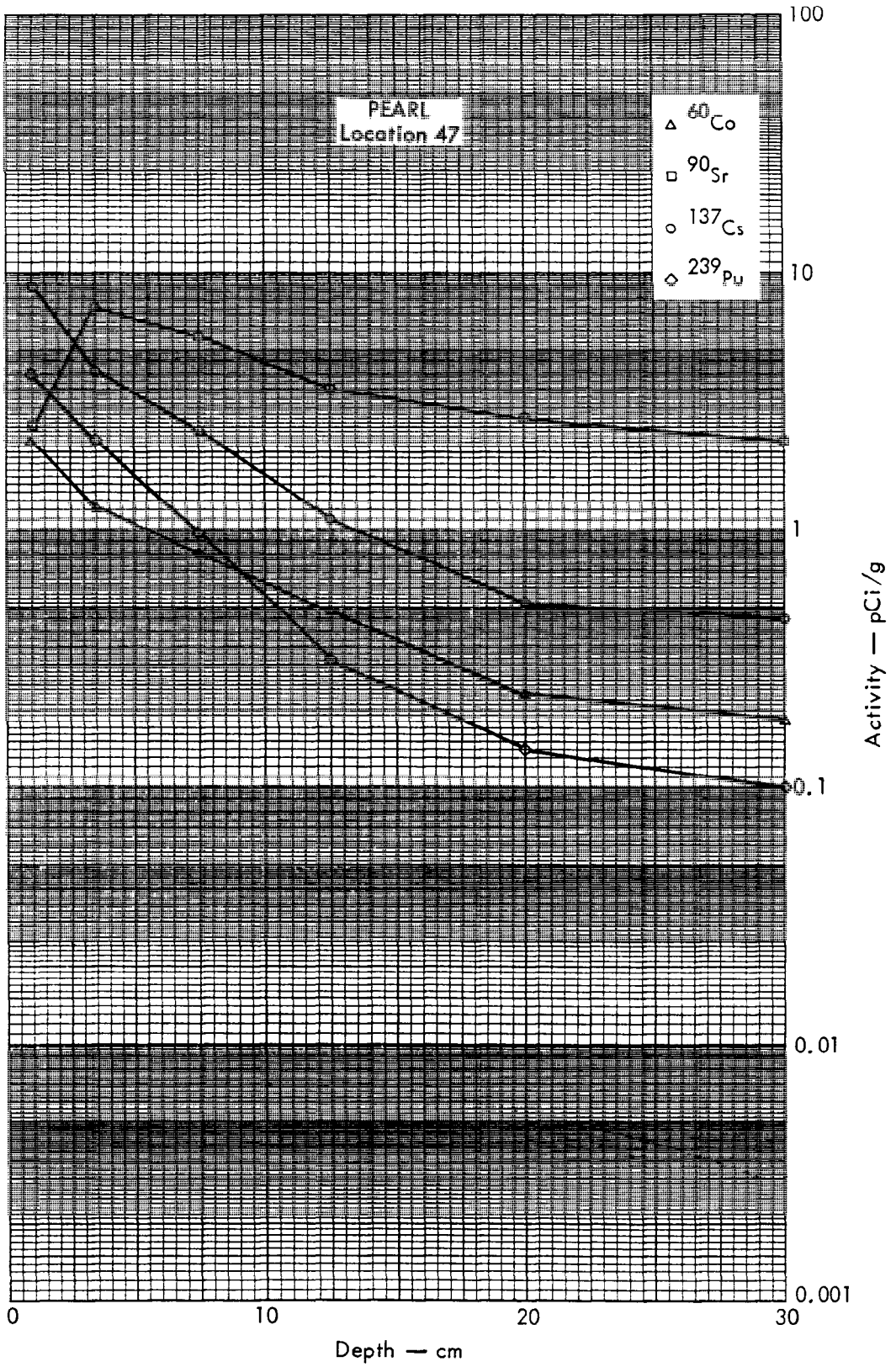

Fig. B. 15. 2c. Activities of selected radionuclides as a function of soil depth.

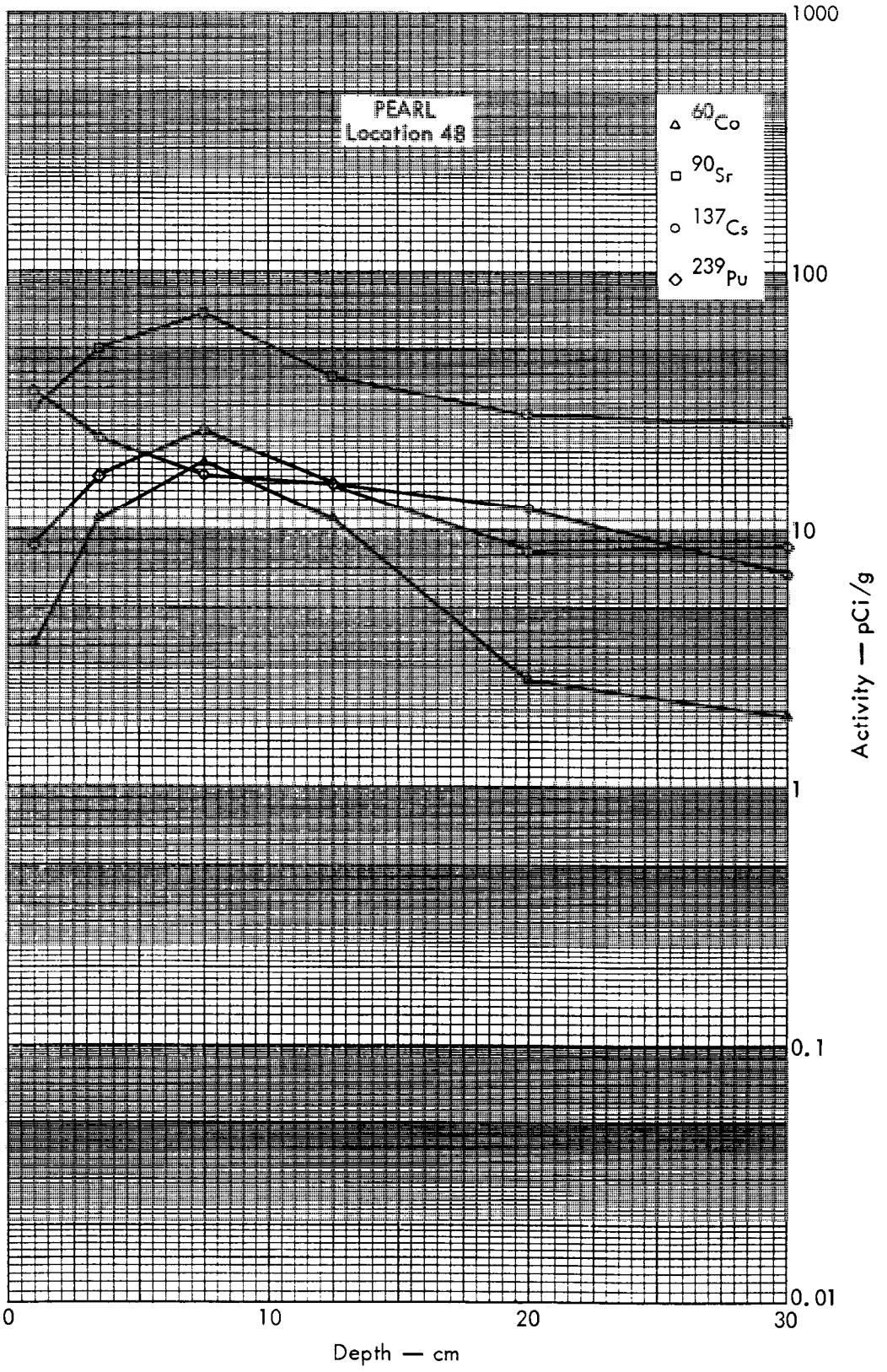

Fig. B. 15.2d. Activities of selected radionuclides as a function of soil depth.

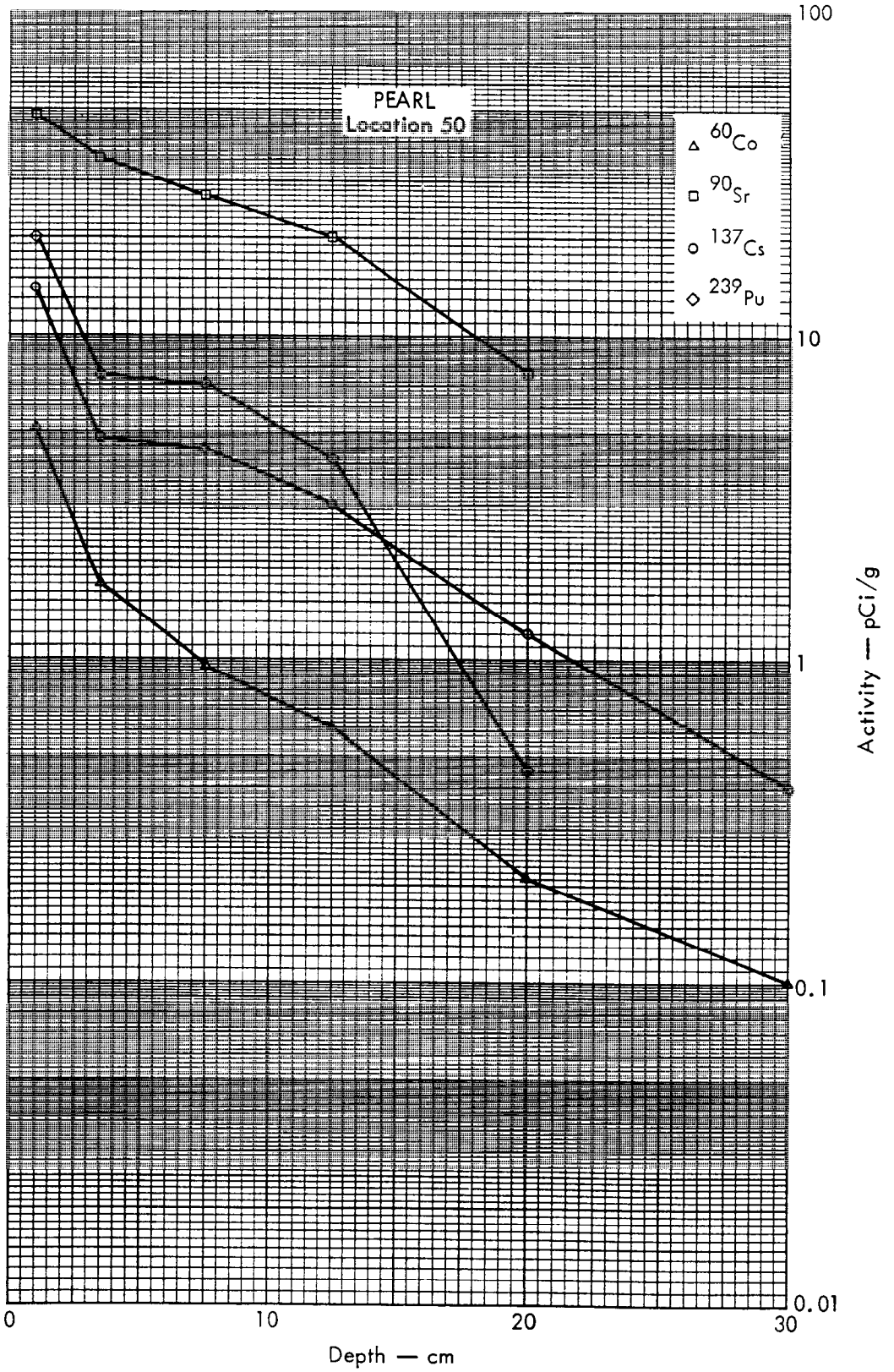

Fig. B. 15. 2e. Activities of selected radionuclides as a function of soil depth.

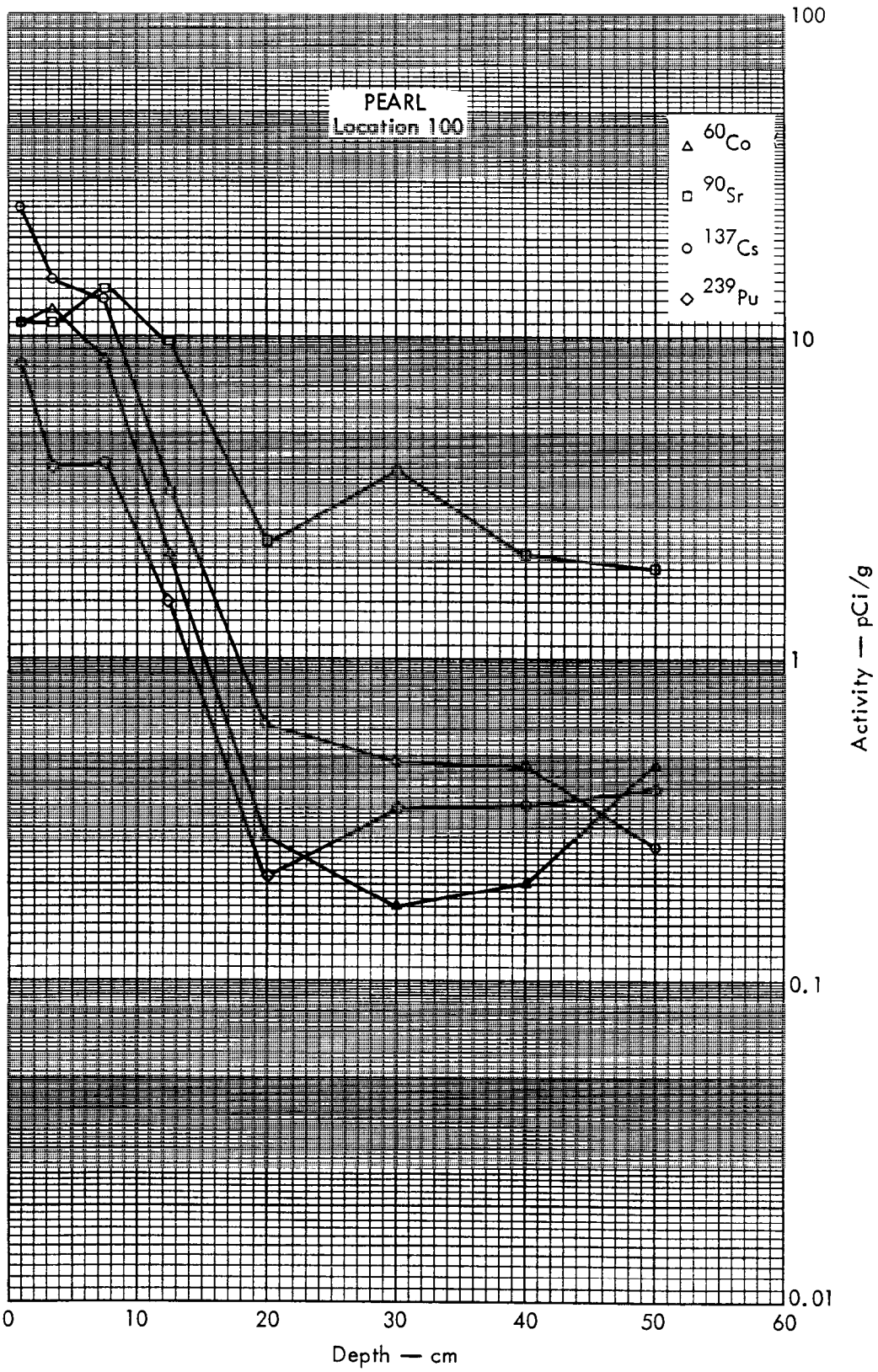

Fig. B. 15. 2f. Activities of selected radionuclides as a function of soil depth.

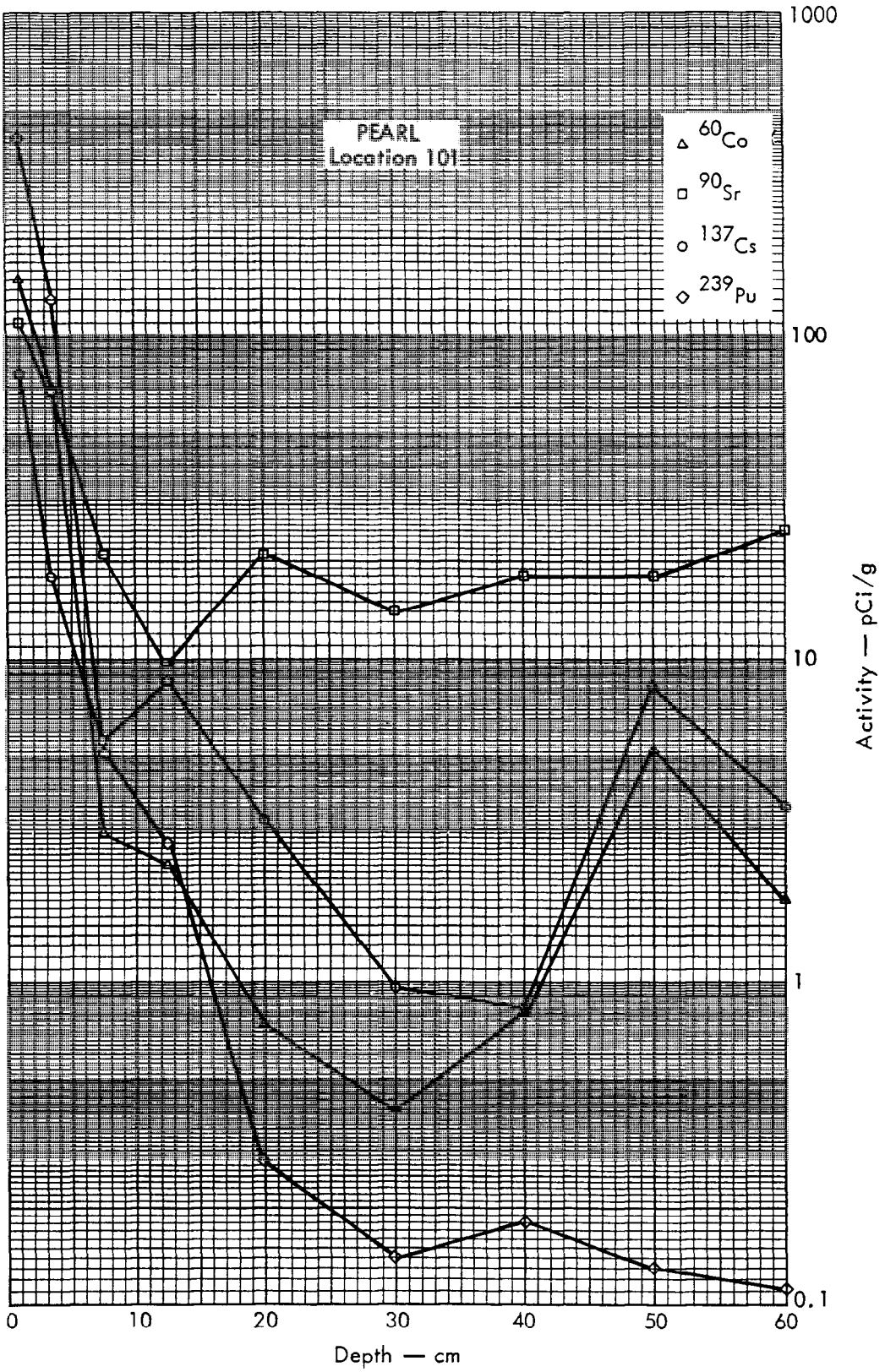

Fig. B.15.2g. Activities of selected radionuclides as a function of soil depth.

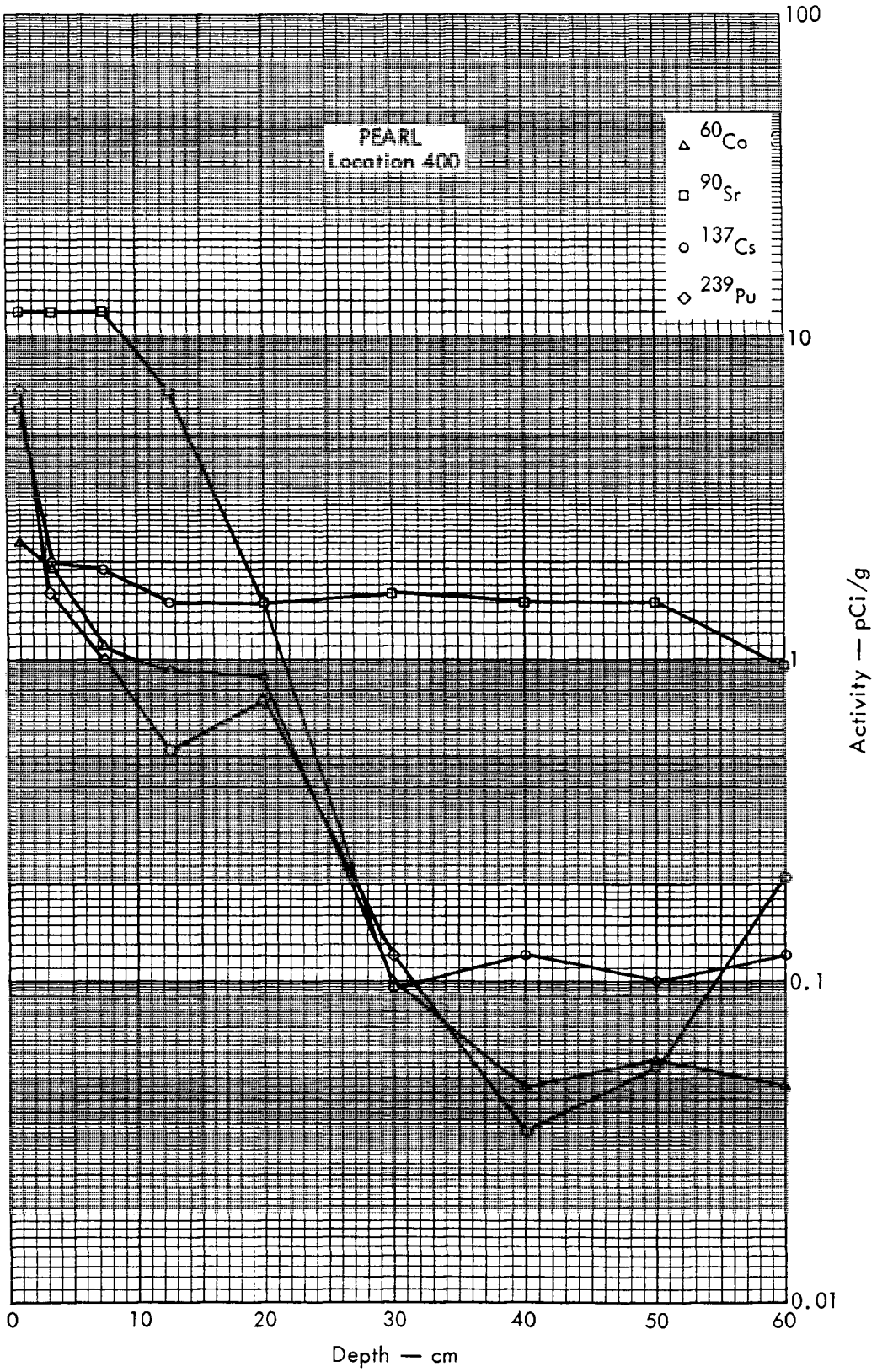

Fig. B. 15.2h. Activities of selected radionuclides as a function of soil depth.

Fig. B.16.1.a.

Fig. B.16.1.b. **Gross count isoexposure contours.** (Refer to alphabetic symbol key in this appendix.)

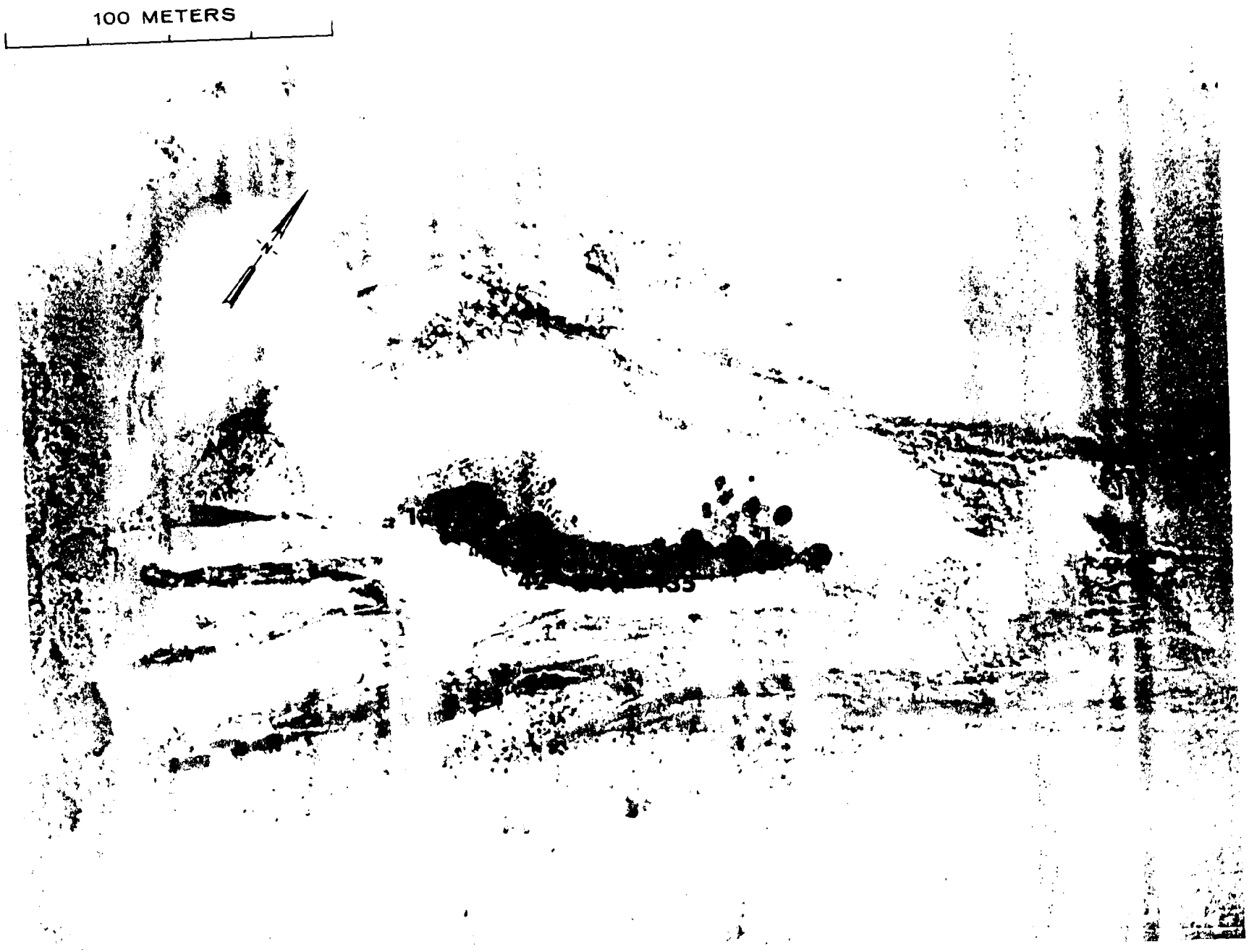

Fig. B.16.1.d. The gamma background exposure rate (μR/hr) at 1 m above the ground, measured with a portable NaI scintillation counter.

Fig. B.16.1.f. Soil-sample locations.

Fig. B.16.1.g. Vegetation sample locations.

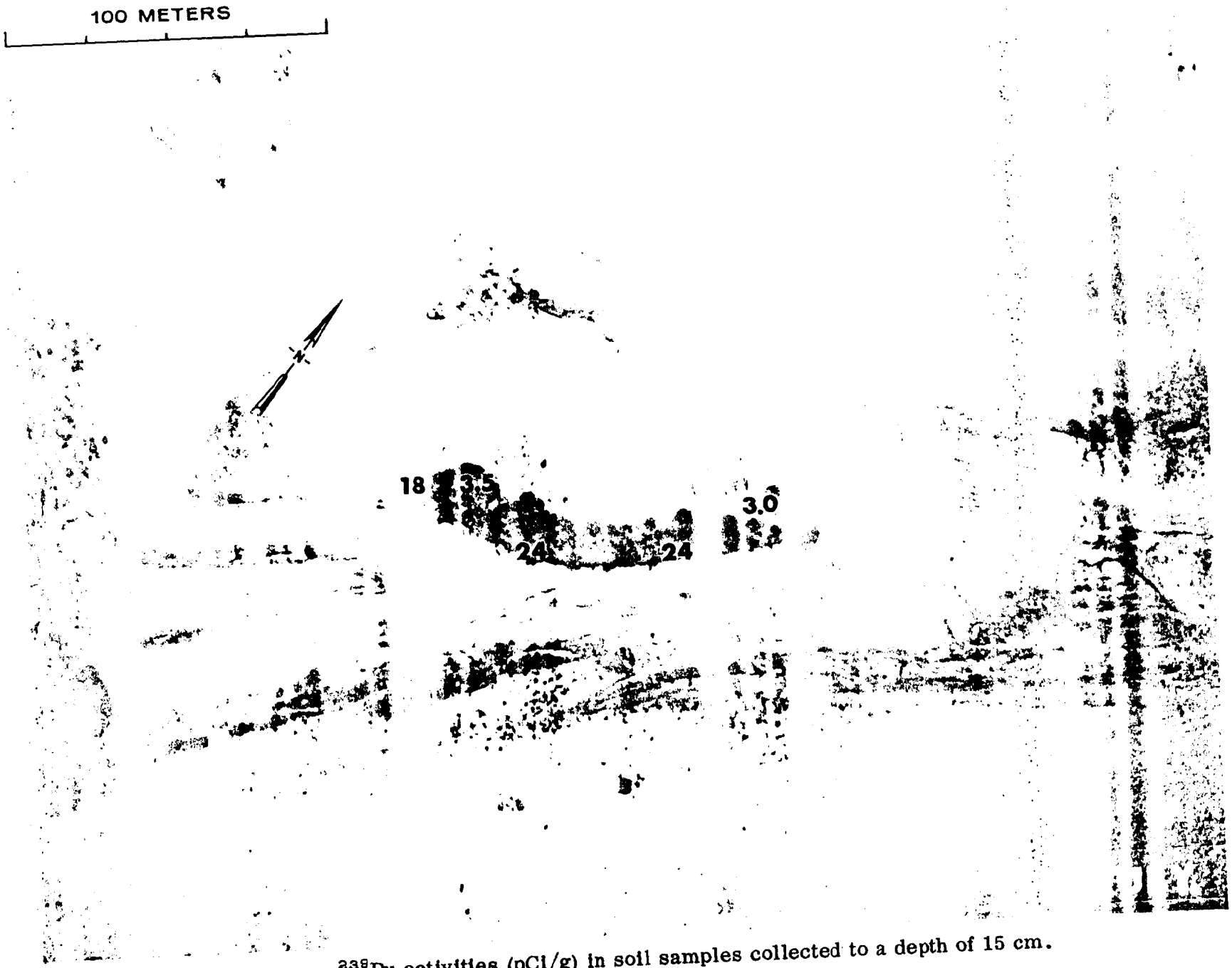

Fig. B.16.1.i. The average ^{239}Pu activities (pCi/g) in soil samples collected to a depth of 15 cm.

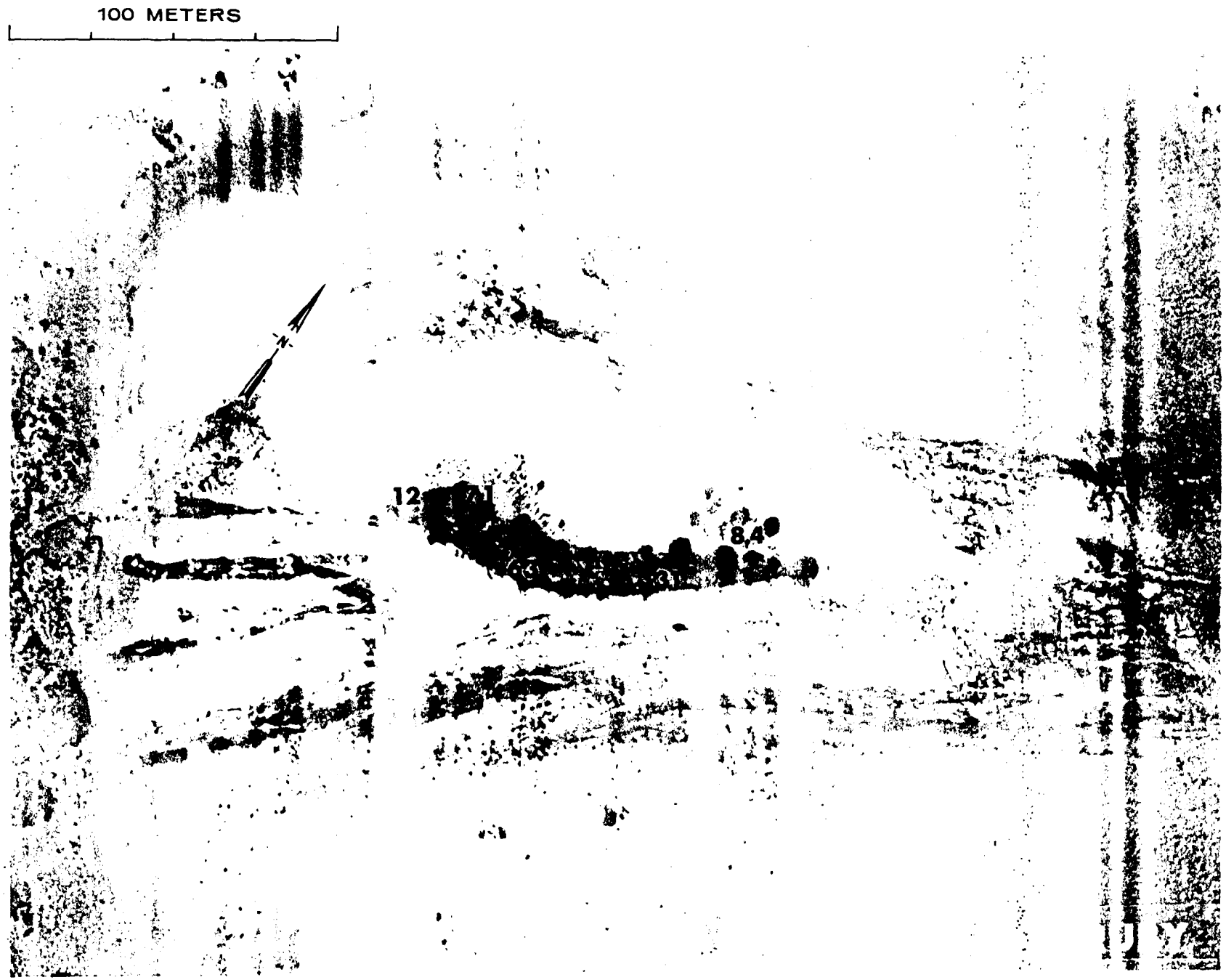

Fig. B.16.1.j. The average ^{90}Sr activities (pCi/g) in soil samples collected to a depth of 15 cm.

Fig. B.16.1.k. ^{137}Cs isoexposure and isoconcentration contours. (Refer to alphabetic symbol key in this appendix.)

Fig. B.16.1.1. The average ^{137}Cs activities (pCi/g) in soil samples collected to a depth of 15 cm.

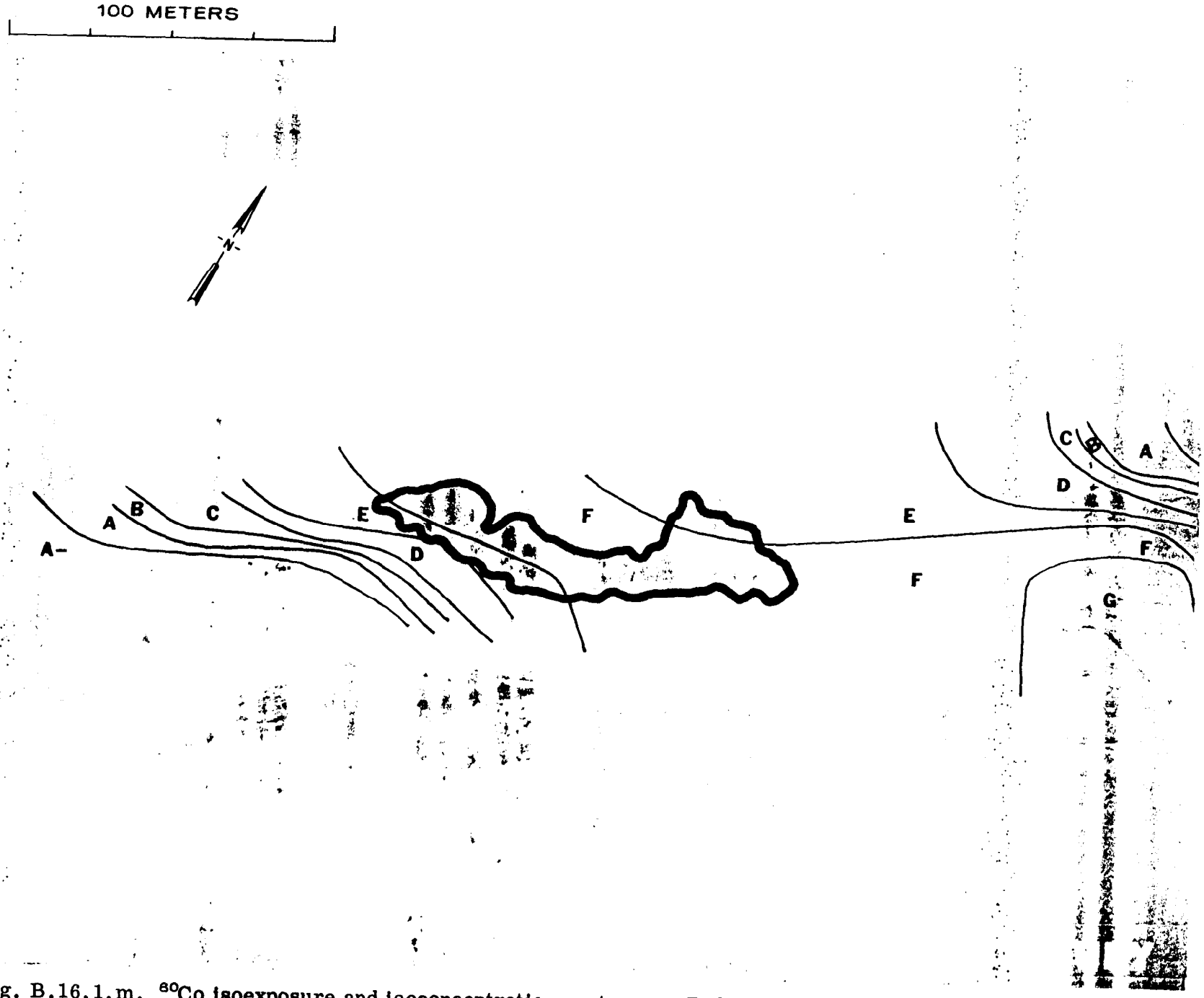

Fig. B.16.1.m. ^{60}Co isoexposure and isoconcentration contours. (Refer to alphabetic symbol key in this appendix.)

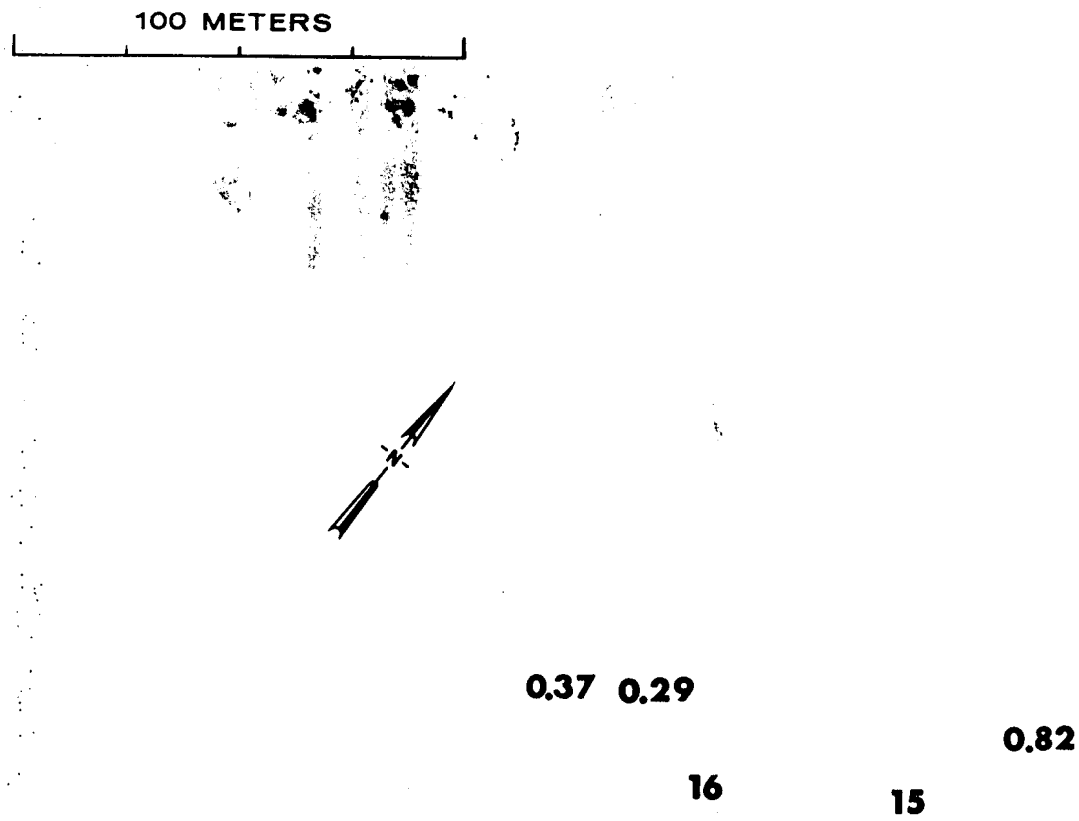

Fig. B.16.1.n. The average ^{60}Co activities (pCi/g) in soil samples collected to a depth of 15 cm.

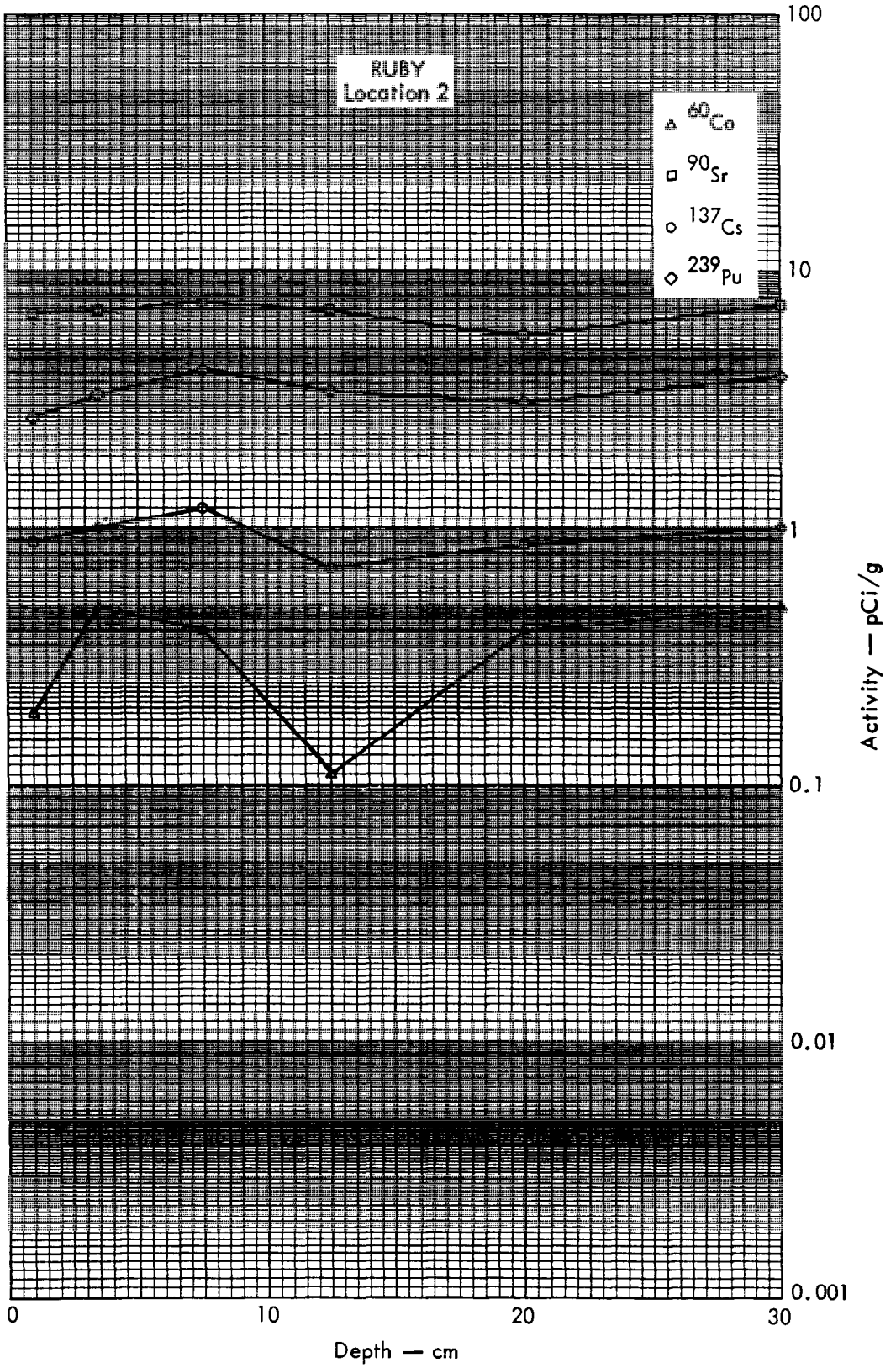

Fig. B.16.2a. Activities of selected radionuclides as a function of soil depth.

Fig. B.17.1.a.

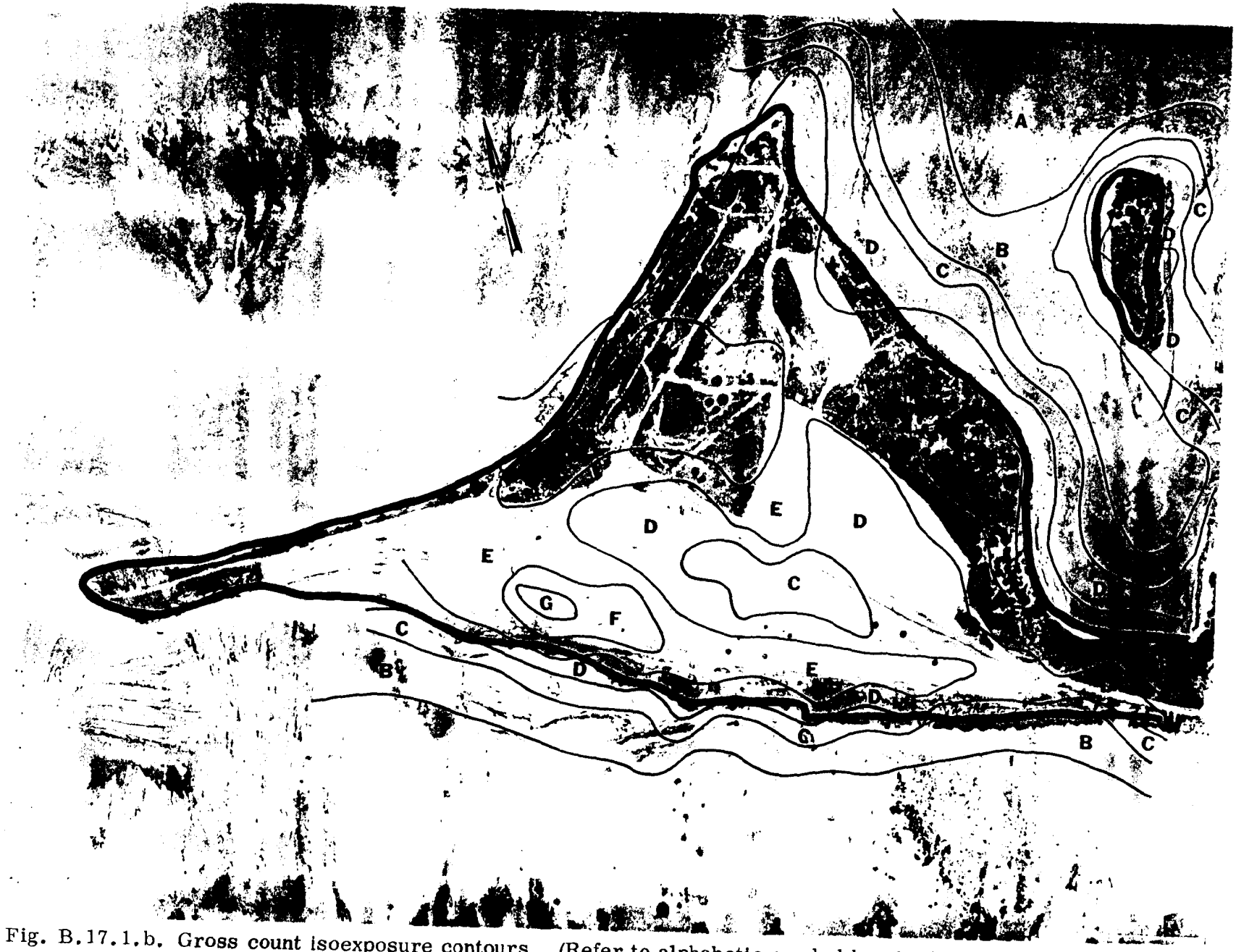

Fig. B.17.1.b. Gross count isoexposure contours. (Refer to alphabetic symbol key in this appendix.)

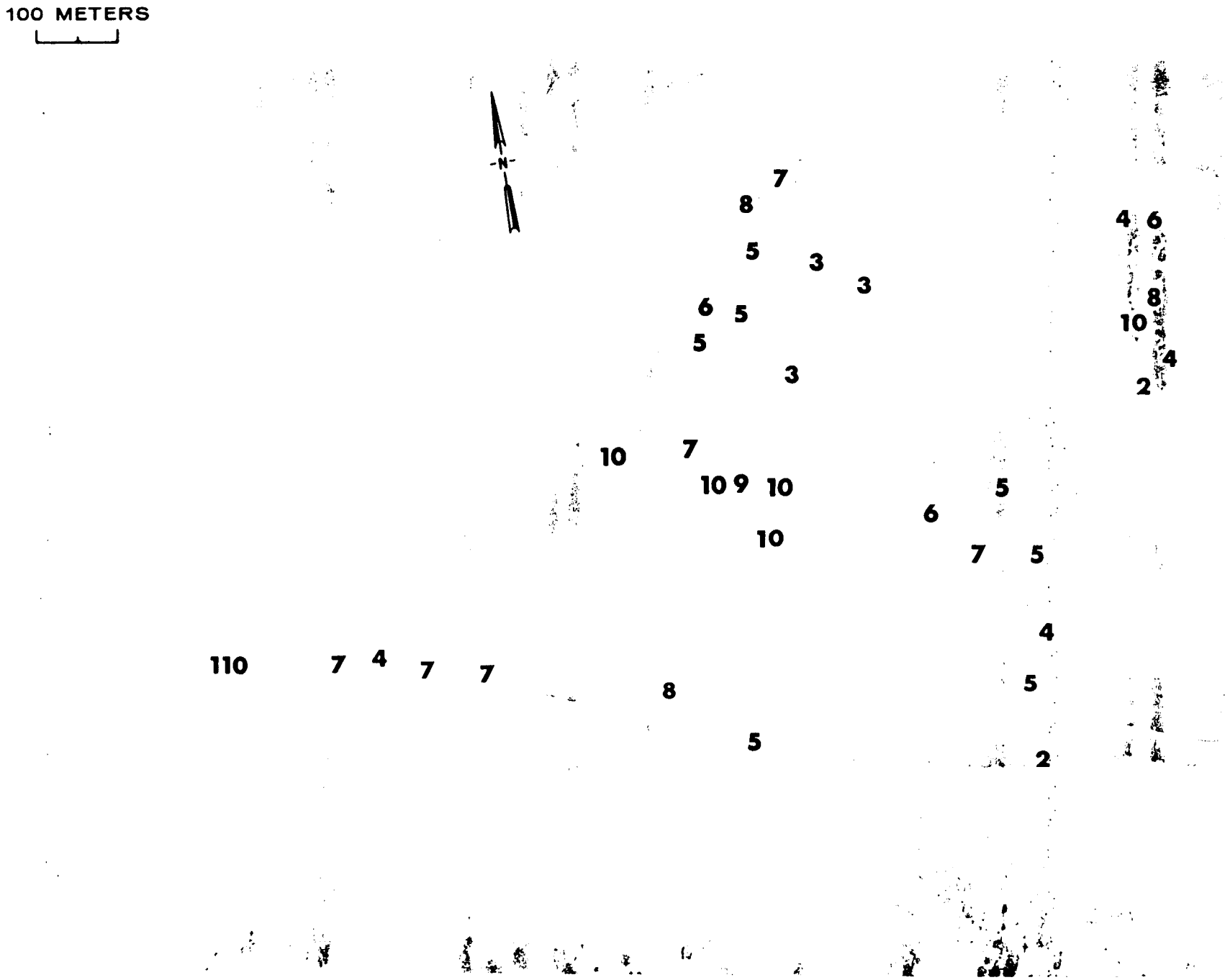

Fig. B.17.1.d. The gamma background exposure rate (μR/hr) at 1 m above the ground, measured with a portable NaI scintillation counter.

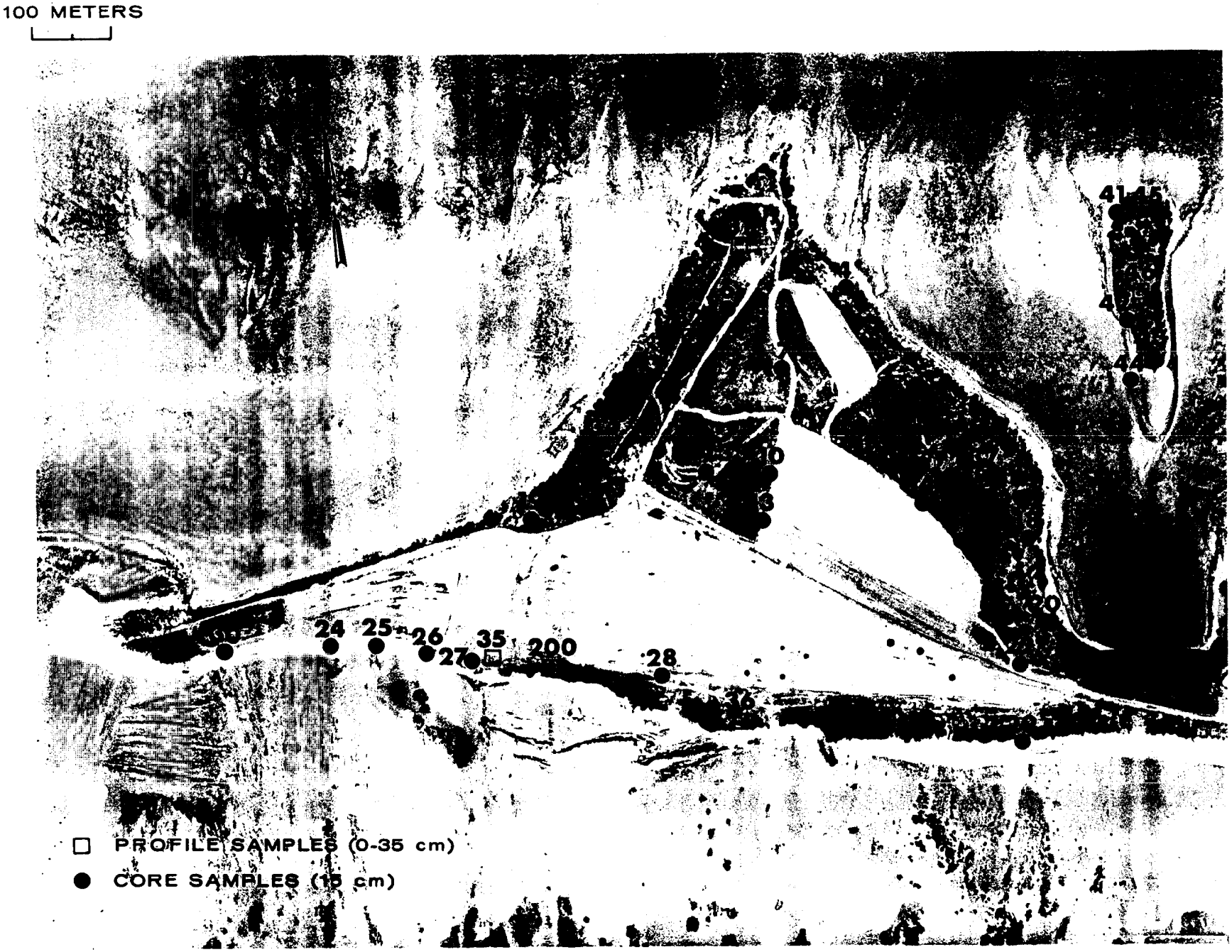

Fig. B.17.1.f. Soil-sample locations.

Fig. B.17.1.g. Vegetation sample locations.

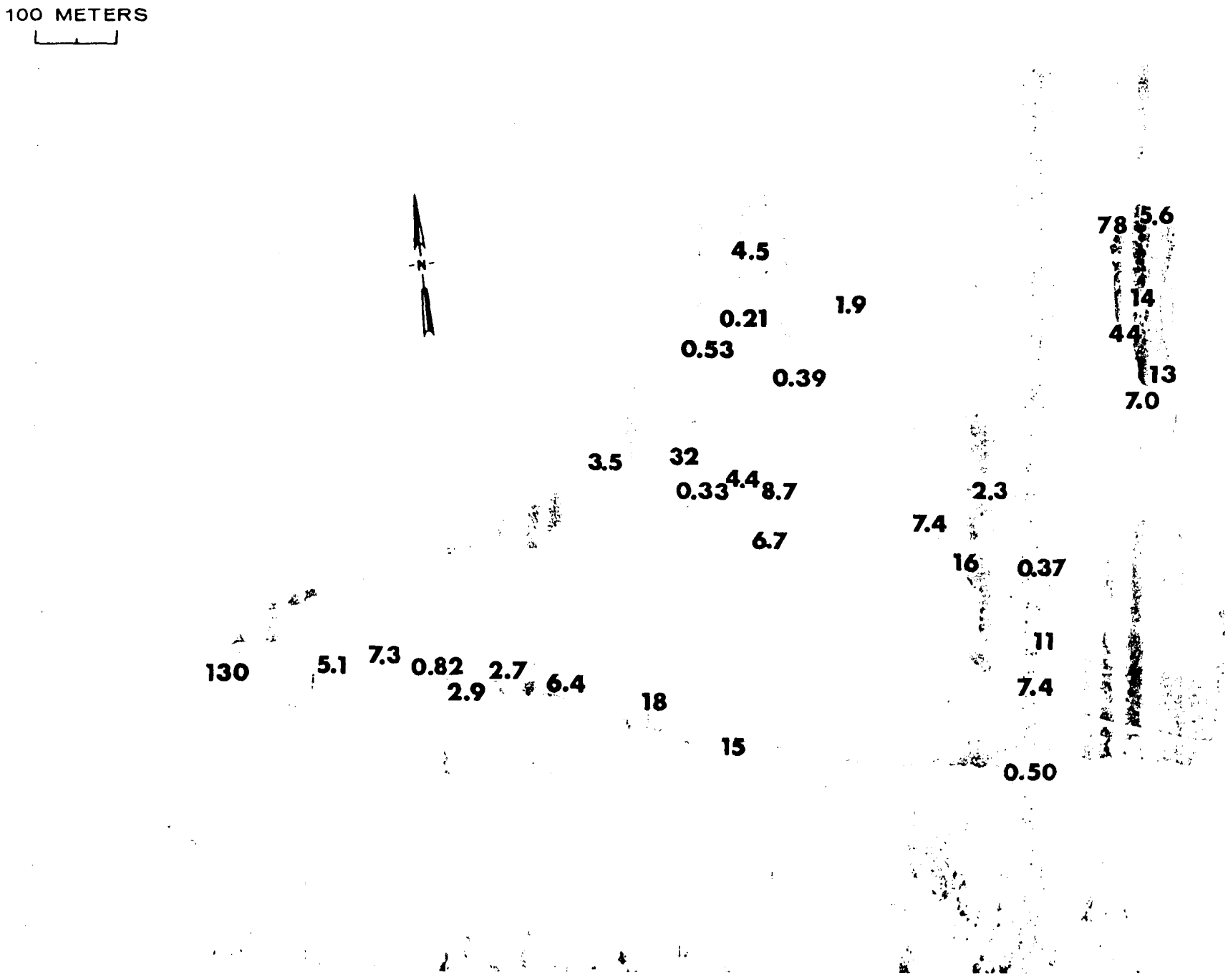

Fig. B.17.1.i. The average ^{239}Pu activities (pCi/gm) in soil samples collected to a depth of 15 cm.

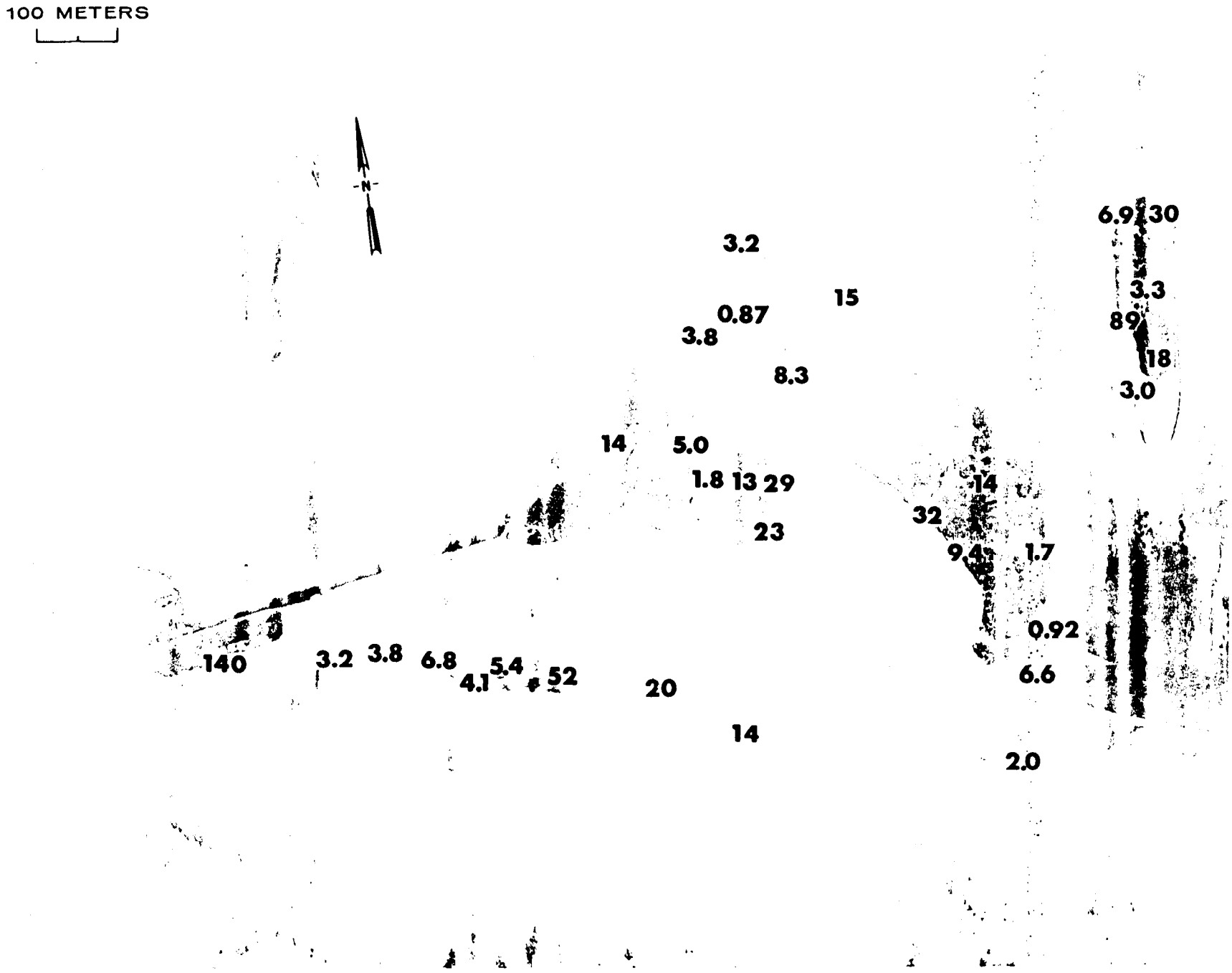

Fig. B.17.1.j. The average ^{90}Sr activities (pCi/gm) in soil samples collected to a depth of 15 cm.

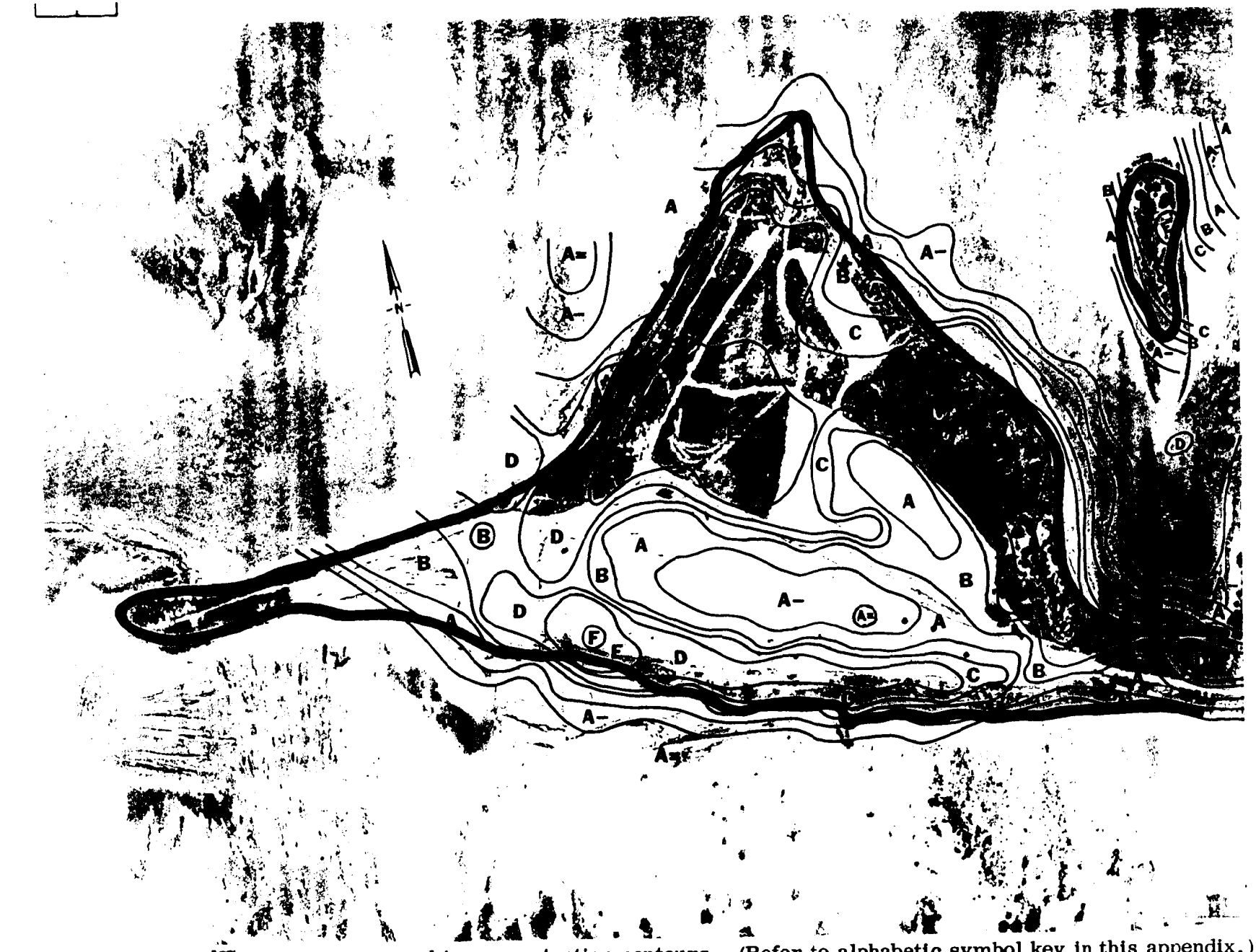

Fig. B.17.1.k. ^{137}Cs isoexposure and isoconcentration contours. (Refer to alphabetic symbol key in this appendix.)

Fig. B.17.1.1. The average ^{137}Cs activities (pCi/gm) in soil samples collected to a depth of 15 cm.

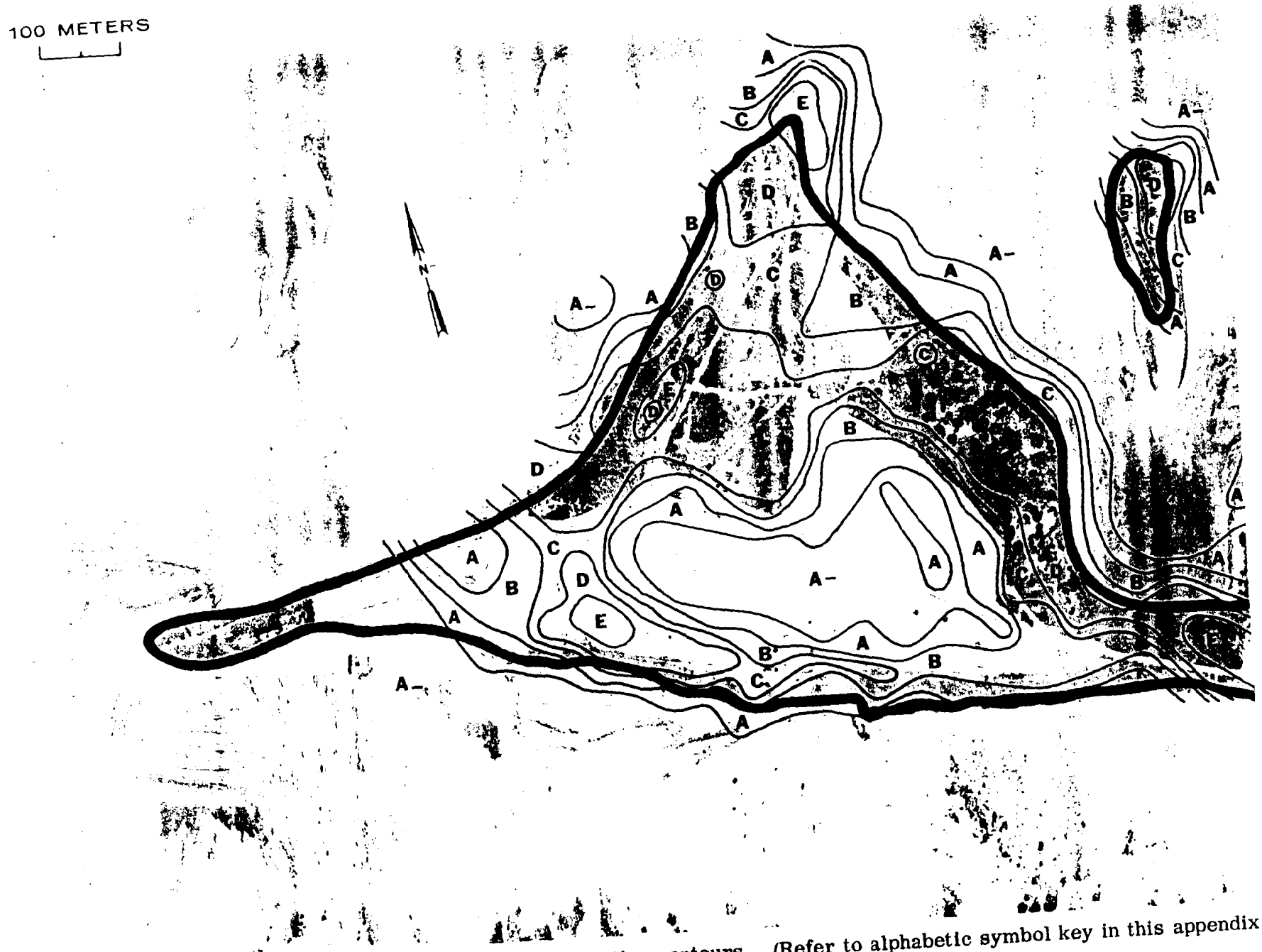

Fig. B.17.1.m. ^{60}Co isoexposure and isoconcentration contours. (Refer to alphabetic symbol key in this appendix.)

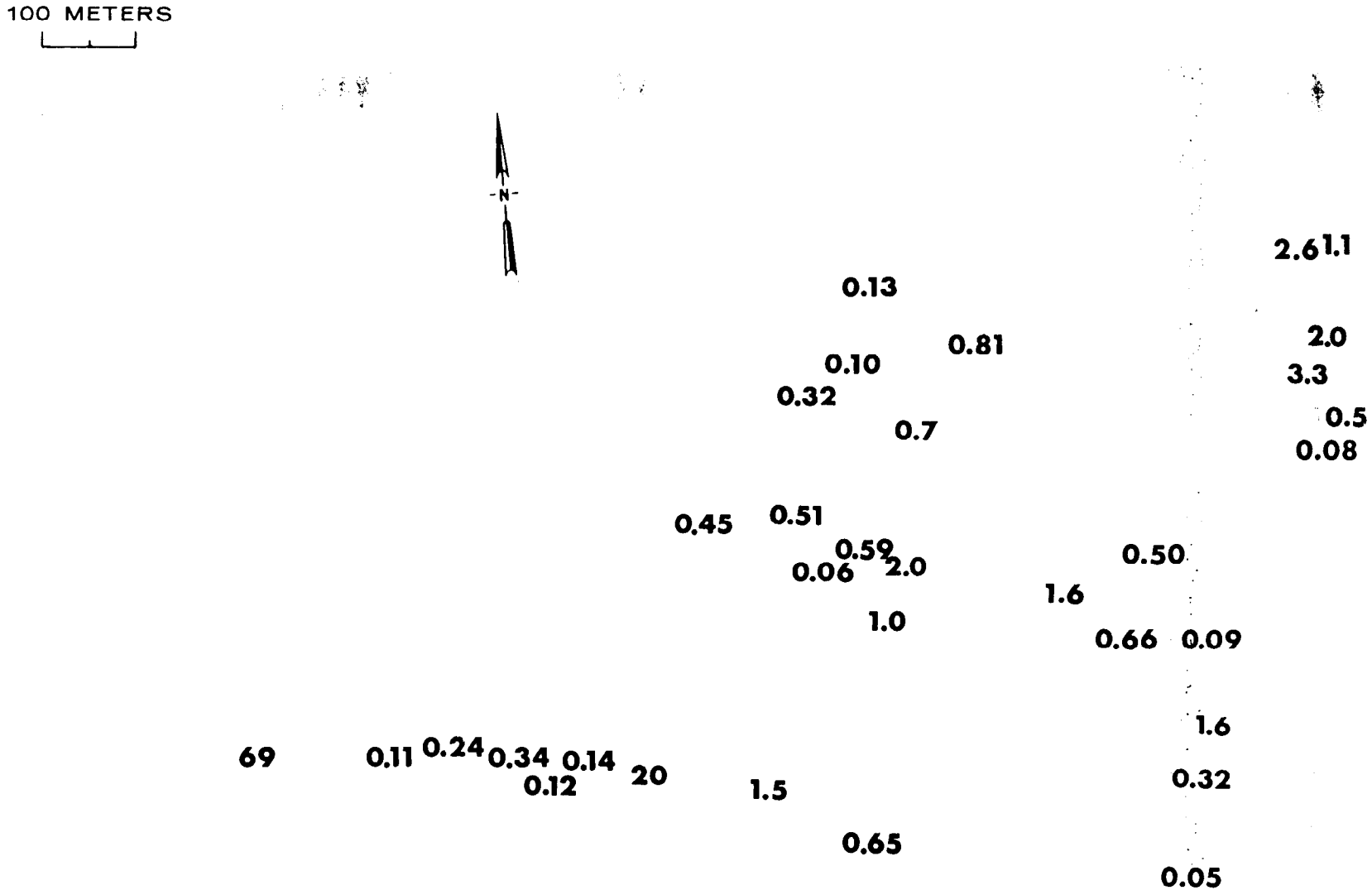

Fig. B.17.1.n. The average ^{60}Co activities (pCi/gm) in soil samples collected to a depth of 15 cm.

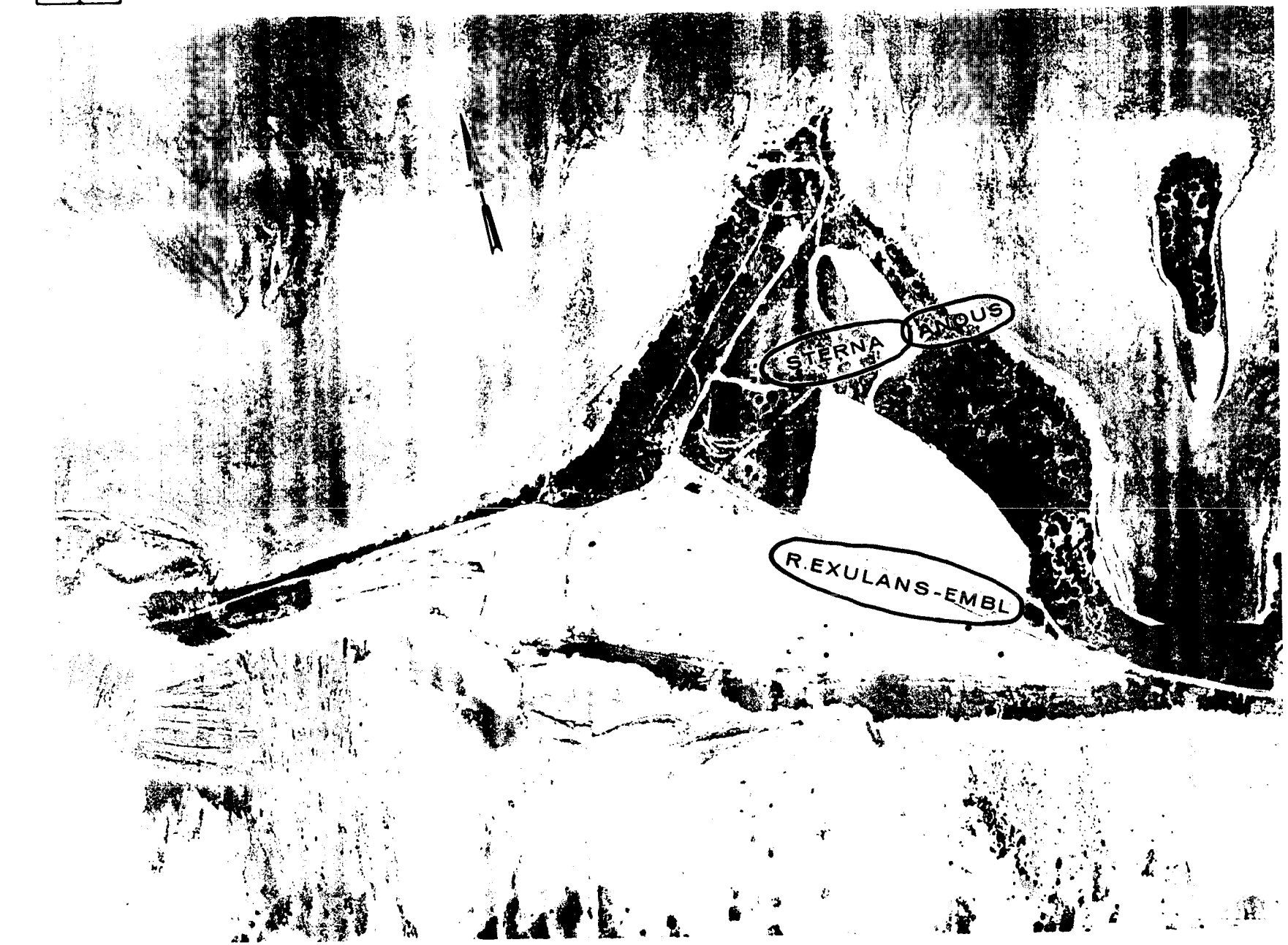

Fig. B.17.1.c. Terrestrial animal sample locations.

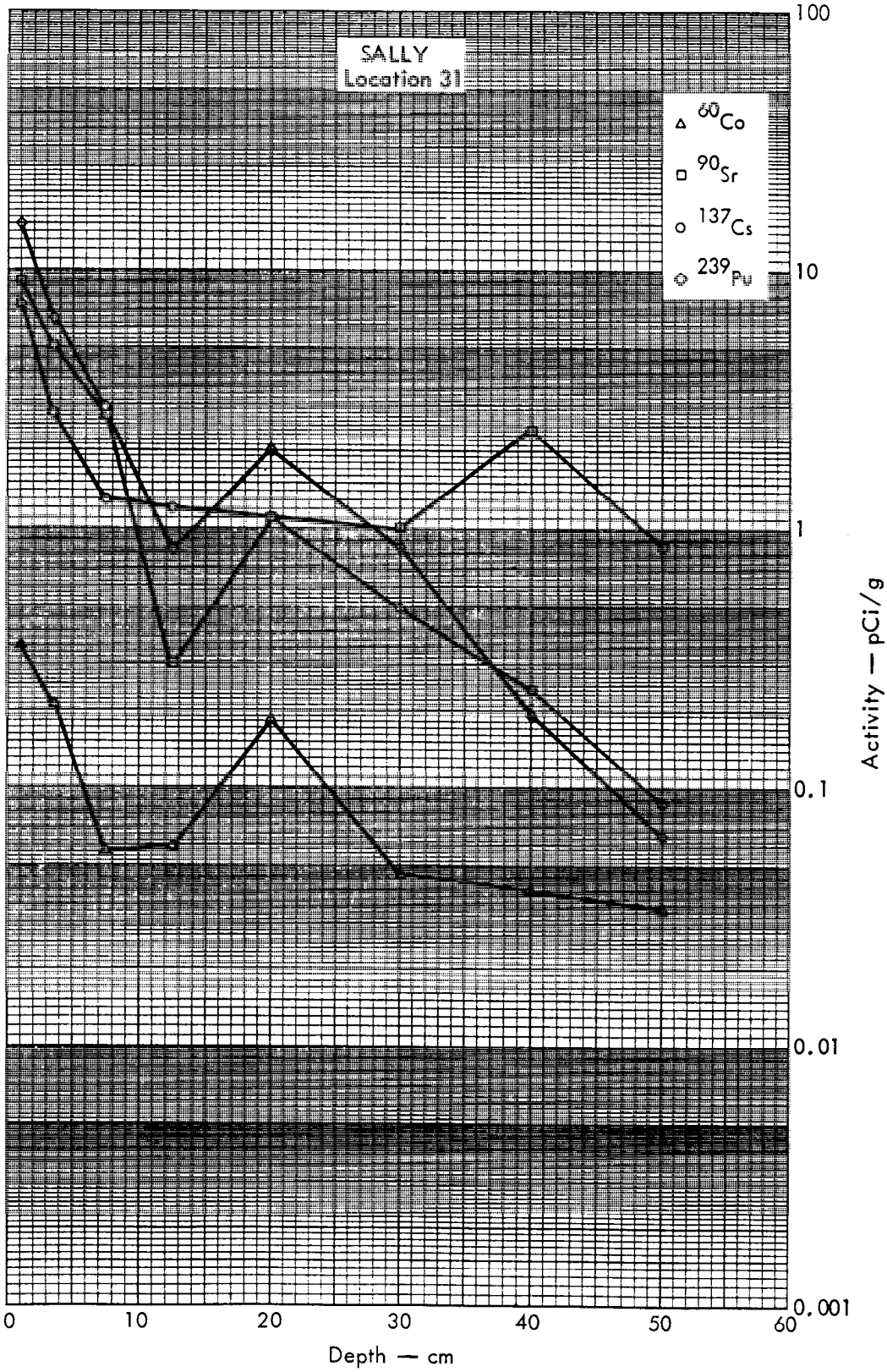

Fig. B. 17.2a. Activities of selected radionuclides as a function of soil depth.

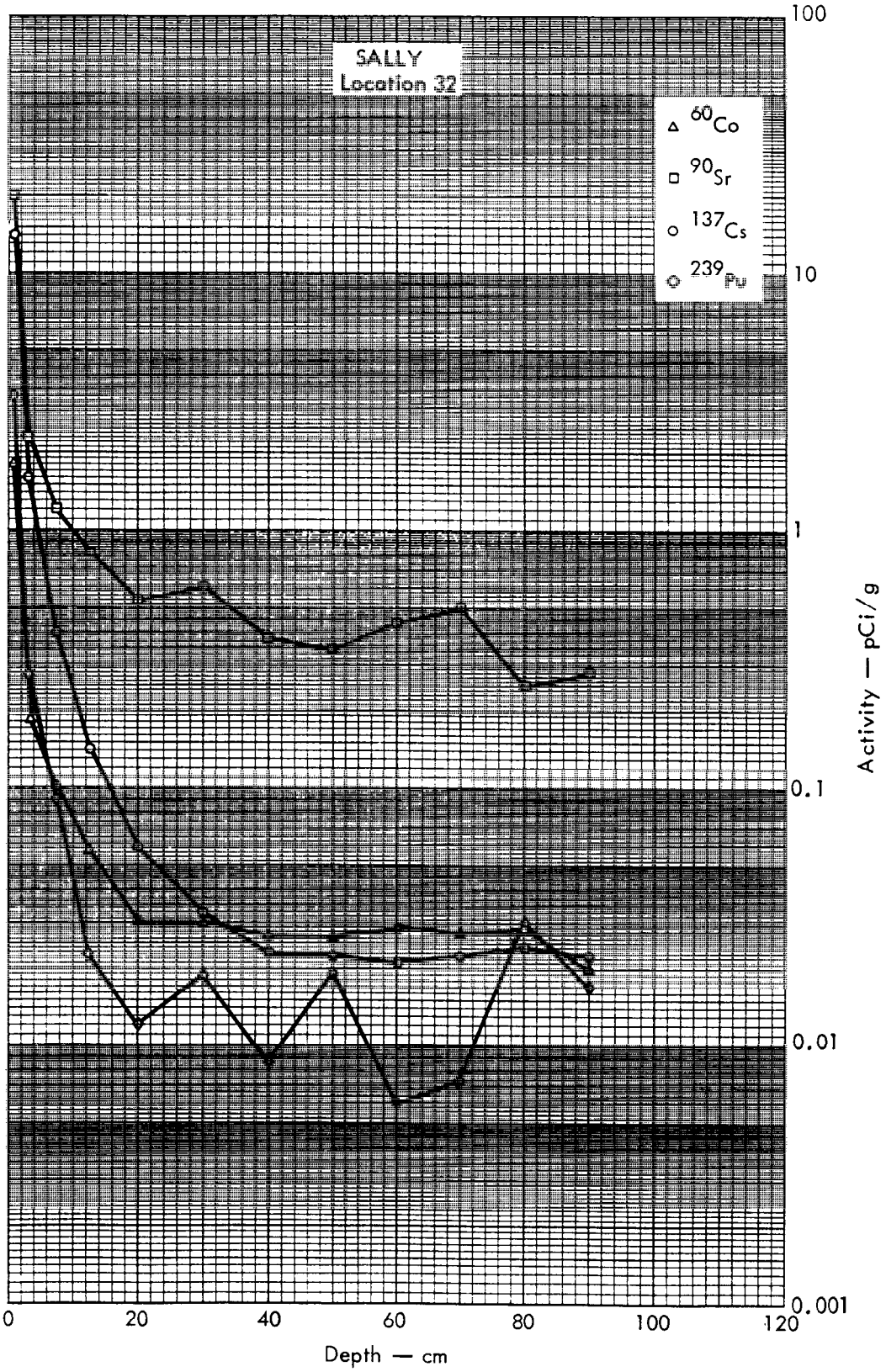

Fig. B.17.2b. Activities of selected radionuclides as a function of soil depth.

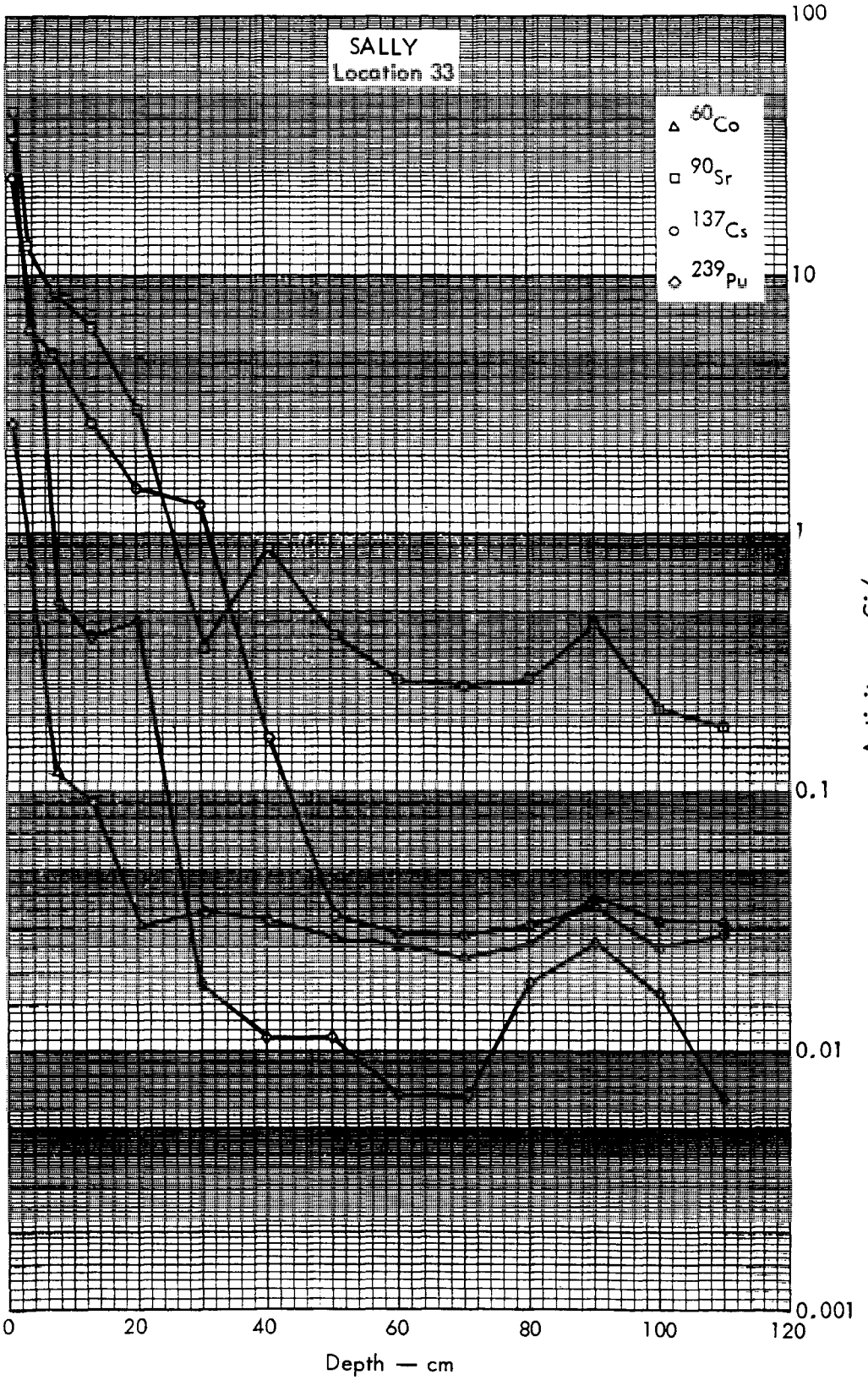

Fig. B. 17.2c. Activities of selected radionuclides as a function of soil depth.

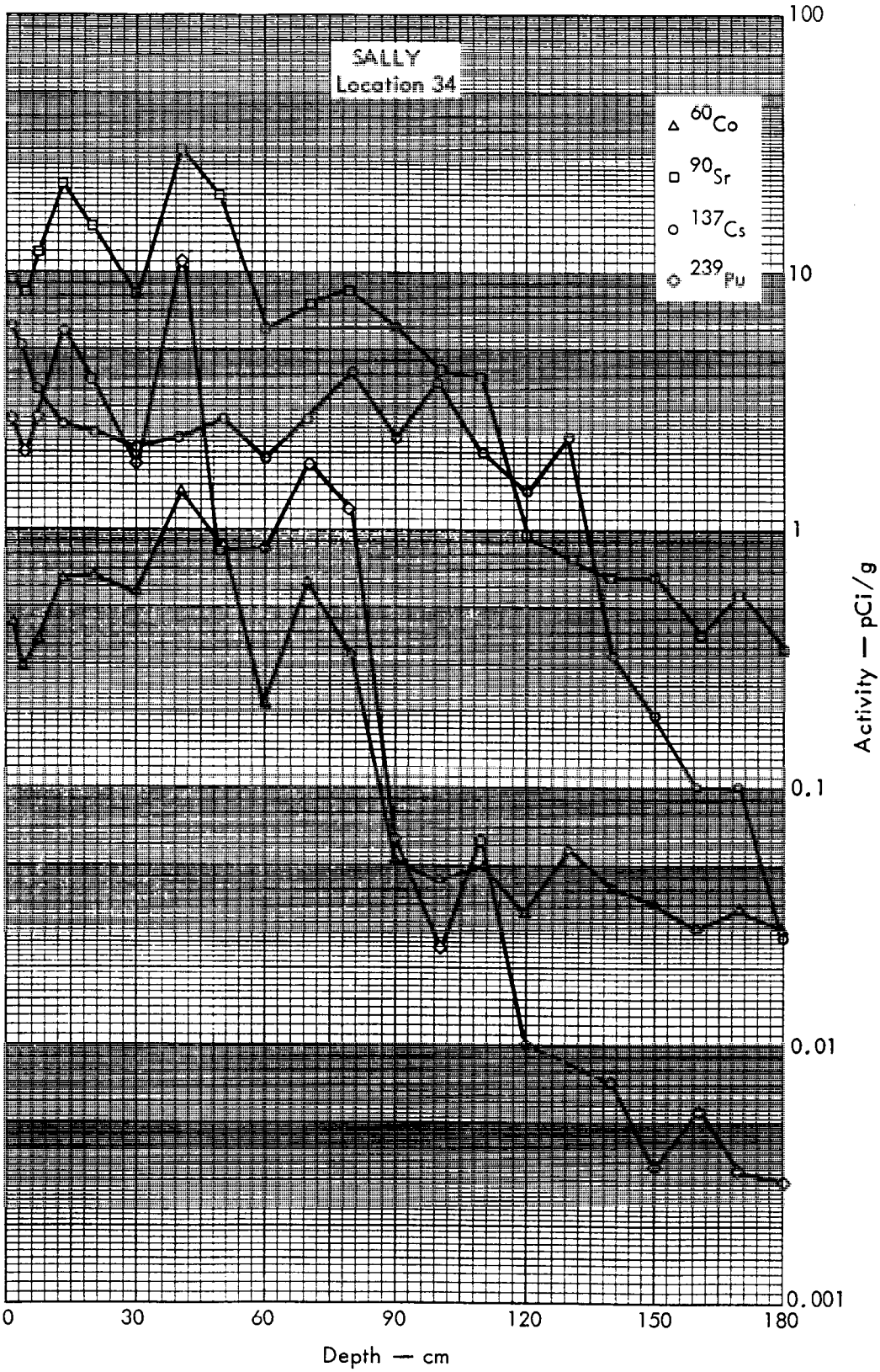

Fig. B. 17.2d. Activities of selected radionuclides as a function of soil depth.

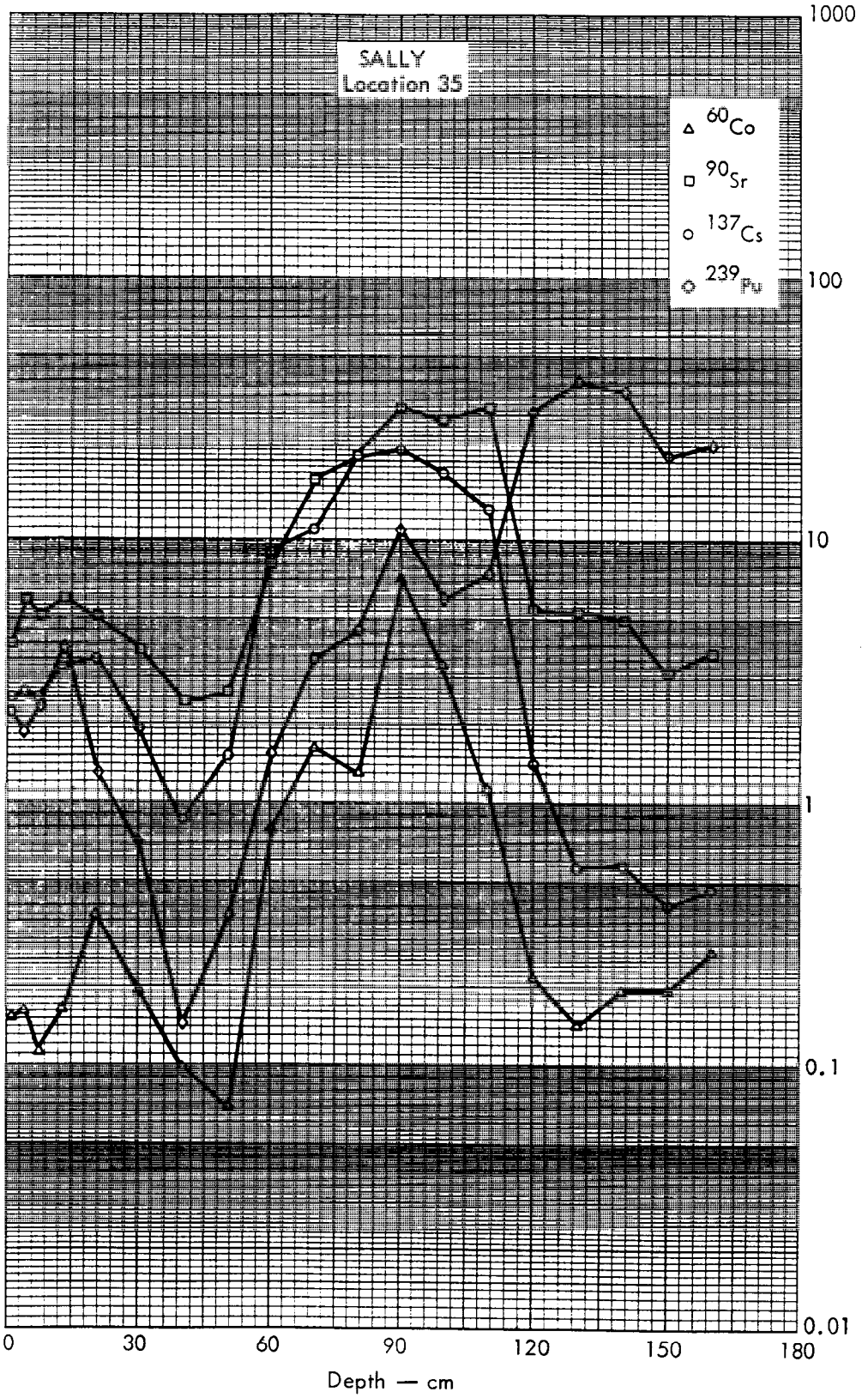

Fig. B.17.2e. Activities of selected radionuclides as a function of soil depth.

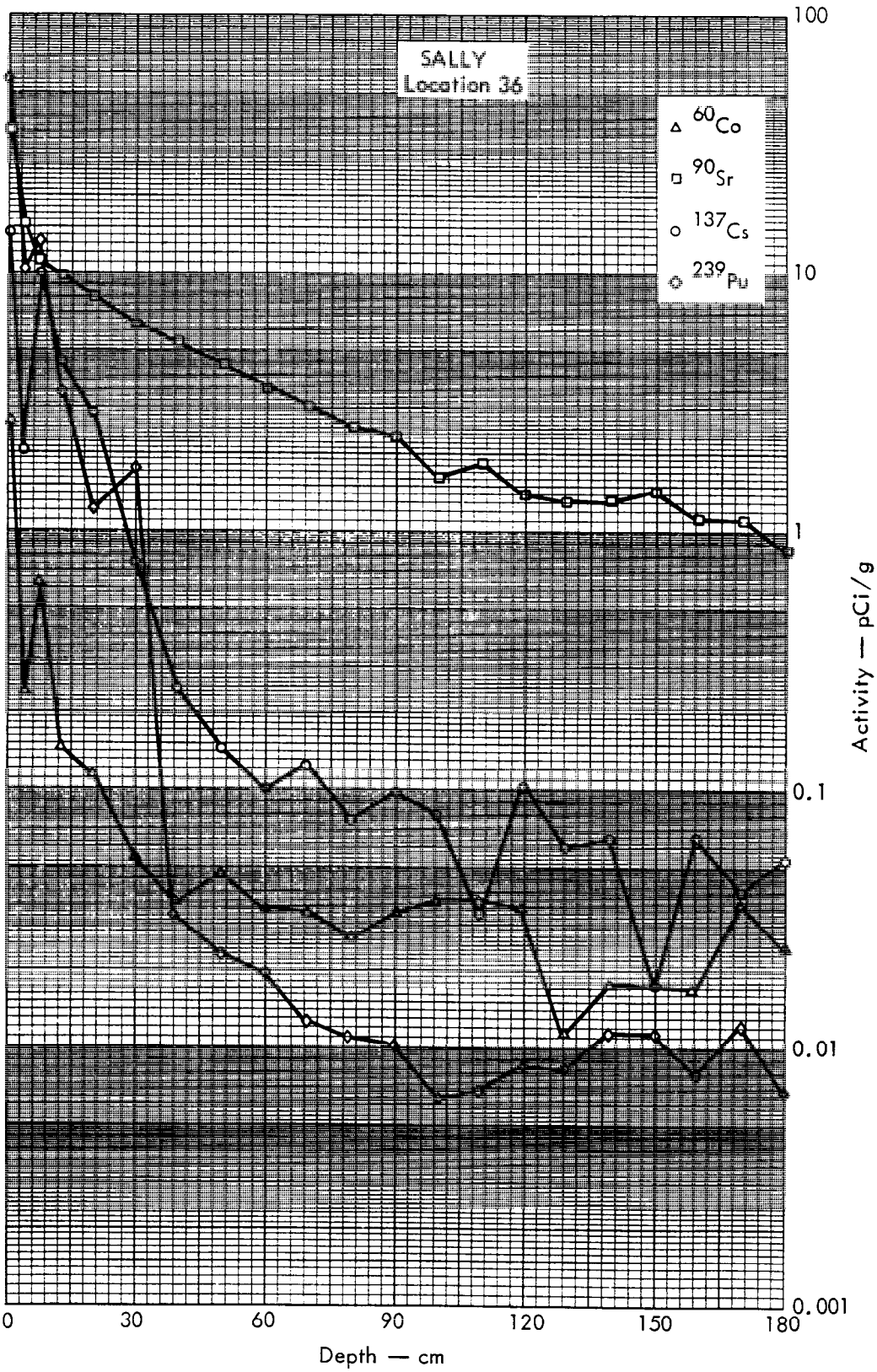

Fig. B. 17.2f. Activities of selected radionuclides as a function of soil depth.

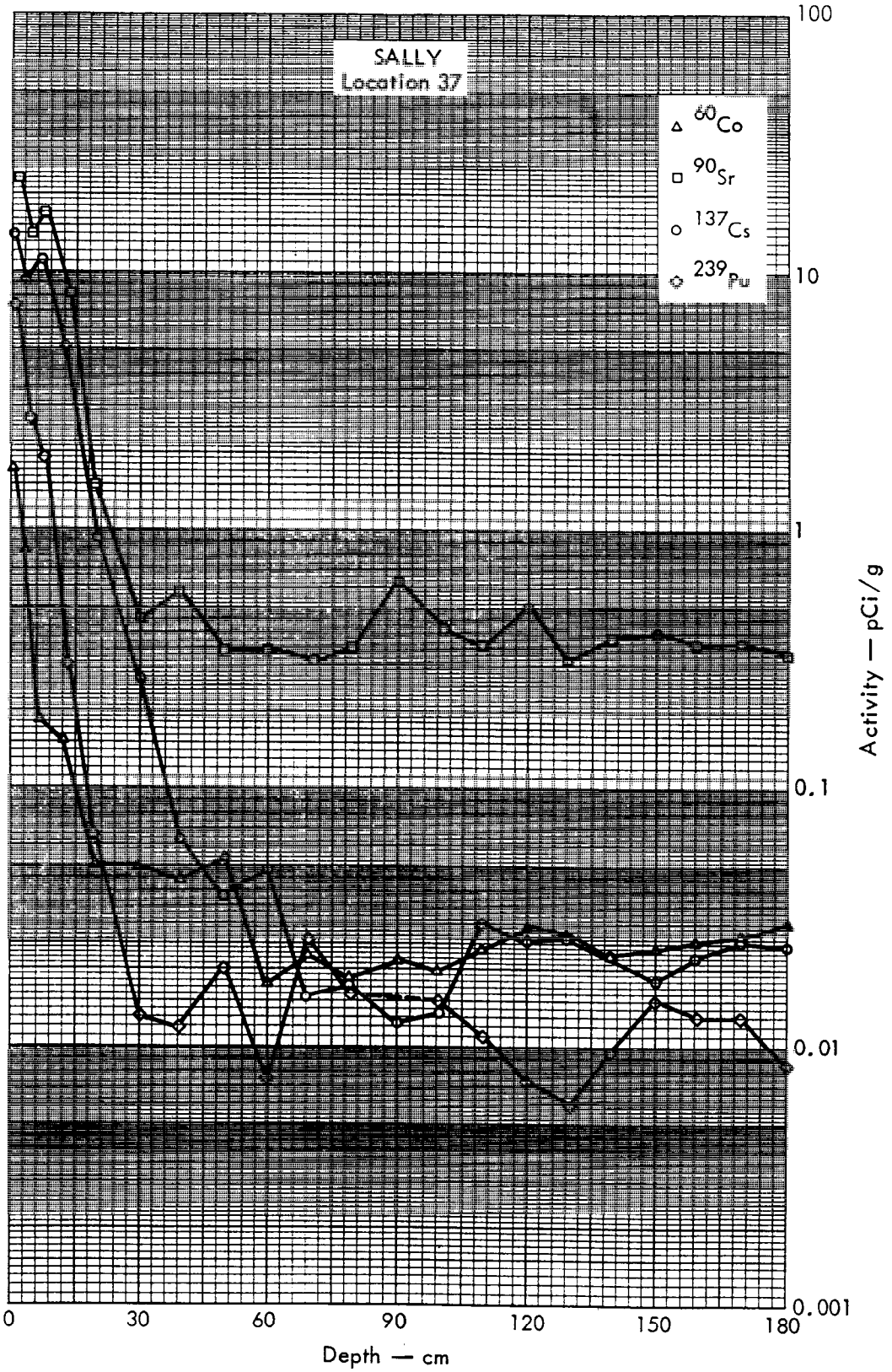

Fig. B. 17.2g. Activities of selected radionuclides as a function of soil depth.

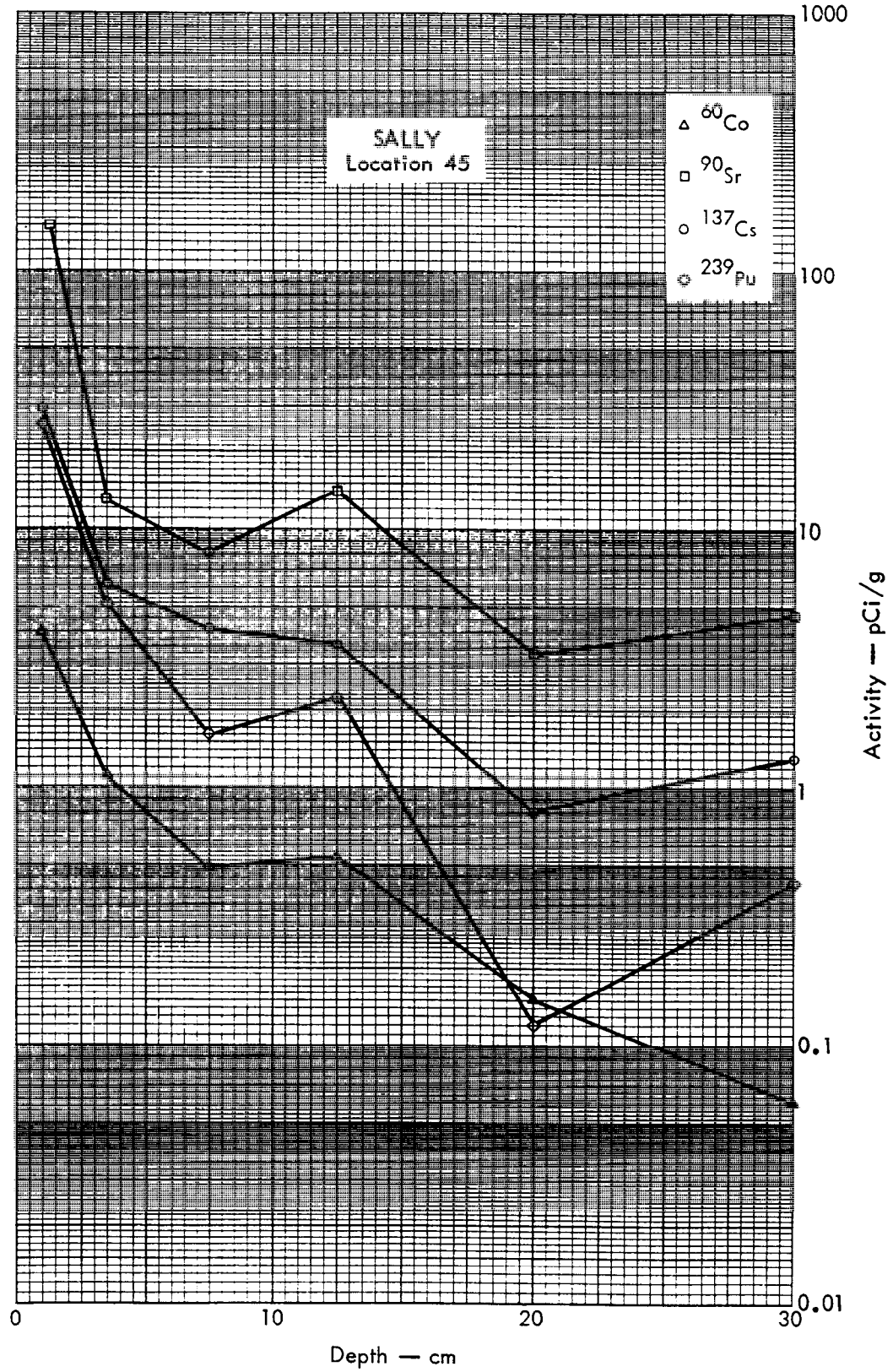

Fig. B. 17.2h. Activities of selected radionuclides as a function of soil depth.

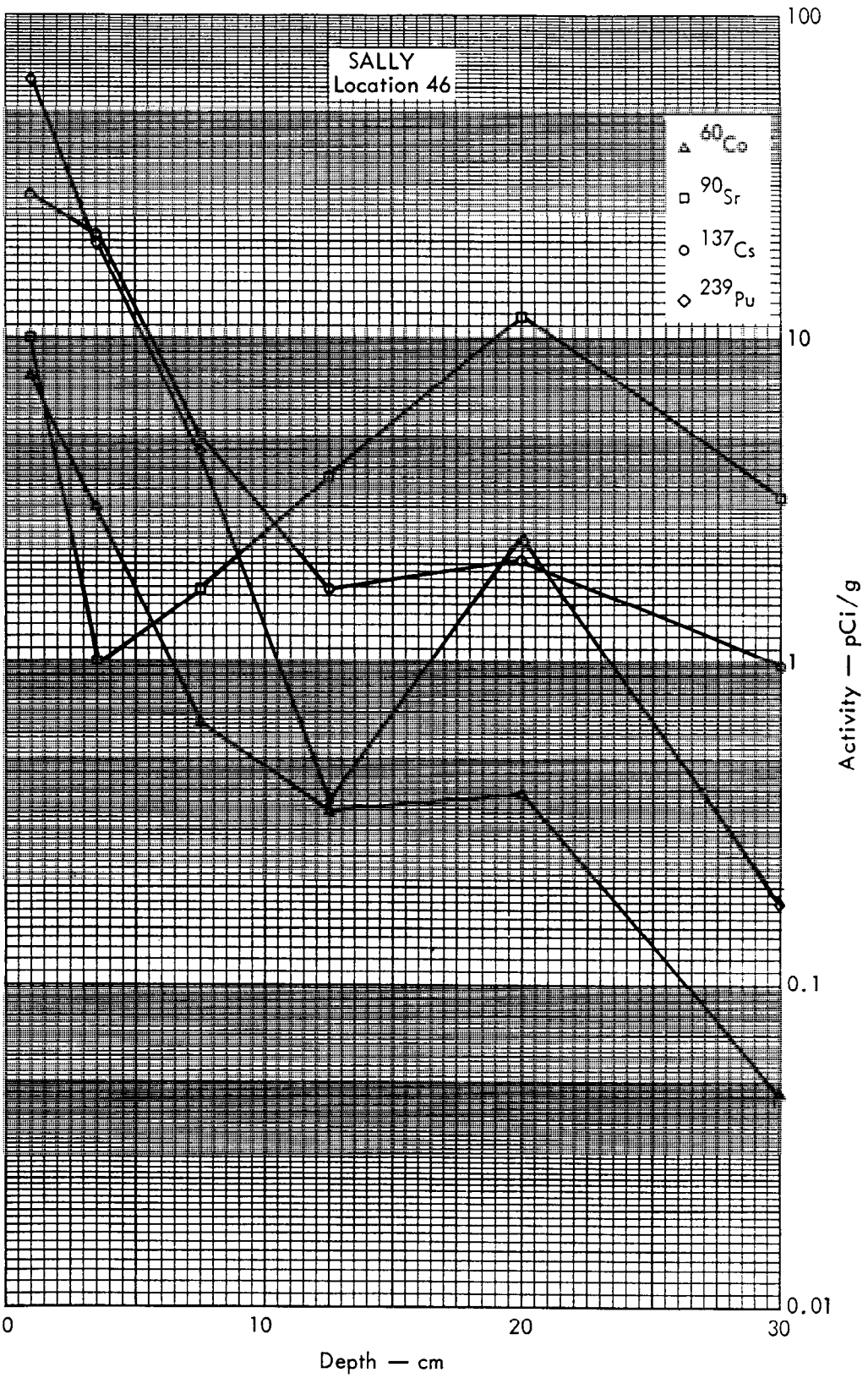

Fig. B. 17. 2i. Activities of selected radionuclides as a function of soil depth.

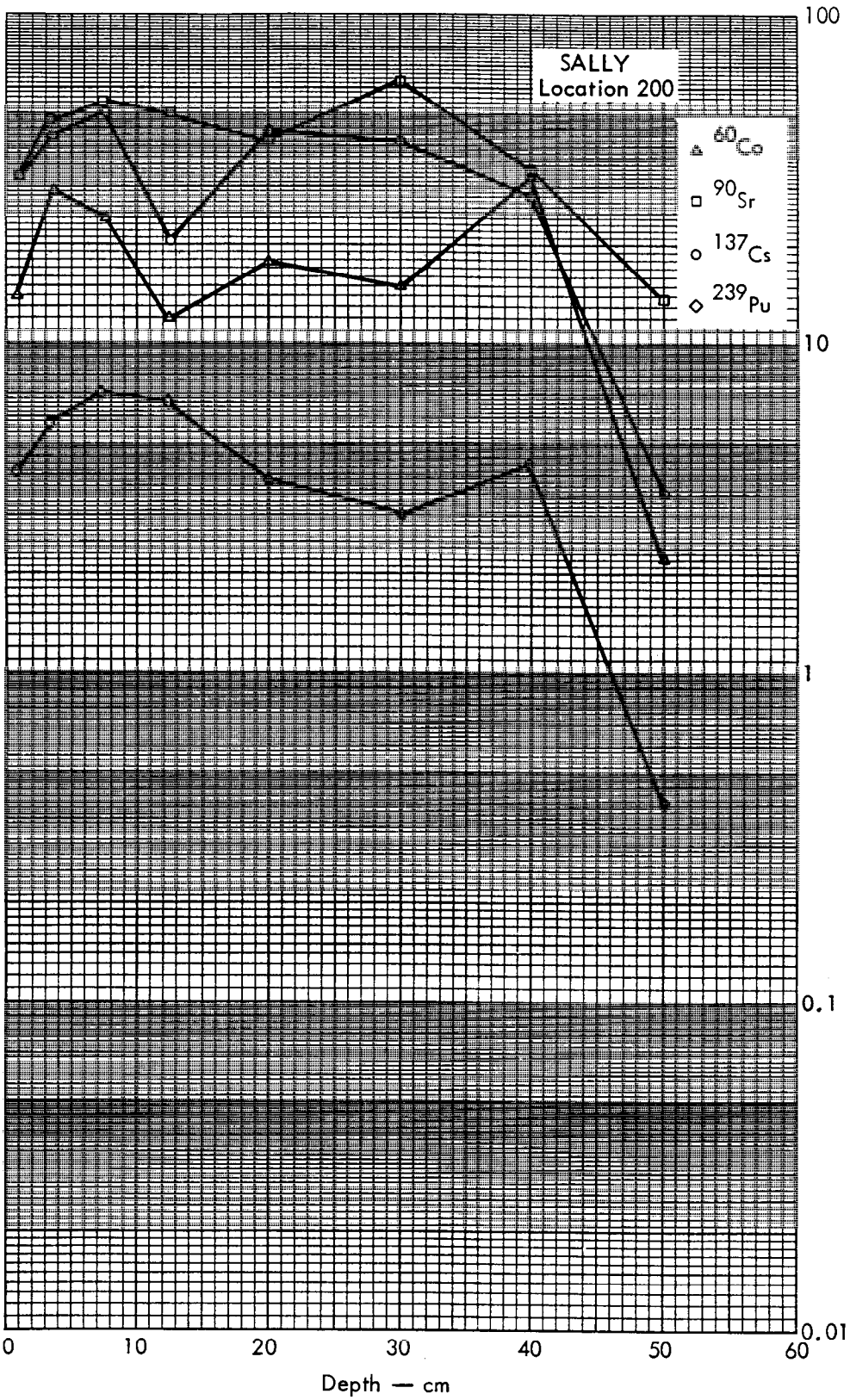

Fig. B.17.2j. Activities of selected radionuclides as a function of soil depth.

Fig. B.18.1.a.

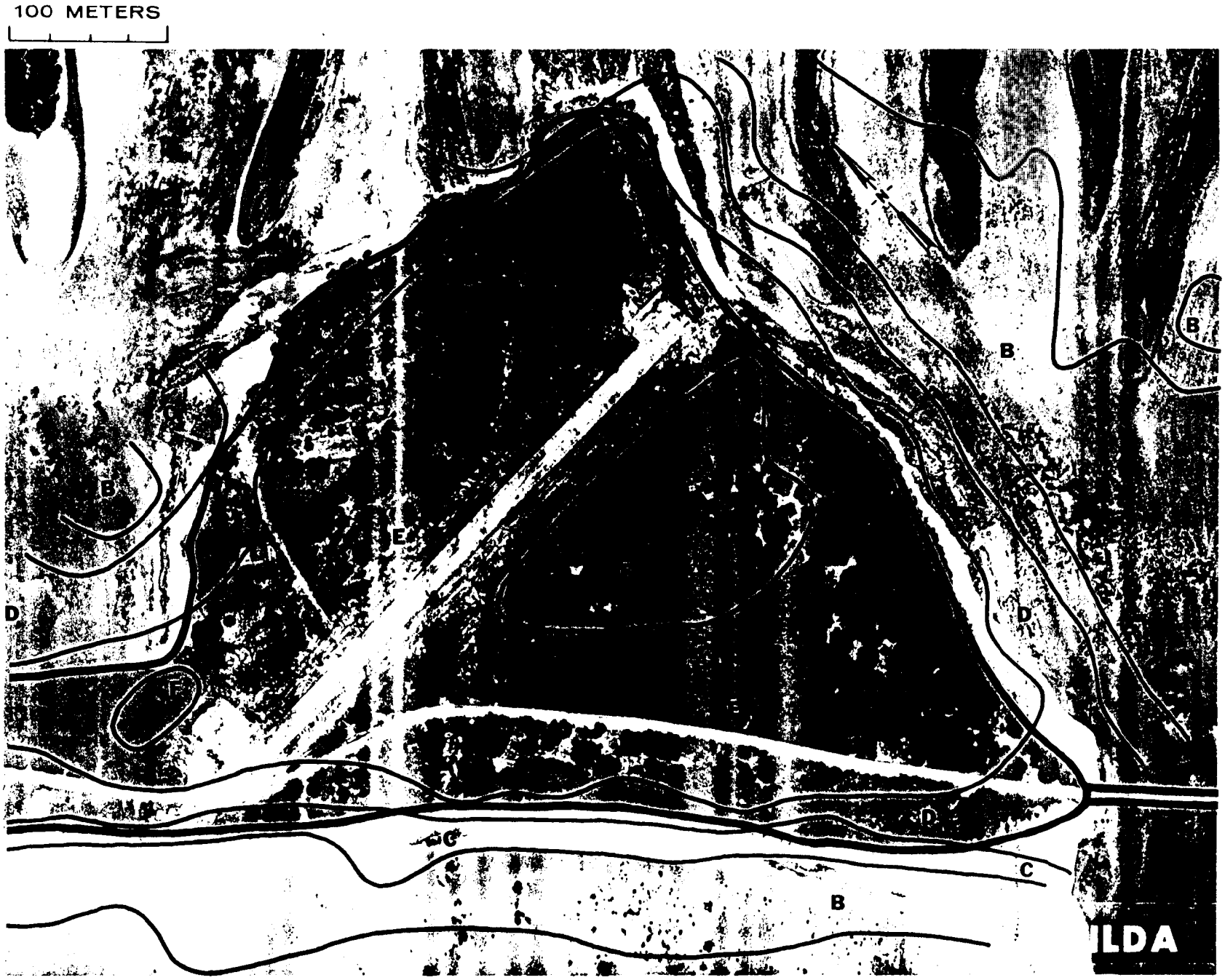

Fig. B.18.1.b. **Gross count isoexposure contours.** (Refer to alphabetic symbol key in this appendix.)

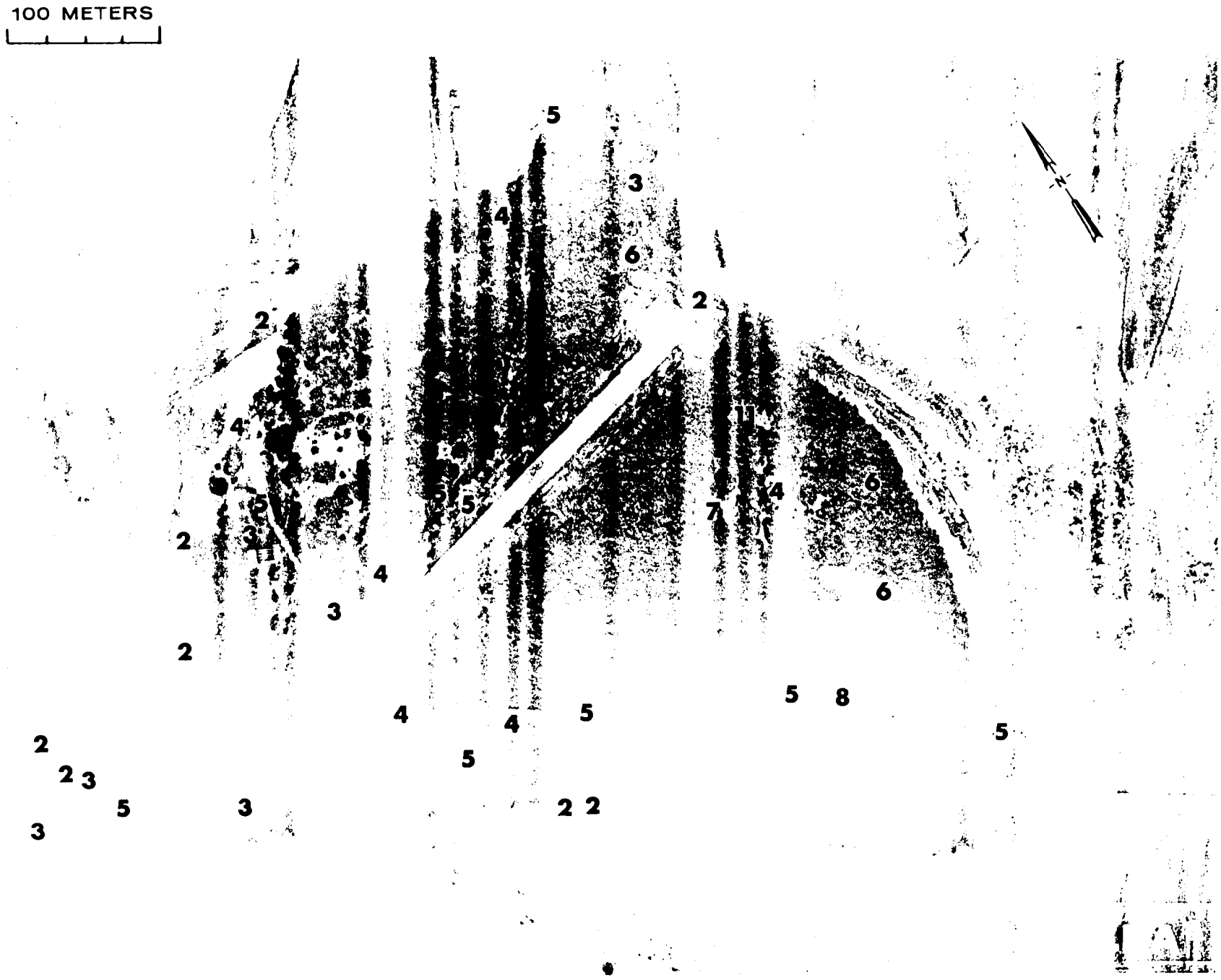

Fig. B.18.1.d. The gamma background exposure rate (μR/hr) at 1 m above the ground, measured with a portable NaI scintillation counter.

Fig. B.18.1.f. Soil-sample locations.

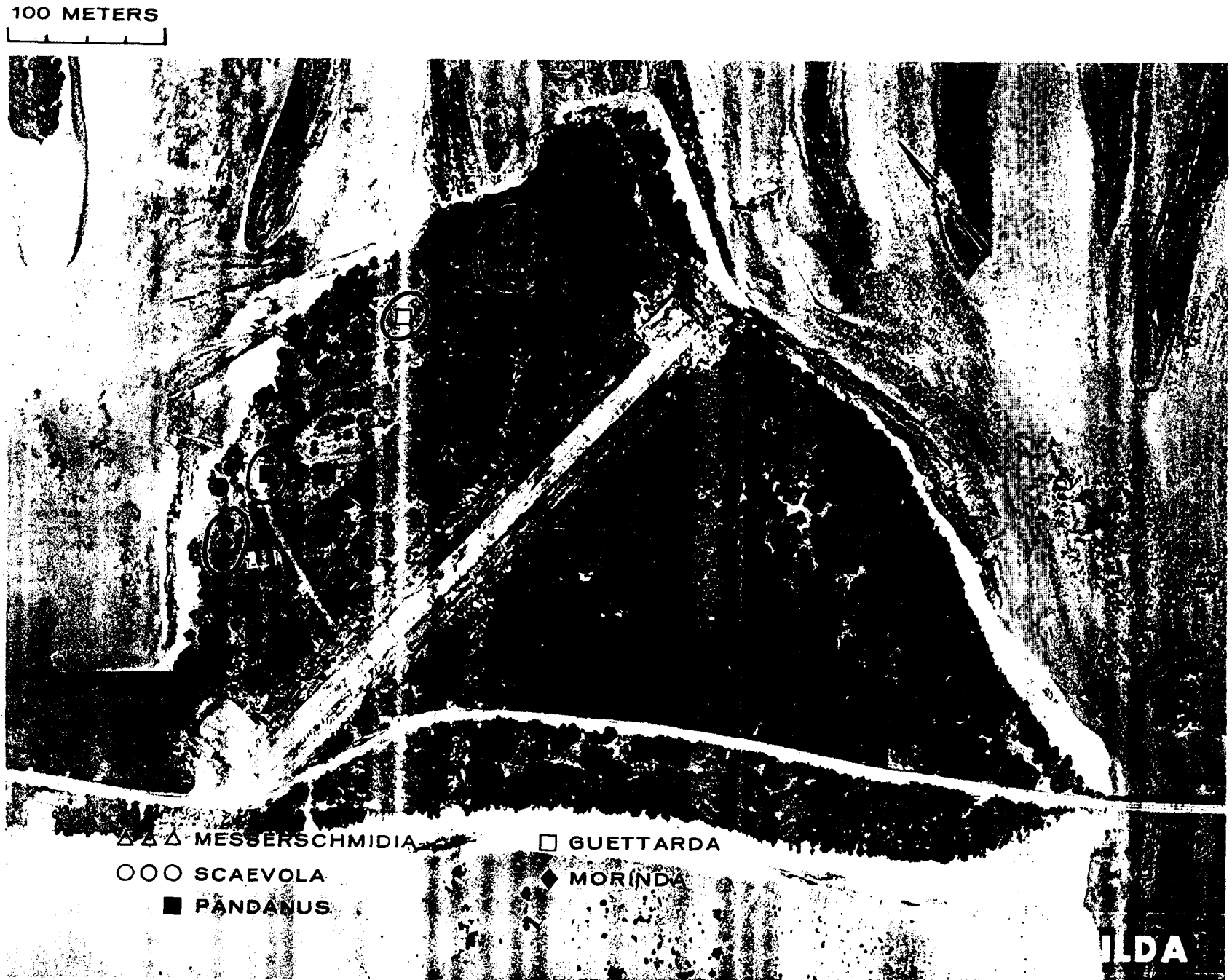

Fig. B.18.1.g. Vegetation sample locations.

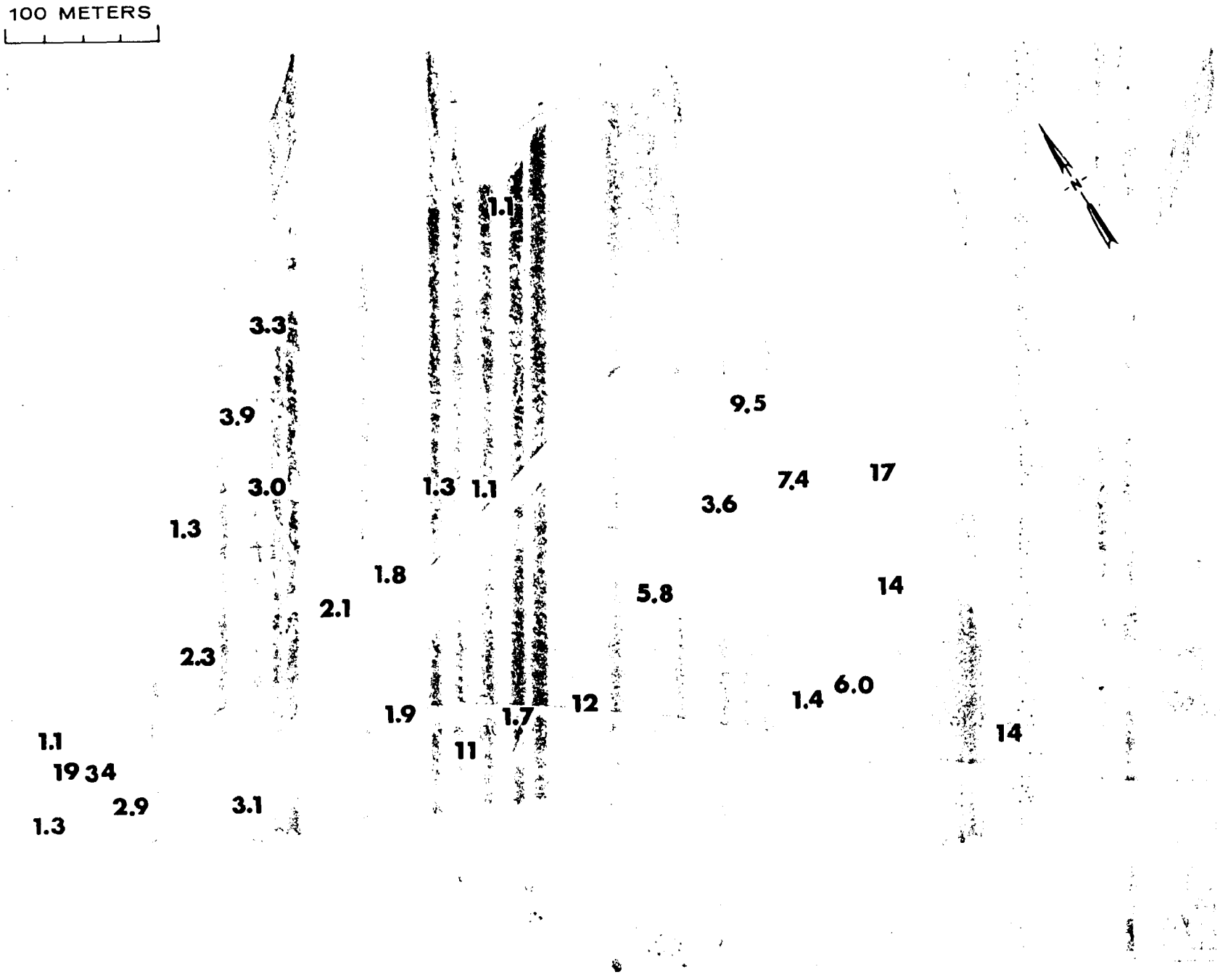

Fig. B.18.1.i. The average ^{239}Pu activities (pCi/gm) in soil samples collected to a depth of 15 cm.

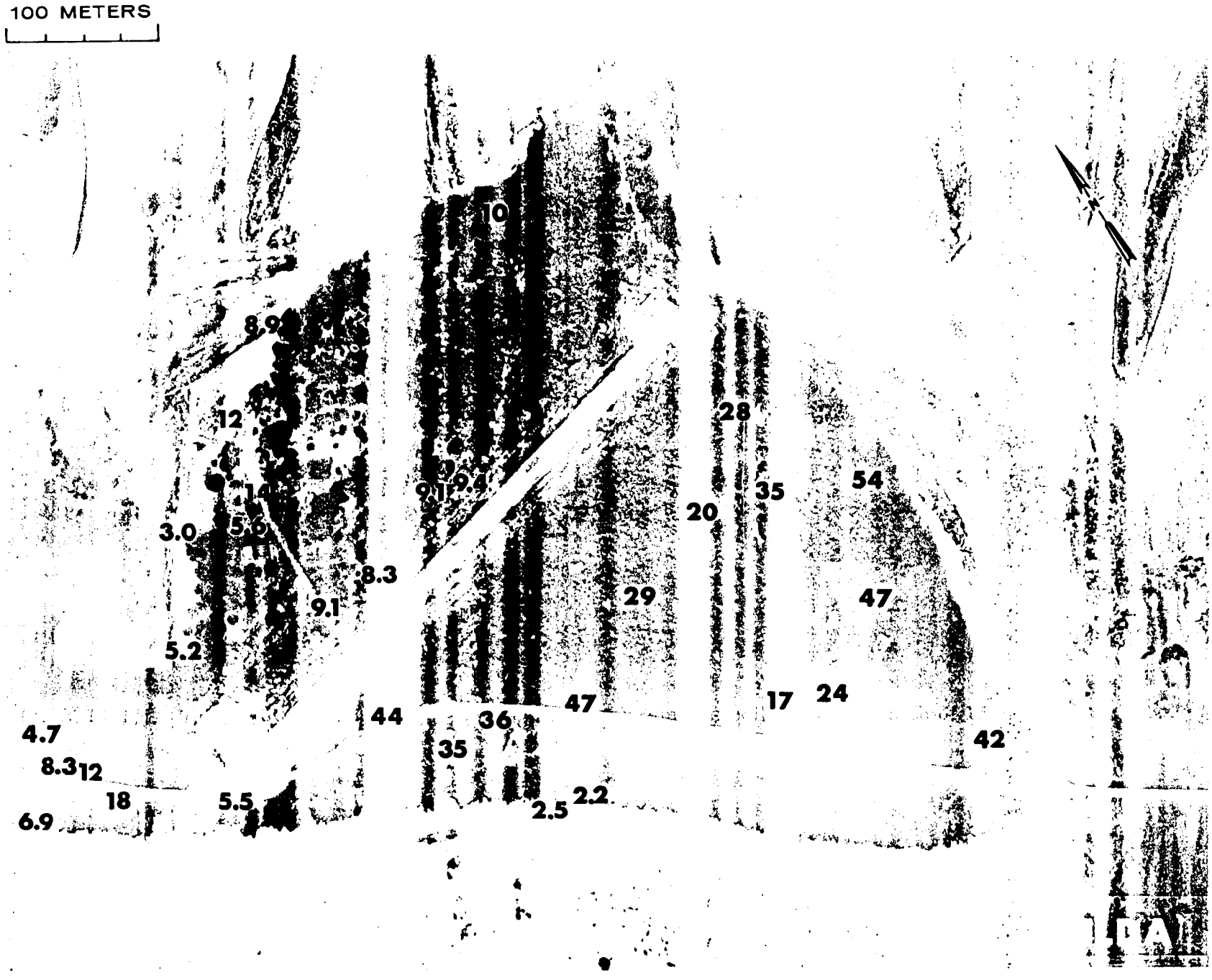

Fig. B.18.1.j. The average ^{90}Sr activities (pCi/gm) in soil samples collected to a depth of 15 cm.

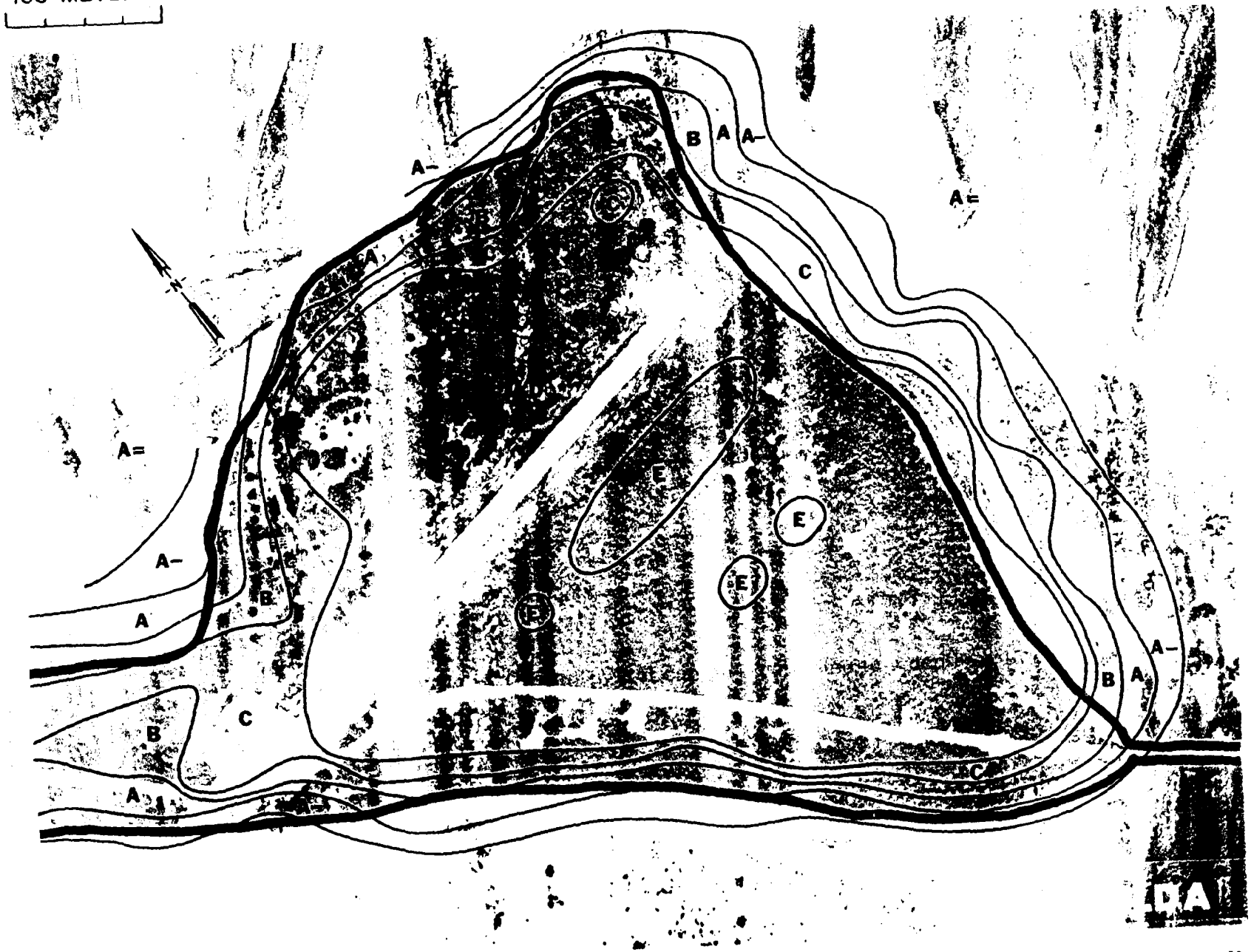

Fig. B.18.1.k. ^{137}Cs isoexposure and isoconcentration contours. (Refer to alphabetic symbol key in this appendix.)

Fig. B.18.1.1. The average ^{137}Cs activities (pCi/gm) in soil samples collected to a depth of 15 cm.

Fig. B.18.1.m. ^{60}Co isoexposure and isoconcentration contours. (Refer to alphabetic symbol key in this appendix.)

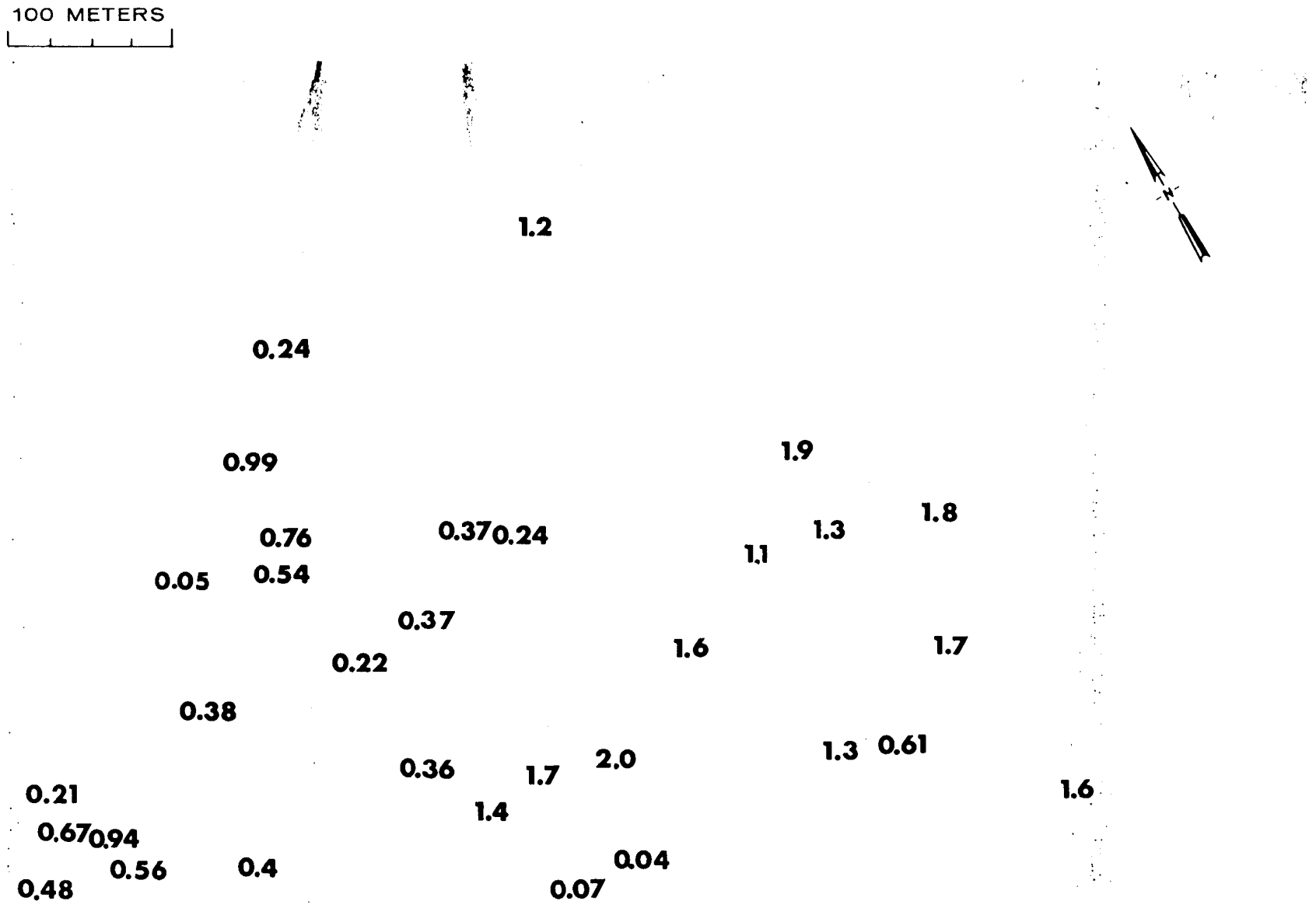

Fig. B.18.1.n. The average ^{60}Co activities (pCi/gm) in soil samples collected to a depth of 15 cm.

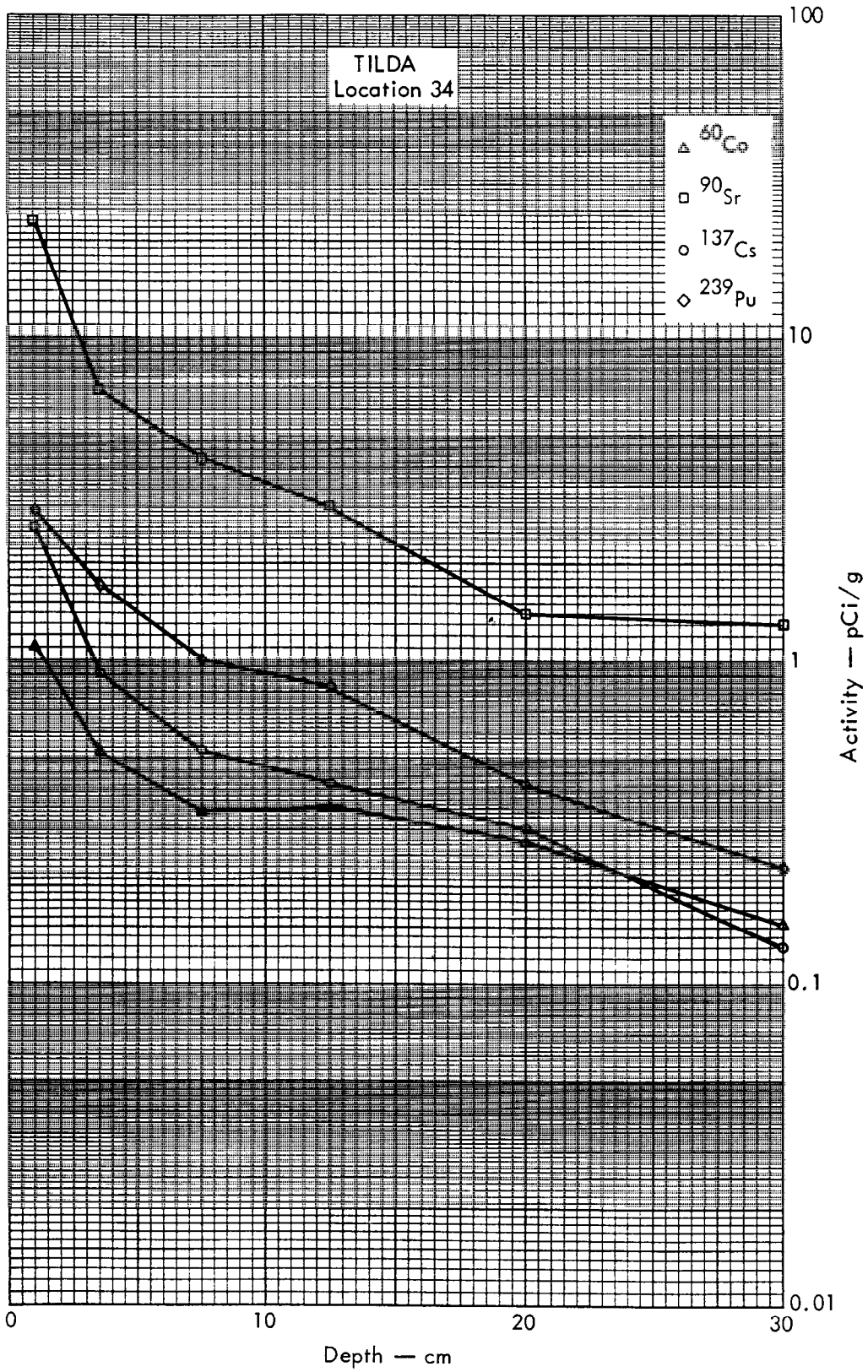

Fig. B. 18. 2a. Activities of selected radionuclides as a function of soil depth.

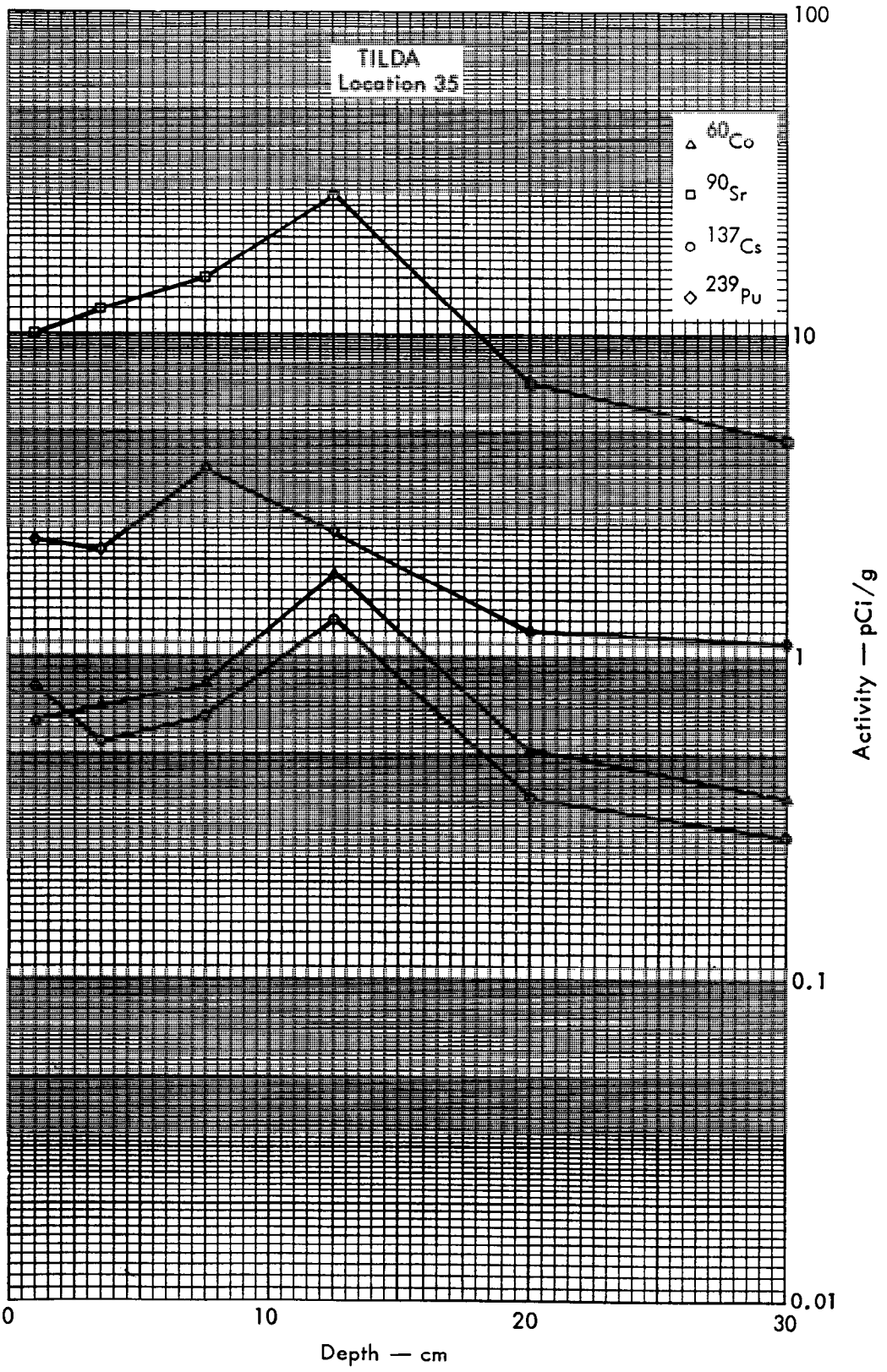

Fig. B.18.2b. Activities of selected radionuclides as a function of soil depth.

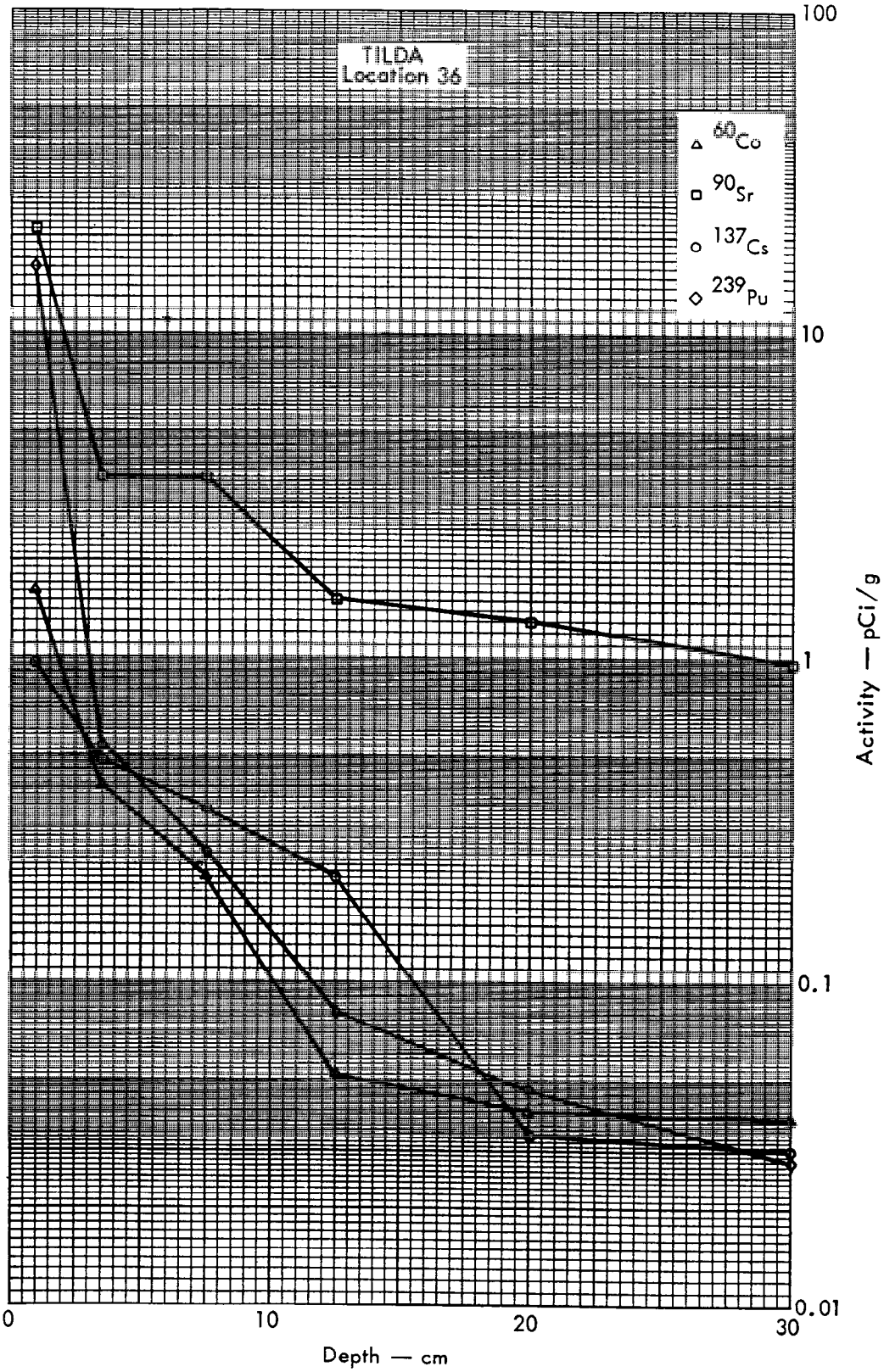

Fig. B.18.2c. Activities of selected radionuclides as a function of soil depth.

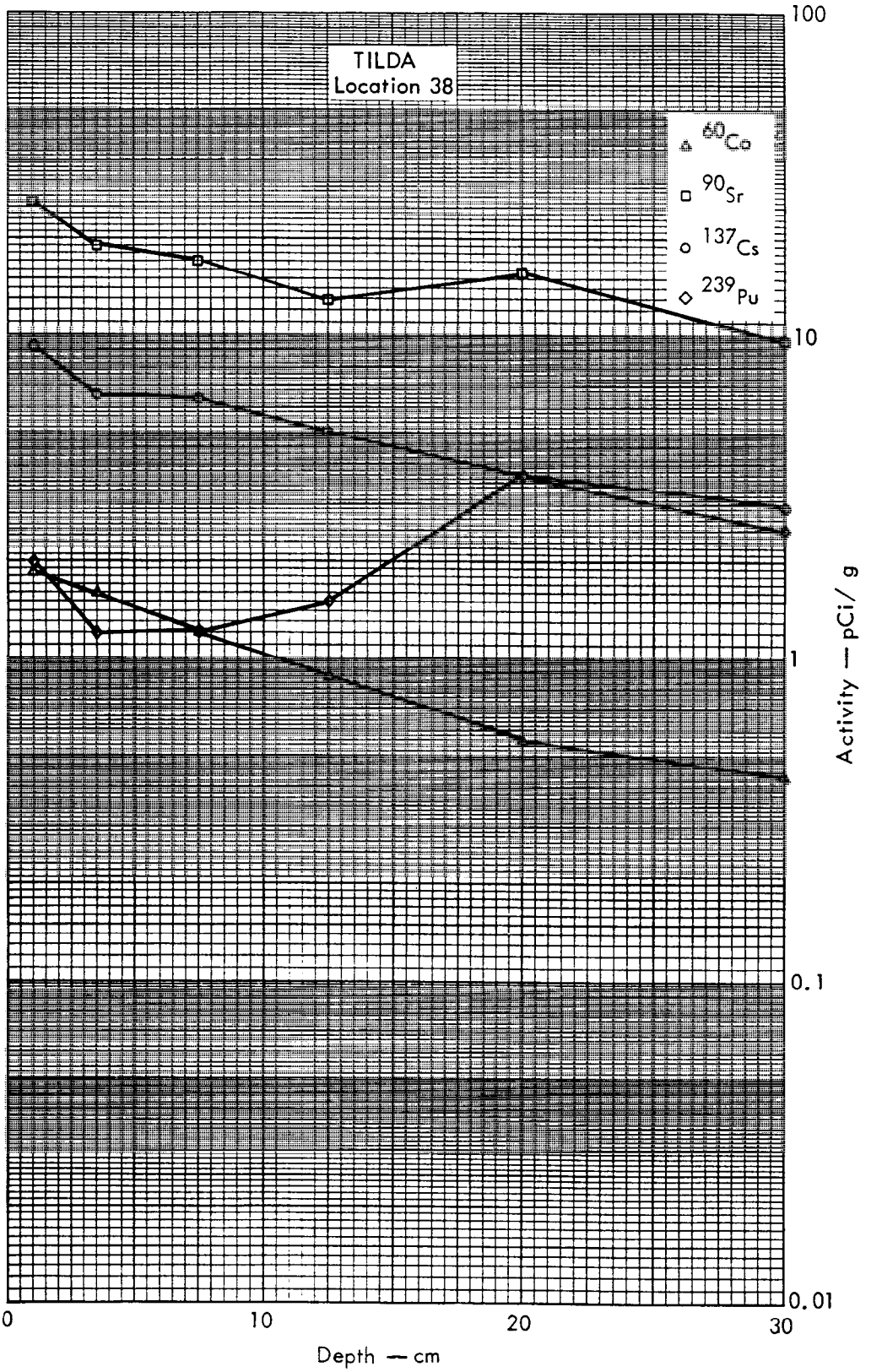

Fig. B. 18. 2d. Activities of selected radionuclides as a function of soil depth.

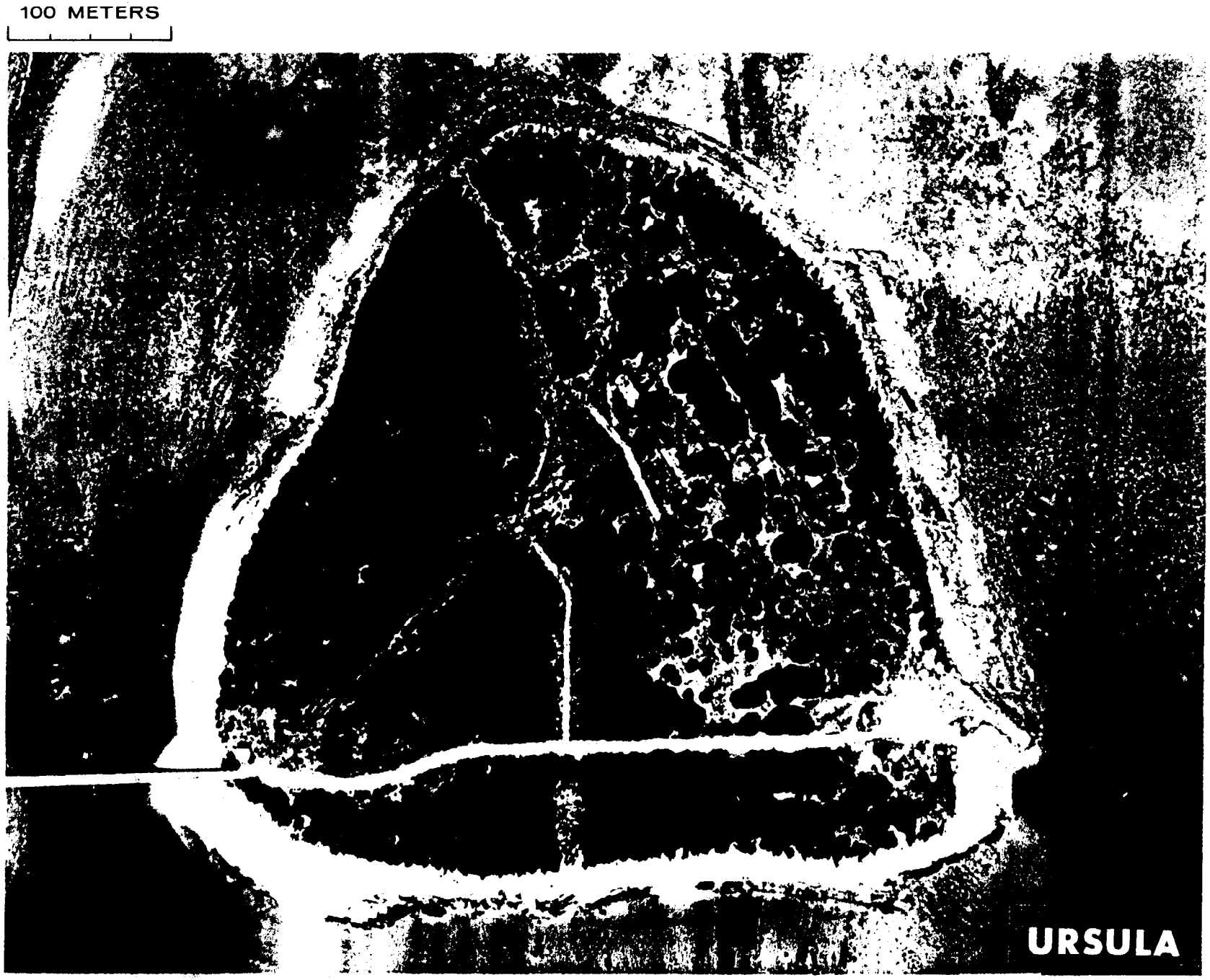

Fig. B.19.1.a.

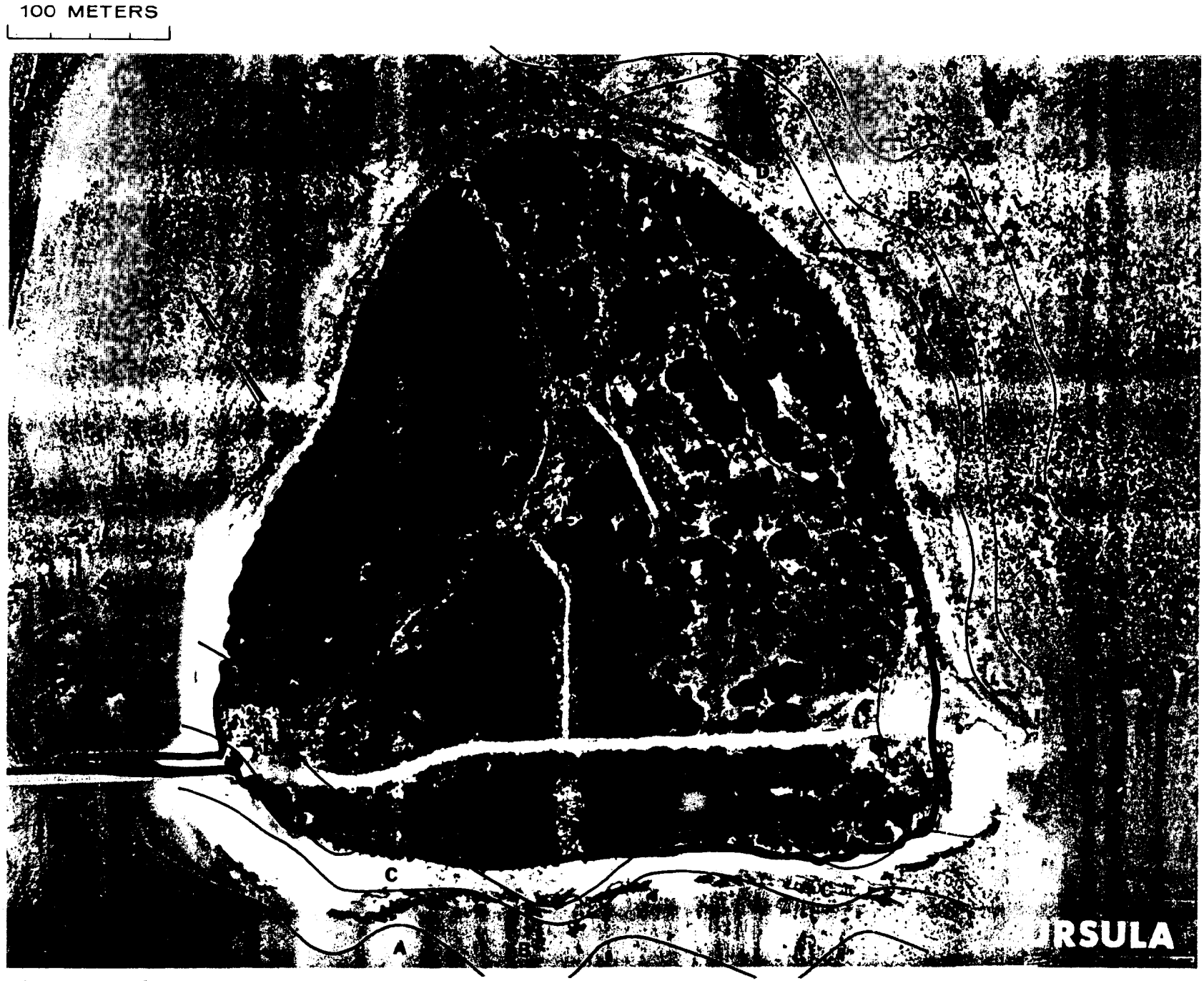

Fig. B.19.1.b. **Gross count isoexposure contours.** (Refer to alphabetic symbol key in this appendix.)

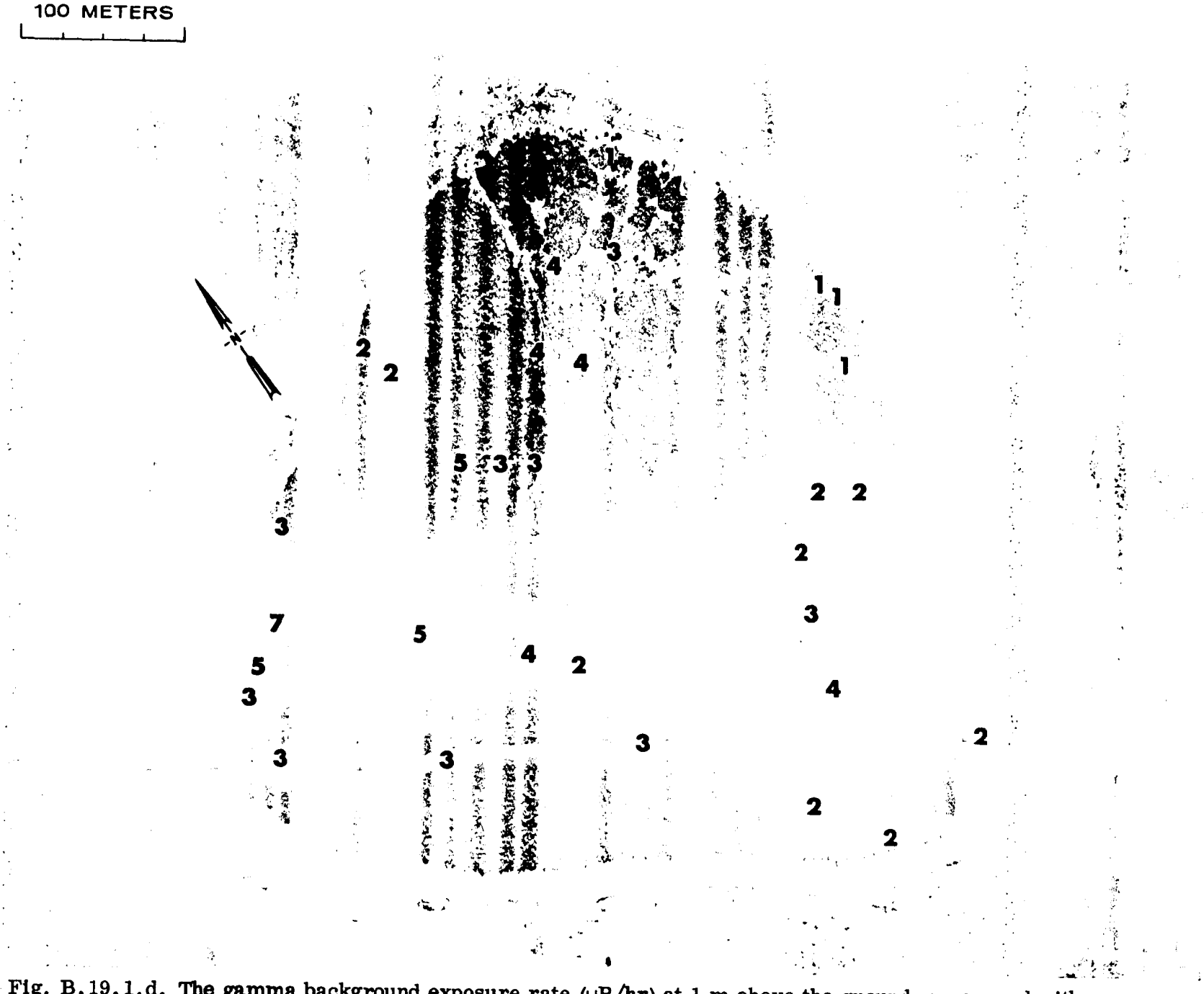

Fig. B.19.1.d. The gamma background exposure rate (μR/hr) at 1 m above the ground, measured with a portable NaI scintillation counter.